

**Structural and Functional Characterization  
of the Interactions of Platelet-Derived Chemokines  
CCL5, CXCL4 and CXCL4L1**

Von der Fakultät für Mathematik, Informatik und Naturwissenschaften der Rheinisch-  
Westfälischen Technischen Hochschule Aachen zur Erlangung des akademischen Grades  
eines Doktors der Naturwissenschaften genehmigte Dissertation

vorgelegt von

Diplom-Biologe

Alisina Sarabi

aus

Kabul, Afghanistan

Berichter:

Universitätsprofessor Christian Weber

Universitätsprofessor Rainer Fischer

Tag der mündlichen Prüfung: 31.01.2011

The results of this work were in part published in:

Rory R Koenen, Philipp von Hundelshausen, Irina V Nesmelova, Alma Zerneck, Elisa A Liehn, **Alisina Sarabi**, Birgit K Kramp, Anna M Piccinini, Søren R Paludan, M Anna Kowalska, Andreas J Kungl, Tilman M Hackeng, Kevin H Mayo & Christian Weber (2009). Disrupting functional interactions between platelet chemokines inhibits atherosclerosis in hyperlipidemic mice. Nat Med **15** (1): 97-103.

**Alisina Sarabi**, Birgit K Kramp, Maik Drechsler, Tilman M Hackeng, Oliver Soehnlein, Christian Weber, Rory R Koenen and Philipp von Hundelshausen (2010). CXCL4L1 inhibits angiogenesis and induces undirected endothelial cell migration without affecting endothelial cell proliferation and monocyte recruitment. J Thromb Haemost **9** (1): 209-19 [Epub ahead of print DOI:10.1111/j.1538-7836.2010.04119.x.] PMID: 20961394.

## Table of Contents

<b>Table of contents</b> .....	i
<b>Abbreviations</b> .....	vi
I Introduction .....	1
I.1 Atherosclerosis .....	1
I.2 Chemokines .....	2
I.3 Interaction of chemokines .....	4
I.4 Chemokine receptors .....	6
I.4.1 Alternative signaling mechanism .....	8
I.5 Platelets.....	8
I.6 Platelet-derived chemokines CXCL4, CXCL4L1 and CCL5 .....	10
I.6.1 CXCL4 .....	10
I.6.2 CXCL4L1 .....	14
I.6.3 CCL5 .....	15
I.7 Aims of the study.....	17
II Material and methods .....	18
II.1 General equipment.....	18
II.2 Molecular biology .....	19
II.2.1 General work with <i>E. coli</i> .....	19
Bacteria growth media.....	20
Preparation of heat-shock competent <i>E. coli</i> .....	20

	Heat-shock transformation of competent <i>E. coli</i> .....	21
II.2.2	Bacterial strains .....	21
II.2.3	Plasmids.....	21
II.2.4	Polymerase chain reaction.....	21
II.2.5	Cloning of CXCL4 and CXCL4L1 .....	22
II.2.6	Miniprep: Small-scale purification of plasmid DNA .....	23
II.2.7	Midiprep and maxiprep: Large-scale purification of plasmid DNA .....	24
II.2.8	Restriction endonuclease digestion of DNA .....	24
II.2.9	Agarose gel electrophoresis.....	24
II.2.10	Quantification of DNA .....	25
II.2.11	Sequencing of DNA .....	25
II.3	Protein analysis.....	25
II.3.1	Protein concentration assay .....	25
II.3.2	SDS-polyacrylamide gel electrophoresis (PAGE) .....	26
II.3.3	Tricine gel.....	27
II.3.4	Coomassie blue staining.....	28
II.3.5	Silver staining.....	28
II.3.6	Western blot analysis.....	28
II.3.7	Dot blot.....	29
II.3.8	Primary antibody .....	29
II.3.9	Secondary antibody .....	30
II.4	Protein expression and purification .....	30
II.4.1	CCL5 expression and purification.....	30
II.4.2	CCL5 FPLC (fast protein liquid chromatography) .....	31
	Sephacryl S-100HR.....	31
	HiTrap chelating HP.....	31
	MonoS™ 5/50 GL .....	32
	Resource™ Reverse Phase Chromatography (RPC).....	32

## Table of Contents

---

II.4.3	CCL5 HPLC (high performance liquid chromatography).....	33
II.4.4	CXCL4 and CXCL4L1.....	34
II.4.5	CXCL4 and CXCL4L1 FPLC.....	34
	HiLoad 16/10 SP-Sepharose™.....	34
	MonoS™ 5/50 GL or Capto™ S.....	35
	Resource™ RPC.....	35
II.4.6	CXCL4 and CXCL4L1 HPLC.....	35
II.4.7	Chemical synthesis of CXCL4L1.....	36
	Peptide synthesis and native chemical ligation.....	36
II.5	Biochemical analysis of the CCL5-CXCL4 heterodimer.....	39
II.5.1	Molecular dynamics simulations.....	40
II.5.2	Differential scanning calorimetry.....	40
II.5.3	Interaction of CXCL4 or CXCL4L1 with CCL5.....	41
	Ligand blot.....	41
	Isothermal fluorescence titration.....	41
II.6	Cell culture.....	42
II.6.1	General.....	42
II.6.2	Cell lines.....	42
II.6.3	Culturing of adherent cell monolayers.....	42
II.6.4	Culturing of cells in suspension.....	43
II.6.5	Freezing and thawing of cells.....	43
II.7	Functional assays.....	43
II.7.1	Angiogenesis <i>in vitro</i> .....	43
II.7.2	Endothelial migration.....	43
	Transwell assay.....	43

## Table of Contents

---

	The $\mu$ -Slide Chemotaxis chamber .....	44
II.7.3	Endothelial cell proliferation .....	44
II.7.4	Monocyte recruitment.....	45
	In vitro .....	45
	In vivo.....	45
II.7.5	Heparin neutralization .....	46
II.7.6	Protein C activation .....	46
II.7.7	Data illustration and statistic analysis .....	46
III	Results .....	47
III.1	Protein expression and purification .....	47
III.1.1	Expression and purification of recombinant CCL5.....	47
III.2	NMR chemical shift mapping of CCL5-CXCL4 heterodimer .....	51
III.3	CXCL4/CXCL4L1 Purification .....	54
III.4	Chemical synthesis of CXCL4L1.....	59
III.5	Functional analysis of CXCL4L1 and CXCL4 .....	64
III.5.1	CXCL4L1 and CXCL4 inhibit tube formation .....	64
III.5.2	CXCL4L1 induces endothelial cell chemokinesis.....	65
III.5.3	CXCL4L1 does not inhibit endothelial cell proliferation.....	66
III.5.4	Hetero- and homooligomerization differ in CXCL4L1 and CXCL4 .....	67
III.5.5	CXCL4L1 interaction with CCL5 does not enhance CCL5-triggered .....	
	monocyte arrest .....	69
III.5.6	Influence of CXCL4L1 on heparin neutralization and APC generation ..	70
IV	Discussion.....	72
IV.1	Different expression strategies for obtaining the CCL5, CXCL4 and .....	
	CXCL4L1 .....	72

## Table of Contents

---

IV.2	Structural differences between CXCL4 and CXCL4L1 .....	74
IV.3	CXCL4-CXCL4L1 functional comparison .....	75
V	Summary.....	80
VI	Zusammenfassung .....	82
VII	Acknowledgement.....	84
VIII	References .....	85
IX	Curriculum Vitae .....	93

## Abbreviations

aa	amino acid
APC	activated protein C
apoE	apolipoprotein E
APS	ammonium persulfate
aPTT	activated partial thromboplastin time
bFGF	basic fibroblast growth factor
BMC	1,2-bis(2-mercaptoacetamido) cyclohexane
CAD	coronary artery disease
CD	cluster of differentiation
CVD	cardiovascular disease
DDT	dithiothreitol
DMF	dimethylformamide
DMSO	dimethylsulphoxid
<i>E. coli</i>	<i>Escherichia coli</i>
ECMs	extracellular matrix proteins
FCS	fetal calf serum
Fmoc	9-Fluorenylmethoxycarbonyl
FPLC	fast protein liquid chromatography
GAG	glycosaminoglycan
GDP	guanosine diphosphat
Gnd-HCL	guanidine-HCL
GPCR	G-protein-coupled receptors
GTP	guanosine triphosphat
HDMEC	human dermal microvascular endothelial cells



## Abbreviations

---

HEPES	4-2-hydroxyethyl-1-piperazineethanesulfonic acid
HF	hydrofluoric acid
HPLC	high pressure liquid chromatography
HRP	horseradish peroxidase
HSA	human serum albumin
HSQC	$^{15}\text{N}$ - $^1\text{H}$ heteronuclear single quantum coherence
HUVEC	human umbilical vein endothelial cell
IFN- $\gamma$	interferon-gamma
IMAC	immobilized metal affinity chromatography
IP3	inositol triphosphate
IPTG	isopropyl- $\beta$ -D-thiogalactopyranoside
$K_d$	dissociation constant
kDa	kilo Dalton
LB	Lauria-Bertani broth
LDL	low-density lipoprotein
MAPK	mitogen-activated protein kinase
MBHA	methylbenzhydramine
MM6	mono mac 6
MPA	mercaptoproprionic acid
NMR	nuclear magnetic resonance
o.n.	over night
PBS	phosphate buffered saline
PF4	platelet factor 4
PI3K	phosphoinositide-3 kinase
PIP2	phosphatidylinositol bisphosphate
PIP3	phosphotidylinositol-3,4,5-trisphosphate

## Abbreviations

---

PKA	protein kinase A
PKC	protein kinase C
PLC	phospholipases C
PMN	polymorphonuclear cells
RANTES	regulated on activation, normal T-cell expressed and secreted
rt	room temperature
SDS-PAGE	sodium dodecyl sulfate-polyacrylamide gel electrophoresis
SPPS	solid-phase peptide synthesis
TB	terrific broth
t-Boc	tert-Butyloxycarbonyl
TBS	tris buffered saline
TEMED	N,N,N',N'-tetramethylethylenediamine
TFA	trifluoroacetic acid
TM	thrombomodulin
TNF- $\alpha$	tumor necrosis factor-alpha
TSS	transformation and storage solution
VEGF	vascular endothelial growth factor
VWF	von Willebrand factor

# I Introduction

## I.1 Atherosclerosis

Cardiovascular disease (CVD) is a major cause of morbidity and mortality in developed countries, thus imposing an already substantial and still increasing socio-economic burden (Koenen 2008). Atherosclerosis, which can be best characterized as a chronic inflammation of the vessel wall, is the underlying cause of coronary artery disease (CAD). Recent developments in vascular biology have shown that lesion progression in atherosclerosis is driven by the influx of inflammatory cells from the blood stream (Hansson 2006).

Atherosclerosis is characterized as a chronic inflammation, where due to endothelial dysfunction and production of pro-inflammatory mediators by platelets, monocytes are recruited to the surface of endothelial cells (Fig.I.1 A). Ensuing the transmigration through the endothelial layer into the intima, monocytes transform to macrophages and further to foam cells through engulfing and accumulating lipids (Fig.I.1 B). More inflammatory cells are attracted and a lipid-rich and necrotic core (plaque) is formed. Neovascularization, which emerges from the adventitia into the plaque, is responsible for leakage of blood components and hemorrhage (Fig.I.1 C). The progression of the plaque formation leads to the formation of a fibrous cap, which is composed of collagen rich extracellular matrix, T cells, macrophages and smooth muscle cells that overlay the plaque. Proteases that are released from the activated immune cells weaken the fibrous cap and this can lead to the rupture of the plaque. The exposure of cell debris and tissue factor to the blood triggers the coagulation cascade, which finally ends in the formation of thrombosis and occlusion of the artery (Fig.I.1 D) (Weber 2008).

Chemokines appear to play an important role in the regulation and control of this process by orchestrating the interactions between circulating blood cells and arterial wall.

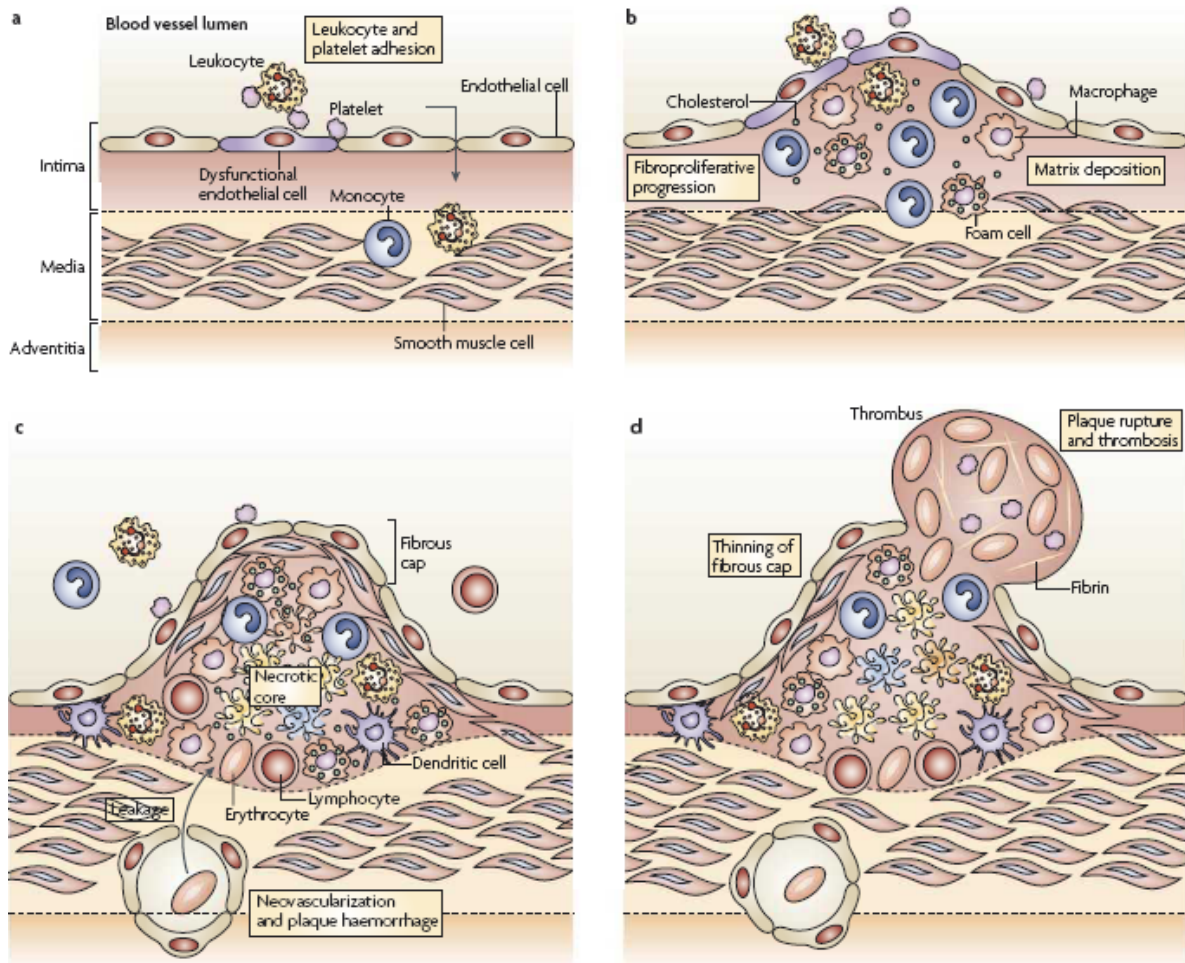


**Fig.1.1: Development of atherosclerosis.** (A) Endothelial-cell dysfunction leads to early platelet and leukocyte adhesion and increased permeability of the endothelium. (B) Recruited monocytes accumulate lipids and transform into macrophages or foam cells (fatty streaks). (C) Creation of a necrotic core by apoptosis of macrophages and other plaque cells. A fibrous cap formation that consists of matrix and a smooth-muscle-cell layer is formed. Also neovascularization can occur from the adventitia within the plaque, which can lead to plaque hemorrhage. (D) Progression of the plaque leads to a thinning of the fibrous cap, which can ultimately result in plaque rupture due to matrix degradation by proteases (Weber 2008).

## I.2 Chemokines

Chemokines (an abbreviation of *chemoattractant cytokines*) are a family of structurally related proteins which can influence the most profound aspects of a cell's life, including not only activation, adhesion and chemotaxis but also proliferation, maturation, differentiation, apoptosis, malignant transformation, and dissemination (Rossi 2000). They are single polypeptides ranging from 70 to 100 amino acids in length, approximately 8 to 10 kDa in molecular weight and share 20-50% gene and amino acid sequence homology. The chemokines are classified into four subfamilies according to the position of the N-terminal cysteines. The  $\alpha$ -chemokines, also known as CXC chemokines, contain a single random amino acid between the first and second cysteine residues (Kobayashi 2006). Up to

now 17 different CXC chemokines have been described. This group can be further divided into chemokines containing the amino acid motif glutamic acid-leucine-arginine (ELR-positive) at the N-terminus and those without the motif (ELR-negative). An example for an ELR-positive chemokine is CXCL8 (IL-8) and for an ELR-negative chemokine CXCL4 (Platelet Factor 4, PF4).  $\beta$  or CC chemokines have two adjacent cysteine residues near the N-terminus. At least 28 chemokines are allocated to this group e.g. CCL5 or RANTES (Regulated on activation normal T cell expressed and secreted) (Charo 2004). The C or  $\gamma$  group has two members XCL1 (lymphotactin- $\alpha$ ) and XCL2 (lymphotactin- $\beta$ ) which lacks two of the four cysteines, but shares homology at its carboxyl terminus with the C-C chemokines (Kelner 1994). CX3CL1 (Fractalkine) is a C-X3-C chemokine with three random amino acid residues between the first two cysteines and constitutes alone the fourth subgroup. CX3CL1 is the only chemokine besides CXCL16 that can be found as membrane bound whereas the rest is soluble.

Previously, chemokines were divided broadly into two categories according to their function in pro-inflammatory and homeostatic chemokines (Moser 2004). Pro-inflammatory chemokines act in a SOS response where they are expressed by induction of a stimulus that alters the cellular homeostasis and are responsible for the recruitment of immune cell to the site of the inflammation and infection. Whereas the homeostatic chemokines are expressed constitutively and play an important role in basal leukocyte trafficking and forming the architecture of secondary lymphoid organs (Gerard 2001). Recent findings indicate that many chemokines cannot be classified in either of these groups. Such chemokines with dual function participate in immune defense functions as well as in targeting non-effector leukocytes at sites of leukocyte development and immune surveillance. Many chemokines with dual-function are highly selective for lymphocytes and have a role in T-cell development in the thymus, as well as in T-cell recruitment to sites of inflammatory (Moser 2004). Although there are numerous of chemokines, structurally they are similarly shaped (Fig.I.2).

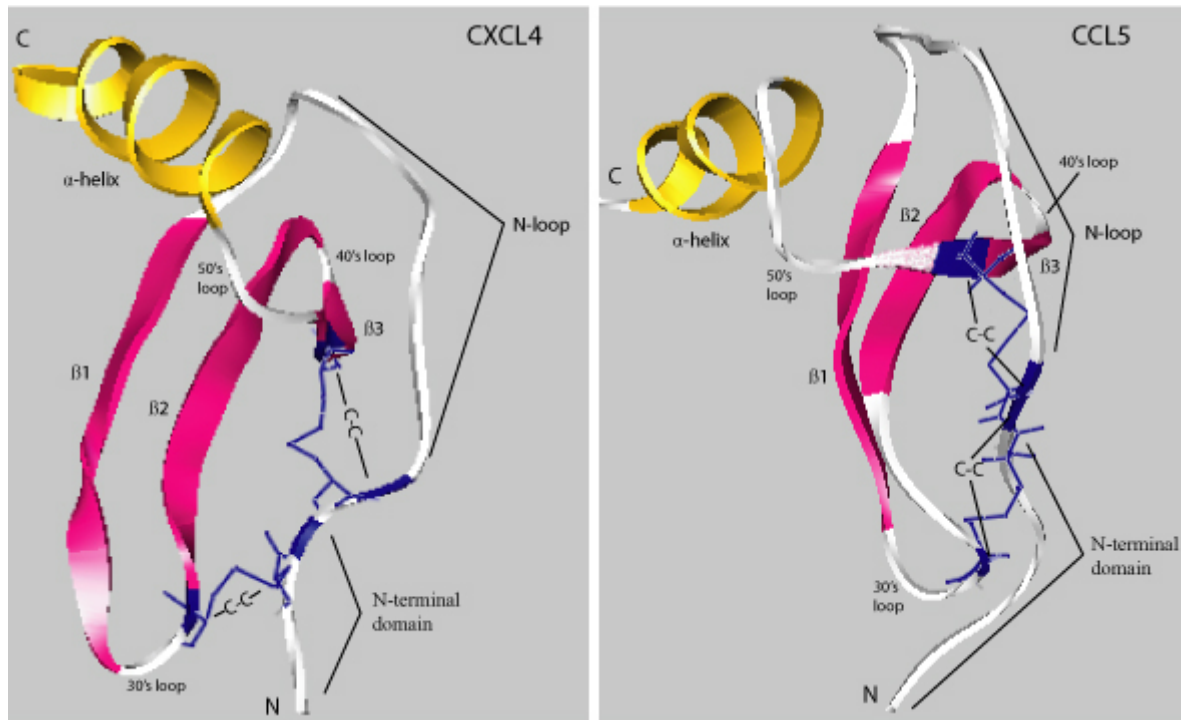


**Fig.1.2: Typical 3D structure of a CXC (CXCL4) and CC (CCL5) chemokine.** The chemokine topology consists of an elongated N-terminus followed by first two cysteines. A loop of about ten residues shapes the N loop, which has an important functional role. Then after the three anti-parallel  $\beta$ -strands a C-terminal  $\alpha$ -helix is succeeded. Each  $\beta$ -strand unit is connected by turns known as the 30s, 40s and 50s loops, which reflects the numbering of residues in the mature protein. The 30s and 50s loops possess the latter two of the four cysteines characteristic of the family of CXC chemokines (generated with 3D-Mol Viewer).

### I.3 Interaction of chemokines

Chemokines can form heterophilic interactions, which then can lead to enhancement or suppression of the primordial function. Moreover a functional chemokine ‘interactome’ (protein-protein interaction) can be constituted by different interactions in particular microenvironments, where a given chemokine could exercise different functions dependent on the composition of a specific milieu and dependent on the interaction partner. These interactions can expand the plasticity of the regulatory chemokine network, which can evoke the possibility of regulating and orchestrating of the leukocytes to the inflammatory sites (Weber 2006). It has been reported that the heterodimerization of CCL3 and CCL4 protects them from enzymatic digestion thus stabilizing their activity or might induce receptor heterodimerization to affect signaling (Guan 2001). The CCR7 agonists CCL19 and CCL21 can form heterodimers with unrelated non-agonist chemokines (CCL19/CCL22 or CCL21/CXCL13) which can lead to the activation of CCR7 at lower agonist concentrations than in the presence of CCL19 or CCL21 alone (Paoletti 2005). Other examples for heterophilic interaction are CXCL4 with CXCL8 (Dudek 2003;

Nesmelova 2005) or CXCL4 with CCL5 (von Hundelshausen 2005). There are two types of interactions between CC and CXC chemokines, the CC-type and the CXC-type. In the CC-type the N-termini from two monomer subunits are involved in the interaction forming a small  $\beta$ -sheet (Sticht 1999). In the CXC type, the first  $\beta$ -strand from each monomer subunit interacts with the first  $\beta$ -sheet of the other monomer subunit in an extended six-stranded  $\beta$ -sheet domain (Clore 1995).

Chemokines also form robust interactions with GAGs (glycosaminoglycan) of the extracellular matrix and endothelial cell (Kuschert 1999). There are several classes of GAGs, the most ubiquitous being HS (heparan sulfate), a polysaccharide that is expressed on virtually every cell in the body and comprises 50–90% of total endothelial proteoglycans (Proudfoot 2006). Other classes of GAGs include heparin, which is produced almost exclusively by mast cells and has been exploited therapeutically as an anticoagulant, chondroitin sulfate and dermatan sulfate, which, like HS, are found on cell surfaces and the extracellular matrix, keratan sulfate and hyaluronic acid, which have important supportive skeleton functions. A common feature of GAGs is their overall negative charge due to the sulfate and carboxylate groups, which suggests an electrostatic interaction with cationic basic proteins, such as chemokines. However, while the driving force for binding is principally electrostatic, this interaction is not only based on overall charge interactions, because also acidic chemokines like CCL3 or CCL4 interact with GAGs (Kuschert 1999).

A common heparin-binding motif for several chemokines has been described as a classical BBXB motif, where B represents a basic amino acid residue, on the 40s loop for example for CCL5, CCL3 and CCL4 (Proudfoot 2006). GAG binding is a prerequisite of chemokine activity *in vivo* because of the creation of a high local concentration of chemokines by retention on the luminal lining of the vessel. Without this tethering mechanism, chemokine accumulation would be hampered by diffusion, especially under flow conditions, diluted to a concentration below the threshold required for binding, and distributed uniformly throughout the vasculature. Thus no localized chemotactic signal would be generated for leukocytes to follow. GAGs, that are present on the cell surface, facilitate also oligomerization of chemokines to enhance luminal presentation (Hoogewerf 1997). Furthermore, it has been shown that chemokines with mutations in the GAG binding site lose their ability to recruit monocytes *in vivo*, even though the chemotactic

activity *in vitro* is retained (Proudfoot 2003). This demonstrates that interaction with GAGs *in vivo* is essential, and further show that GAG interaction and oligomerization are closely linked features of chemokines.

## **I.4 Chemokine receptors**

Chemokines act through rhodopsin-like, class A, seven-transmembrane-domain (7TMD), G-protein coupled receptors (GPCR). These chemokine receptors are part of a much bigger superfamily of G-protein coupled receptors that include receptors for hormones, neurotransmitters, paracrine substances, inflammatory mediators, certain proteinases, pheromones, taste, odorant molecules, and even photons and calcium ions (Murdoch 2000).

According to their ligands (e.g. CXC-, CC-chemokine) that they bind, chemokine receptors are classified into 4 groups, CXCR, CCR, XCR and CX3CR. Up to date 7 CXCR, 10 CCR, 1 XCR and CX3CR receptor family members are known. Each chemokine receptor has distinct chemokine specificity, but the specificities can overlap considerably, because many chemokines can bind multiple receptor subtypes, and many receptors can bind multiple chemokines (Murphy 2000). Nevertheless, binding of CC-chemokine receptors is restricted to CC-chemokines and the same holds true for CXC-chemokine receptors.

The receptors have a length of 320-370 amino acids (aa) and show a 25-80% aa sequence identity, indicating a common ancestor. Moreover they share some common features including an acidic extracellular N-terminal segment with tyrosine sulfation motif, a 7  $\alpha$ -helical transmembrane domain with 3 intracellular and 3 extracellular connecting loops composed of hydrophilic amino acids that are oriented perpendicularly to the plasma membrane. Highly conserved cysteines in extracellular loops 1 and 2 are linked by a disulfide bond. The sequence DRYLAIVHA, or slight variations, in the second intracellular loop as well as a basic third intracellular loop and a cysteine in each of the four extracellular domains are also present in all the receptors. The intracellular C-terminal segment is rich with serine and threonine residues (Fig.I.4) (Murphy 2000).

Chemokine GPCRs carry out three fundamental parts of the chemokine-induced “cellular reflex”: message acquisition, semantic extraction (decoding), and initiation of cell responses (Rot 2004). Sequence analysis of the chemokine receptors shows high homology, except for the N-terminal and C-terminal residues. Low sequence homology among the receptor N-terminal residues suggests that the N-domain is involved in ligand



binding, and play a direct role in mediating ligand specificity whereas the cytoplasmic C-terminal tail contains serine and threonine residues as potential phosphorylation sites, which are important for the regulation of the receptor activity. The ligand-receptor interaction is based on a general two-site mechanism model. Binding involves interactions between the ligand N-loop and receptor N-domain (site-I), and ligand N-terminal and receptor exoloop residues (site-II) (Rajagopalan 2006).

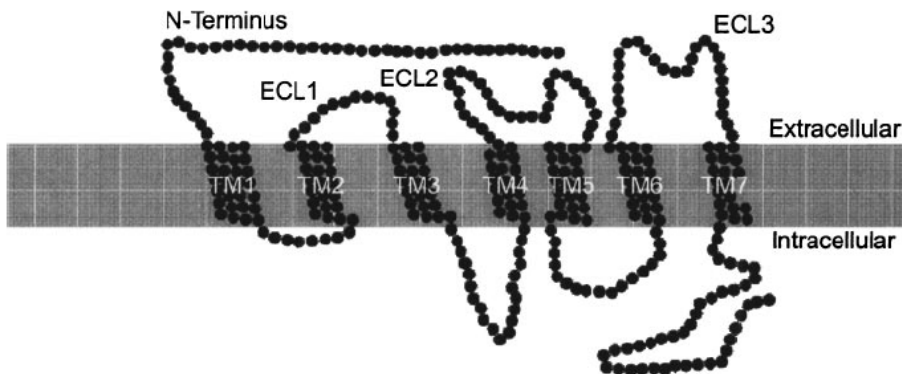


**Fig.I.4: Topology of a typical chemokine receptor.** A G-protein coupled receptor is composed of an extracellular N-terminus followed by sequential changes of the intracellular loops and extracellular loops (ECL1-3) which are connected by the hydrophobic transmembrane domains (TM1-TM7) embedded in the bilayer of the cell surface, ending with an intracellular C-terminal tail (Fernandez 2002).

After agonist binding, GPCRs expose intracellular sites involved in the interaction with the G-protein heterotrimer, which contains  $\alpha$ ,  $\beta$  and  $\gamma$  subunits. This catalyses the dissociation of GDP bound to the  $G\alpha$  subunit and its replacement with GTP, and leads to dissociation of  $G\alpha$  from  $G\beta\gamma$  subunits. Chemokine receptors can be coupled to several different  $G\alpha$  isoforms. Both  $\alpha$ -GTP subunits and  $G\beta\gamma$  subunit complexes then stimulate several downstream effectors. For example chemokines that mediate signals through the pertussis toxin-sensitive  $G_{i1}$  proteins activate the phosphoinositide-3 kinases (PI3K), which then leads to generation of phosphatidylinositol-3,4,5-trisphosphate (PIP3), which then further activates other signal transduction component that results finally in chemotaxis (Rot 2004). Other downstream signaling molecules are for example, phospholipase C (PLC), phosphatidylinositol bisphosphates (PIP2), inositol triphosphate (IP3) and protein kinase C (PKC) that results in the MAPK cascade activation cascades that regulates the nuclear expression of growth-promoting genes. Ultimately, the G-protein-coupling specificity of each receptor determines the nature of its downstream signaling targets (Dorsam 2007).

The simultaneous presence of two different chemokines can induce homo- or

heteromerization of the receptors. In the case of heteromerization, distinct signaling can be triggered through another G protein subunit (Rodríguez-Frade 2001).

#### **I.4.1 Alternative signaling mechanism**

An outside-in signaling of chemokines can be mediated also by binding to sulfated sugars of the GAG family, such as heparan sulfate and chondroitin sulfate on the surface of cells. For example, CCL5 signals in HeLa-CD4 cells that express GAGs and are completely devoid of GPCRs, but does not signal in mutant cells that lack GAGs (Chang 2002). This GPCR-independent signal was mediated by GAG-decorated CD44 (Roscic-Mrkic 2003). CXCL4 may also signal through chondroitin sulfate-decorated membrane molecules on neutrophils, monocytes, and lymphocytes (Brandt 2000). GAGs on a target cell membrane may also influence chemokine signals by another mechanism, for example by facilitating GAG bound chemokines the presentation to their GPCRs in cis by GAG binding-induced changes in their secondary structure.

### **I.5 Platelets**

Platelets are small, 2-3  $\mu\text{m}$  in diameter, anuclear megakaryocyte-derived cells that lack genomic DNA but contain megakaryocyte-derived messenger RNA (mRNA) and the translational machinery needed for protein synthesis. Pre-mRNA splicing, a typical nuclear function, has been detected in the cytoplasm of platelets and the platelet transcriptome contains approximately 3000 to 6000 transcripts. After leaving the bone marrow, platelets circulate in the blood system for about 10 days (Davi 2007). Platelets play an important role in thrombosis and hemostasis. Mature platelets patrol through the circulation in an inactive state and are cleared after 8-10 days by macrophages in the spleen and liver (Von Hundelshausen 2008). Their contact with macromolecules, such as von Willebrand factor (VWF) and subendothelial extracellular matrix proteins (ECMs), of the injured vessel wall or constituents of a ruptured atherosclerotic plaque entails activation, aggregation, and adhesion through various receptors (Varga-Szabo 2008). While these events help to prevent blood loss in the case of injury, they are the initial steps of thrombus formation and can induce acute arterial occlusion. Receptors on the platelet surface are the initiators of activation signaling and subsequent platelet activities. Most of the platelet-activating signals rely on the binding of agonists to G-protein coupled receptors (Offermanns 2006).

After platelet activation multiple cellular responses are mediated, including the release of granule contents and formation of microparticles. A considerable portion of the secretory proteins and ingredients are multiple chemokines that are stored in the  $\alpha$ -granules (von Hundelshausen 2007). These products play an important role in the protective hemostasis as well as in the pathologic thrombus formation (Jennings 2009). For the many platelet-derived substances, chemokines are an especially intriguing family of proteins that are stored in their  $\alpha$ -granules and exert numerous biological activities (von Hundelshausen 2007). A variety of chemokines has been found to be expressed by platelets (Table 1) share characteristic chemophysical properties, e.g. a positive charge and high affinity for negatively charged glycosaminoglycans which enables their retention on the surface of endothelial cells even in the presence of shear forces (Baltus 2005). They are involved in the adhesion and transmigration of monocytes, PMN (polymorphonuclear cells), and bone marrow derived progenitor cells in the vessel wall. In addition they participate in the process of forming and extending atherosclerotic plaques (Davi and Patrono 2007). Among them, the most abundant are CXCL4 (PF4), CXCL7 (CTAP-III), CCL5 (RANTES), and CXCL-12 (SDF-1). Platelet chemokines do not form only homo-aggregates, but also heterophilic interactions occur, which leads to significant modulation of their biological activities (Weber and Koenen 2006).

Tab.1: Chemokines known to be stored in platelets.

<b>Chemokine</b>	<b>Alternative name</b>	<b>Receptor</b>	<b>System</b>
CXCL1	GRO- $\alpha$	CXCR2, CXCR1	human
CXCL4	PF4	GAG, CXCR3B	human, mouse
CXCL4L1	PF4alt	Unknown	human
CXCL5	ENA-78	CXCR2	human
CXCL7	PBP, CTAPIII NAP-2, $\beta$ -TG	CXCR2	human
CXCL8	IL-8	CXCR1, CXCR2	human
CXCL12	SDF-1 $\alpha$	CXCR4	human, mouse
CCL2	MCP-1	CCR2	human, mouse

<b>Chemokine</b>	<b>Alternative name</b>	<b>Receptor</b>	<b>System</b>
CCL3	MIP-1 $\alpha$	CCR1	Human
CCL5	RANTES	CCR1, CCR3, CCR4, CCR5	human, mouse
CCL17	TARC	CCR4, CCR8	human

## **I.6 Platelet-derived chemokines CXCL4, CXCL4L1 and CCL5**

### **I.6.1 CXCL4**

Platelet factor 4 (PF4) or CXCL4 is an abundant platelet  $\alpha$ -granule protein that is a founding member of the CXC chemokine family. CXCL4 was one of the first chemokines to be discovered (Deuel 1977). For a certain time, CXCL4 expression and storage was solely believed to occur in megakaryocytes and the  $\alpha$ -granules in platelets. Expression has also been shown in other different cell types including monocytes, T cells, neutrophils and smooth muscle cells (Lasagni 2007). The human CXCL4 gene encodes a protein of 70 amino acids and is located on chromosome 4q13.3 (Zlotnik 2006). Although CXCL4 was the first chemokine that was isolated, unlike other chemokines, it may not have a clear role in inflammation, since it does not behave like a “classic” chemokine exerting no significant chemotactical properties on immune cells. And also unlike most CXC-chemokines, CXCL4 does not contain an N-terminal Glu-Leu-Arg (ELR) motif, which is critical for the activation of the chemokine receptor CXCR2 and for the promotion of angiogenesis (Strieter 1995). Only at concentrations several orders of magnitude higher than those of other prototypic members of this family, e.g. CXCL8 (interleukin 8, IL-8) CXCL4 has chemotactic and functional priming activity on neutrophils (Petersen 1998). Despite its relative impotence as a chemotaxin, CXCL4 has pleiotropic activities. The most salient feature of this abundant protein (20 mg/10<sup>9</sup> platelets) is its high affinity for the anionic heparin ( $K_d$  4.4 nM) (Dudek 1997), which can lead to HIT (heparin induced thrombocytopenia), an immune mediated reaction in which auto-antibodies against a complex of heparin and CXCL4 activate platelets. This could lead to a reduction of circulating platelet counts and is recognized as a risk factor for thromboembolic complications. The interaction between heparin and CXCL4 is not based on unspecific surface charges but on specific interactions between the positively charged amino acid

residues of CXCL4 (arginine, lysines at the C-terminal region) and the negatively charged sulfate group of the heparin polymer. CXCL4 mainly exists in solution as a tetramer (Mayo 1995).

Along with a number of related (e.g. CXCL8) and unrelated chemokines (e.g. CXCL10) it has been reported to inhibit proliferation of early committed hematopoietic progenitors at concentrations in the low nanomolar range *in vitro* (Dudek 2003). It is known that this cationic chemokine exhibits a strong antiangiogenic activity *in vitro* (Maione 1990) and *in vivo* (Hagedorn 2001). It suppresses growth of various tumors and metastases *in vivo* (Tanaka 1997). This effect is related to their antiangiogenic action and not to tumor cell proliferation (Bello 2002). Although CXCL4 is one of the first agents discovered to have an antiangiogenic action in *ex vivo* systems (Maione 1990), the specific receptor-related mechanisms that transduce the antiangiogenic signal of CXCL4 are still poorly understood. Recently it has been shown that CXCL4 binds also to integrins ( $\alpha v\beta 3$ ,  $\alpha v\beta 5$  and  $\alpha 5\beta 1$ ). This interaction had inhibitory as well as enhanced effects on integrin-dependent endothelial cell migration. Soluble CXCL4 mediated the inhibition of cell adhesion and migration, whereas immobilized CXCL4 promoted cell migration and sprouting (Aidoudi 2008).

Unlike virtually every other member of the chemokine family, a G protein-coupled receptor for CXCL4 analogous to the other well-defined CXC and CC chemokine receptors has yet to be characterized (Murdoch 2000). There has been a single report that CXCL4 binds to CXCR3B, an alternatively spliced product from the *CXCR3* gene (Lasagni 2003). CXCR3B is 52 amino acid residues longer at its N-terminus compared with the previously recognized form, now termed CXCR3A. Unlike CXCR3A, which bound its agonists CXCL9, CXCL10, and CXCL11 exclusively, CXCR3B bound CXCL4 as well. The high affinity of CXCL4 to CXCR3B with a  $K_d$  of about 4 nM, which was comparable to its other described ligands, suggested that CXCL4 may be a natural ligand for this receptor. Furthermore they showed that the activation of CXCR3A was G $\alpha_i$  protein coupled, which is pertussis toxin-sensitive and activates cellular proliferation, by contrast the activation of CXCR3B was carried out by bound G $\alpha_s$  protein, which was pertussis toxin-resistant and led to cellular apoptosis via formation of cAMP and activation of PKA. Nevertheless the biological relevance of this single observation is still not clear.

It has been shown that CXCL4 mediates signaling via binding to the GAG chondroitin sulfate (Petersen 1998). Another study has shown that CXCL4 binds via GAG to the (low-

density lipoprotein) LDL receptor and disrupts the endocytosis of LDL, which results in retention on the cell surface (Sachais 2002). Also, CXCL4 mediates endothelial cell response and negative regulation of megakaryopoiesis via LDL receptor related protein 1 (Lambert 2009).

However, binding to biochemically and functionally different receptors may constitute the molecular basis for the heterogeneity of CXCL4 functions on various cell types. CXCL4 is therefore notable among the chemokines by virtue of its abundance, lack of potency to influence leukocyte function, and absence of a clearly defined high-affinity receptor.

Platelets play an important role in thrombus formation. As CXCL4 is one of the most abundant proteins released during platelet plug formation, it exhibits both pro- and antithrombotic *in vitro* effects, depending on the context. Prothrombotic effects are exerted by binding to heparin and heparin-like molecules and thereby preventing the activation of antithrombin (AT) or by inhibiting the activation of FXII of the intrinsic pathway of thrombus formation (Sachais 2004). Recently, it has been reported that CXCL4 inhibits the anticoagulant function of activated protein C (APC) (Preston 2009). Contrary to that, the antithrombotic effect was shown by the enhancement of the activation of the activated protein C (APC) complex (Slungaard 2003). Here, CXCL4 binds and stimulates the cofactor activity of thrombomodulin (TM), an endothelial cell surface glycoprotein that binds thrombin and promotes the activation of protein C which restrains thrombin production and thrombus growth. The ability of CXCL4 to accelerate the activation of protein C by purified thrombomodulin (TM) is dependent on the presence of TM-associated GAG (Dudek 1997). Mouse *Cxcl4* knock out (*Cxcl4* *-/-*) and human CXCL4 overexpression in mice studies revealed no detectable phenotypes in steady-state. But in the ferric chloride (FeCl<sub>3</sub>) carotid artery injury model of thrombosis they showed a defect in the formation of occlusive thrombi compared with wild-type controls (Eslin 2004).

Angiogenesis is another field where CXCL4 has an important role. CXCL4 was one of the first antiangiogenic agents discovered, inhibiting endothelial cell growth *in vitro* and preventing blood vessel proliferation in the chicken chorioallantoic membrane system in a dose dependent manner (Maione 1990). By binding to bFGF (basic fibroblast growth factor), CXCL4 inhibits their activating effect on endothelial cells. The mitogenic activity of bFGF requires interactions with both a high affinity receptor and a cell-surface heparan sulfate proteoglycan as co-receptor. The interaction with heparan sulfate and therefore the activity of bFGF is inhibited by CXCL4 (Watson 1994). This in turn inhibits its binding to

FGFR-1 (fibroblast growth factor receptor-1) and subsequent dimerization, which is responsible for receptor activation and internalization (Perollet 1998). In the same manner the VEGF (vascular endothelial growth factor) activity is inhibited by CXCL4 (Jouan 1999). The heparan sulfate proteoglycan-dependent binding of VEGF to its receptors VEGFR1-3 (Stuttfeld 2009), which belong to the platelet-derived growth factor tyrosine kinase family of receptors is blocked by CXCL4. The receptor binding of the shorter VEGF isoform with 121 residues, which lacks the heparin binding capacity, is not influenced by CXCL4 (Sachais 2004).

Both of the above angiogenesis inhibitory systems are heparin dependent and require high concentrations of CXCL4 ( $\sim 10 \mu\text{M}$ ). This coincides with the reports that the lysine rich C-terminus region of CXCL4 (residue 47-70) is involved in the interaction of heparin and heparin-binding proteins VEGF and bFGF (Ragona 2009).

Multiple studies displayed the important role of platelet-derived chemokines in promoting atherosclerotic lesion formation. Chemokines (e.g. CXCL4, CCL5) from activated platelets are delivered to endothelial cell and leukocytes in the atherosclerotic plaques where they contribute to the exacerbation of atherosclerosis (Huo 2003). A study using carotid endarterectomy specimens from 132 consecutive patients with critical carotid stenosis revealed colocalization of CXCL4 with endothelial cell and plaque macrophages (Pitsilos 2003). A causal role of CXCL4 in atherogenesis was also suggested by reduced lesion sizes in CXCL4-deficient *ApoE*<sup>-/-</sup> mice (Sachais 2007). One of the important insights of CXCL4 which could enhance atherosclerosis is its ability to bind the LDL (low-density lipoprotein) receptor via GAG which enables the inhibition of LDL binding. Also the LDL that bound in the presence of CXCL4 was neither rapidly internalized nor degraded, but remained in clusters on the cell surface that also contained the LDL receptor, a process that could promote the formation of oxidized LDL (ox-LDL) (Sachais 2002). Furthermore, it was shown that CXCL4 could bind oxidized LDL (ox-LDL), but not native LDL, thereby promoting the binding of ox-LDL to endothelial cells, smooth muscle cells, and macrophages, and causing a ten fold increase in the esterification of ox-LDL (Nassar 2003).

Heterodimerization dramatically modulates the biological activities of these chemokines. For example, the formation of CXCL8-CXCL4-heterodimers increases the anti-proliferative activity of CXCL4 against endothelial cells (Nesmelova 2005). The co-presence of CXCL4 and CXCL8, in turn, attenuates the CXCL8-mediated rise in

intracellular calcium in a myeloid progenitor cell line and enhances CXCL8-induced migration of bone marrow-derived pro-B-cells (Baf/3) (Dudek 2003).

It has been reported that CXCL4 homodimerization is electrostatically unfavorable because of the proximity of positively charged residues (histidine-35, lysine-46, lysine-61, lysine-65, lysine-31) which oppose each other at the homodimer interface. In contrast to CXCL4, electrostatic interactions for CXCL8 homodimer formation are favorable. For CXCL4/CXCL8 heterodimer formation, there are significant changes in energetic contributions. Although heterodimerization for CXCL8 energetically, is unfavorable compared to homodimerization, due to the excess of CXCL4 concentration CXCL4/CXCL8 heterodimers are formed. These highly favorable associations drive CXCL4 tetramer to disrupt and more likely to form a heterodimer with CXCL8 (Nesmelova 2008).

## **I.6.2 CXCL4L1**

CXCL4L1 is a non-allelic variant of CXCL4 and a good feature of increasing the biological diversification of the human chemokine family by gene duplication. Unlike CXCL4, there has been no evidence of existence of murine orthologue, suggesting that the gene duplication occurred after the divergence of the two species (Eisman 1990).

Although the gene had been cloned in the 1989/90 separately by 2 different groups and named PF4var1 (variant1) (Green 1989) and PF4alt (alternative) (Eisman 1990), the mature protein was isolated from thrombin-activated human platelets only recently by Struyf et al (2004). Like CXCL4 the human CXCL4L1 gene is located on chromosome 4q13.3 (Zlotnik 2006). Compared with CXCL4, CXCL4L1 has 14% DNA and 38% amino acid divergence in the signal peptide region, and 2.6% DNA and 4.3% amino acid divergence in the coding region of the mature protein.

The mature protein has, also a length of 70 amino acids but contains three amino acid substitutions (proline 58 → leucine, lysine 66 → glutamic acid and leucine 67 → histidine) near the C-terminus. The latter two substitutions interrupt the alternating dibasic/dihydrophobic repeat found at the C-terminus of CXCL4, which is thought to be critical for high affinity binding to heparin-like molecules (Eisman 1990).

CXCL4L1 compared with CXCL4 has been demonstrated to be a much stronger inhibitor of bFGF-induced endothelial cell chemotaxis (at least 10-fold) *in vitro* and more effective in blocking angiogenesis *in vivo* using the rat cornea micropocket assay (Struyf 2004).



These angiostatic effects, like CXCL4 were based on the inhibition of the angiogenic factors CXCL8 and bFGF. Further, using several animal tumor models it has been shown that the angiogenesis inhibition by CXCL4L1 leads to prevention of tumor metastasis development (Struyf 2007).

Interestingly, CXCL4L1 has been found in other cell types and been shown to be secreted via alternative pathways (Lasagni 2007). Here, the authors showed that CXCL4 is predominantly expressed, stored and secreted by the regulated secretory pathway, whereas CXCL4L1 is synthesized continuously and secreted by the constitutive secretory pathway. Further, mRNA of CXCL4 appeared to be expressed more in almost all cells types (platelets, T cells, monocytes, endothelial cells) except in smooth muscle cells, where CXCL4L1 expression dominated. A possible reason could be the regulation and maintenance of vascular homeostasis and to avoid endothelial cell proliferation and aberrant angiogenesis.

So far, no receptor for CXCL4L1 has been identified.

### **1.6.3 CCL5**

CCL5 (regulated on activation, normal T cell expressed and secreted, RANTES) is a 7.852 kDa and 68 amino acid long chemokine belonging to the  $\beta$  family. In search of T cell-specific genes, the coding sequence of CCL5 had been found in a subtracted cDNA library isolated from a functional, antigen-stimulated T-cell line (Schall 1988). The gene coding for CCL5 was located on the chromosome 17q12 (Zlotnik 2006). It became apparent that CCL5 was not only expressed by T cells through the discovery of a protein with chemotactic activity present in the supernatant of thrombin-stimulated platelets which could be identified as CCL5 (Kameyoshi 1992). CCL5 was detected for the first time in the  $\alpha$ -granules of human platelets by immunocytochemistry (Klinger 1995). Since then it became clear that many more cell types, such as fibroblasts, epithelial cells, and mesangial cells, express this pro-inflammatory molecule after activation with stimuli like IFN- $\gamma$  and TNF- $\alpha$ . CCL5 is a potent chemoattractant for monocytes, T cells and eosinophilic granulocytes and beyond that exerts a less pleiotropic activity than CXCL4 (Schall 1990). The quaternary structure of CCL5 as a typical CC-chemokine is very different from that of the CXC chemokines since dimer formation occurs mainly at the mobile N-terminal regions, whereas CXC-dimers are assembled by the extension of their antiparallel beta-sheet domains (Nesmelova 2005).

CCL5 binds to the G-protein coupled receptors CCR1, CCR3, CCR4 and CCR5. The first CC chemokine receptor cloned turned out to be the receptor for CCL5 (Neote 1993), and was designated CCR1 according to the receptor nomenclature system (Murphy 2000). Other receptors for CCL5 have been reported to be CCR3 and CCR4, which cause selective chemotaxis of eosinophils and basophils (Combadiere 1995). The last cloned chemokine receptor for CCL5 was designated CCR5 (Raport 1996). CCR1 and CCR5 mediate differential functions, as CCL5-induced arrest of lymphocytes and monocytes is mediated by CCR1, whereas CCR5 is rather responsible for leukocyte transmigration (Weber 2001).

Like CXCL4, CCL5 can also bind to GAGs. Here the interaction is based on the positively charged basic amino acid residues 44-47 in the first loop of CCL5 with the negatively charged sulfate group of heparin and exhibits a  $K_d$  of 32.1 nM (Martin 2001). Mutation of this region of CCL5 showed a decreased binding ability to heparin and a loss of chemotactic activity, which is induced via CCR1 (Proudfoot 2001).

CCL5 deposition by activated platelets on atherosclerotic or inflamed endothelium triggers the arrest of monocytes (von Hundelshausen 2001). In addition CXCL4 enhances the monocyte arrest by forming heterodimers with CCL5 (von Hundelshausen 2005).

## I.7 Aims of the study

Platelets play an important role in the progression of atherosclerosis. It has been shown that platelet derived chemokines interact together and exacerbate lesion formation. CCL5 induced monocyte arrest was enhanced by heterodimerization with CXCL4. Further for the non-allelic CXCL4 variant CXCL4L1, also present in platelets, a more angiostatic effect had been reported.

To shed light into these interactions and to characterize the CXCL4L1 chemokine further, a strategy for the expression and purification of the platelet derived chemokines CCL5, CXCL4 and CXCL4L1 was developed.

First, CCL5 was expressed in *E. coli* in LB and <sup>15</sup>N-isotope enriched media purified by FLPC and the heterodimer formation with CXCL4 was investigated.

Second, CXCL4 and CXCL4L1 were expressed in *E. coli* and purified using FPLC and HPLC methods.

Further the CXCL4L1 was characterized by functional comparison with CXCL4.

While CXCL4 has been intensively studied, its non-allelic variant CXCL4L1 has only been recently discovered and data of its function and structure are scarce. Therefore, the aim of this study was to characterize this protein with regard to its structural and functional properties. A strategy for protein generation had to be developed. Then the proper assays to investigate oligomerization, chemotactic and anti-angiogenic properties in comparison with CXCL4 were performed.

## II Material and methods

All solutions were prepared with Millipore water (Milli-Q Plus ultrapure purification, Millipore, Billerica, USA). Protocols were adapted from standard protocols (Sambrook 2001) if not stated otherwise. All reagents were of analytical grade and purchased from major chemical suppliers such as Sigma-Aldrich (Steinheim, Germany), Carl Roth (Karlsruhe, Germany), Merck (Darmstadt, Germany) and Fluka (Buchs, Switzerland) unless otherwise stated in the text.

### II.1 General equipment

autoclave	Systec 2540EL (Systec, Wetzlar, Germany)
balance	Analytical Plus, (Ohaus, Pine Brook, USA)
centrifuges	Eppendorf 5417C (Eppendorf, Hamburg, Germany), Heraeus Labofuge 400 and Heraeus Multifuge 3 S-R (Heraeus, Osterode, Germany), Beckman Avanti J 30 I (Beckman Coulter, Krefeld, Germany)
electroporator	Gene-pulser II (Bio-Rad, Hercules, USA), Nucleofector device (Amaxa, Cologne, Germany)
flow cytometers	FACSCantoII (BD Biosciences, San Jose, CA, USA)
fluorescence	Microplate reader SpectraFluor Plus (Tecan, Crailsheim, Germany)  LS 55 Fluorescence Spectrometer (PerkinElmer, USA)
FPLC system	Äkta FPLC ( Amersham/GE Healthcare, Uppsala, Sweden)
gel electrophoresis	Mini-sub cell GT (Bio-Rad, Hercules, USA)

HPLC system	Spectra System SCM (Thermo Electron Corp., Thermo Scientific, Waltham, USA), Varion Prostar HPLC System (Varian Inc., Palo Alto, USA), Waters Delta Prep 3000 HPLC System (Waters Corp., Milford, USA)
image reader	LAS 3000 (Fujifilm, Düsseldorf, Germany)
incubator	Innova 4230 (New Brunswick Scientific, USA)
laminar flow hood	Herasafe (Heraeus, Osterode, Germany)
lyophilisator	Alpha 2-4 LD plus (Christ, Osterode, Germany)
microscopes	Olympus IX71, IX50, IX51 (Olympus Optical, Hamburg, Germany)
PCR thermocyclers	MyCycler (Bio-Rad, Hercules, USA)
pH-meter	InoLab level 1 (WTW, Weilheim, Germany)
sonicator	Branson S-250 D Digital Sonifier (Branson, Danbury, USA)
spectrophotometer	GeneQuant (Amersham/GE Healthcare, Uppsala, Sweden), NanoDrop 1000 (PeqLab, Erlangen, Germany)

## II.2 Molecular biology

### II.2.1 General work with *E. coli*

*E. coli* strains were cultured in LB medium at 37°C with vigorous shaking. For growth on solid media, a bacteria suspension was spread on a LB agar plate or a single bacteria colony was inoculated to achieve single colony growth. The LB plates were incubated inverted overnight at 37°C. For culturing of bacteria transformed with a plasmid conferring antibiotic resistance, growth medium was supplemented with the appropriate antibiotic. For long-term storage of bacteria at -80°C, LB medium containing the corresponding

antibiotics was supplemented with glycerol to a final concentration of 25% (v/v). All solutions used for bacteria work were autoclaved or filter-sterilized.

***Bacteria growth media***

Bacteria growth medium was autoclaved for 20 min at 121°C. LB agar medium was allowed to cool to 50°C before addition of antibiotics.

LB medium:	0.5% (w/v) yeast extract
	1% (w/v) peptone
	1% (w/v) NaCl
LB agar medium:	LB medium with 1.4% (w/v) agar
TB medium	1.2% (w/v) peptone
	2.4% (w/v) yeast extract
	0.4% (v/v) glycerol

***Preparation of heat-shock competent E. coli***

*E. coli* cells were inoculated in 5 mL LB medium and incubated overnight at 37°C with vigorous shaking. Then 100 mL LB medium were incubated with 750 µL of the overnight culture for 1 to 2 h at 37°C until the optical density at 600 nm (OD<sub>600</sub>) was approximately 0.4, indicating the early exponential growth phase. OD<sub>600</sub> was measured in a spectrophotometer with pure medium as reference. The culture was centrifuged (10 min/ 3000 g/ 4°C), and the pellet was resuspended in 10 mL ice-cold TSS buffer. 500 µL aliquots were frozen immediately in liquid nitrogen and stored at -80°C.

TSS buffer:	10% (w/v) polyethyleneglycol (PEG) 8000 (Promega)
	5% (v/v) DMSO
	20 mM MgCl <sub>2</sub>
	in 1x LB medium (II.2.1)

***Heat-shock transformation of competent E. coli***

100  $\mu$ l thawed competent *E. coli* were gently mixed with 1-10 ng of plasmid DNA (see II.2.4.), and incubated for 30 min on ice. The bacteria were heat-shock treated for 45 sec in a 42°C water bath, and then incubated for 2 min on ice. After addition of 500  $\mu$ L LB medium, the bacteria were incubated for 1 h at 37°C with gently shaking. The bacteria were spread on selective LB agar plates and incubated overnight at 37°C.

**II.2.2 Bacterial strains**

DH5 $\alpha$	Invitrogen (Karlsruhe, Germany)
XL1-Blue	Stratagene (La Jolla, USA)
Rosetta (DE3) pLysS	Novagen/Merck Bioscience (Darmstadt, Germany)

**II.2.3 Plasmids**

pET-26+	expression vector containing pelB signal sequence for secretion of the recombinant protein into periplasma (Novagen/Merck Bioscience, Darmstadt, Germany)
pET-26+/CXCL4	CXCL4 expression vector, this study
pET-26+/CXCL4L1	CXCL4L1 expression vector, this study
pET-32a	expression vector containing a thioredoxin tag fused with the recombinant protein (Novagen/Merck, Darmstadt, Germany)
pET-32a/CCL5	CCL5 expression vector, this study

**II.2.4 Polymerase chain reaction**

Polymerase chain reaction (PCR) was used to amplify specific DNA sequences (Saiki 1988). In addition, this method allows the introduction of new cleavage sites for restriction

endonucleases or other modifications (II.2.4) useful for the generation of DNA constructs. Primers with specific sequences were commercially synthesized (Eurofins MWG, Ebersberg, Germany). PCR fragments for cloning purposes were amplified with the high fidelity *Pfu* DNA Polymerase (Promega), which minimizes base misinsertions due to a 3'→5' exonuclease proofreading activity. Annealing temperature was optimized for each primer set based on the primer melting temperature.

PCR reaction: 50-200 ng template DNA  
1x PCR reaction buffer  
0.5 μM forward primer  
0.5 μM reverse primer  
200 μM each of dNTPs (dATP, dCTP, dGTP, dTTP)  
1.3 U DNA polymerase *Pfu* (Stratagene, La Jolla, USA) or *Taq* (Promega, Madison, USA)  
H<sub>2</sub>O to final volume of 50 μl

PCR program	Initial denaturation	95°C, 1 min	} 25-30 cycles
	Denaturation	95°C, 30 sec	
	Annealing	55-65°C, 30 sec	
	Extension	72°C 1-6 min	
	Final extension	72°C 5 min	

### II.2.5 Cloning of CXCL4 and CXCL4L1

The coding region of the CXCL4 cDNA was obtained from ImaGenes (ID Hs.81564 Berlin, Germany) and cloned downstream of the *pelB* signal sequence of the pET-26+ (Merck Biosciences, Darmstadt, Germany) expression vector by PCR (II.2.4) using specific primers:

5'-GTG ATG ACG ACG ACA AGG AAG CTG AAG AAG ATG GGG ACC-3' as forward primer and

5'-ACT CGA GCA GCT AGT AGC TAA CTC TCC AAA AG-3' as backward primer.

The correct CXCL4 ligation in the expression vector was verified by restriction analysis and DNA sequencing (see II.2.11). This pET26+/CXCL4 expression vector served as a template to construct the pET26+/CXCL4L1 expressing vector by using the QuikChange®



Site-Directed Mutagenesis Kit (Stratagene, La Jolla, USA) to replace 3 amino acids (proline-58 to leucine, lysine-66 to glutamic acid and leucine-67 to histidine) at the C-terminus end of the CXCL4. Following primers were used:

5'-CAA GCC CTG CTG TAC AAG AAA ATC ATT AAG GAA CAT TTG GAG AGT TAG C-3' as sense primer and

5'- GCT AAC TCT CCA AAT GTT CCT TAA TGA TTT TCT TGT ACA GCA GGG CTT G-3' as anti-sense primer.

The protocol was performed according to the manufacturer's instructions. The mutagenesis was verified by DNA sequencing (II.2.11) and both expression vectors were each transformed into *E. coli* Rosetta (DE3)-pLysS (Merck Biosciences, Darmstadt, Germany) as described in the section II.2.1.

CXCL4 amino acid sequence

EAEEDGDLQC LCVKTTSQVR PRHITSLEVI KAGPHCPTAQ LIATLKNGRK ICLDLQAPLY KKIHKLLLES

CXCL4L1 amino acid sequence

EAEEDGDLQC LCVKTTSQVR PRHITSLEVI KAGPHCPTAQ LIATLKNGRK ICLDLQAL<sup>L</sup>LY KKIHK<sup>E</sup>HLES

## II.2.6 Miniprep: Small-scale purification of plasmid DNA

Plasmid DNA was purified from a bacteria culture by alkaline lysis as described (Sambrook 2001) mL over night (o.n.) culture was centrifuged (1 min/7000 g/rt) and the pellet was resuspended in 100  $\mu$ L buffer 1. For lysis of the bacteria, 200  $\mu$ L of buffer 2 was added followed by gently mixing and 5 min incubation at rt. The mixture was neutralized by 200  $\mu$ L ice-cold buffer 3, gently mixed, and incubated for 5 min at -20°C. The suspension was spun down (20 min/20000 g/rt) to remove proteins, cell debris and chromosomal DNA. The supernatant with plasmid DNA was transferred to a new eppendorf tube mixed with 500  $\mu$ L isopropanol and centrifuged (20 min/20000 g/rt). The pellet with plasmid DNA was washed with 70% (v/v) ethanol, air dried and resuspended in 50  $\mu$ L 10 mM Tris-HCl, pH 8.5.

Buffer 1:                    50 mM glucose  
                                   25 mM Tris-HCl, pH 8.0

10 mM EDTA, pH 8.0

Buffer 2: 200 mM NaOH

1% (w/v) SDS

Buffer 3: 3 M potassium acetate, pH 5.5

### **II.2.7 Midiprep and maxiprep: Large-scale purification of plasmid DNA**

Large-scale purification of plasmid DNA from bacteria on culture was performed using the Qiagen Plasmid Midi or Maxi Kit™ (Qiagen, Hilden, Germany) according to the manufacturer's instructions.

### **II.2.8 Restriction endonuclease digestion of DNA**

Restriction endonucleases (MBI Fermentas, Ontario, Canada) were used to digest double-stranded DNA for analytical purposes. Restriction endonucleases recognize specific palindromic sequences and cleave a phosphodiester bond at each strand at that sequence. Restriction endonuclease digestion of DNA for analytical purpose was done according to the manufactures instructions. 0.2-1  $\mu\text{g}$  DNA were digested with 5-10 U of the restriction enzyme in a volume of 20  $\mu\text{L}$ . Digests were incubated for 1 h at 37°C or as recommended by the supplier. Reaction buffers were supplied by the manufacturer.

### **II.2.9 Agarose gel electrophoresis**

Separation of DNA fragments from digest was done by agarose gel electrophoresis. The negatively charged DNA fragments migrate towards the anode in an electric field at a rate determined by the size. DNA samples were diluted with DNA loading buffer and separated on a 1-2% (w/v) agarose gel dissolved in TAE electrophoresis buffer containing 0.1  $\mu\text{g}/\text{mL}$  ethidium bromide. After electrophoresis at 120 V, the DNA was visualized on a UV light transilluminator and photographed for documentation.

DNA loading buffer (6x):	30% (v/v) glycerol
	6 mM EDTA
	0.25% (w/v) bromophenol blue
	0.25% (w/v) xylene cyanol
TAE electrophoresis buffer (1x):	40 mM Tris-acetate
	1 mM EDTA

### **II.2.10 Quantification of DNA**

DNA concentration was determined by measuring the absorbance at 260 nm ( $A_{260}$ ) in a spectrophotometer using a quartz cuvette or via NanoDrop ND-1000. For double-stranded DNA an  $A_{260} = 1$  corresponds to 50  $\mu\text{g}$  DNA/mL. The absorbance at 280 nm was also measured to estimate DNA purity. Pure DNA has an  $A_{260}/A_{280}$  ratio of 1.8-2.0 at pH 7.0.

### **II.2.11 Sequencing of DNA**

The sequence of DNA constructs were screened by a commercial sequencing service (Eurofins MWG, Ebersberg, Germany) and the sequence data were verified on the basis of the corresponding electropherogram.

## **II.3 Protein analysis**

### **II.3.1 Protein concentration assay**

The DC Protein Assay (BioRad, Hercules, USA) was used to determine the protein concentration of the fractions. The method is similar to the Lowry Assay (Lowry 1951) and is based on the reaction of proteins with an alkaline copper tartrate solution and folin reagent. The measurement was done according to manufacturer's instruction. Briefly, 5  $\mu\text{L}$  of the fractions and BSA as standard were mixed with 25  $\mu\text{L}$  copper tartrate solution and 200  $\mu\text{L}$  folin reagent. The complexation of the protein with copper tartrate and the following reduction of the folin reagent by the complex were measured at 750nm.

### II.3.2 SDS-polyacrylamide gel electrophoresis (PAGE)

After each purification step the fractions or fraction pools were analyzed by SDS-PAGE (Sodiumdodecylsulfate-polyacrylamide-gel electrophoresis) (Laemmli 1970). SDS binds to polypeptides resulting in a negative charge directly proportional to protein size. Protein samples were first concentrated in a stacking gel before migrating into the resolving gel. Electrophoresis was carried out in a Mini-PROTEAN® 3 cell system (Bio-Rad, Hercules, USA) at 120 V until the bromphenol blue dye front reached the bottom of the gel. The resolving gel was analyzed either by coomassie blue, silver staining or western blotting (II.3.4-6).

Resolving gel	12-15% (w/v) acrylamide/Bis
	375 mM Tris-HCl, pH 8.8
	0.1% (w/v) SDS
	0.1% (w/v) ammonium persulfate
	0.1% (v/v) TEMED
Stacking gel:	5% (w/v) acrylamide/Bis
	125 mM Tris-HCl, pH 6.8
	0.1% (w/v) SDS (sodium-dodecylsulfate)
	0.1% (w/v) ammonium persulfate
	0.1% (v/v) TEMED
Electrophoresis buffer:	250 mM Tris base
	1.92 M glycine
	1% (w/v) SDS

### II.3.3 Tricine gel

For a better resolution of the small proteins (<30kDa) a tricine gel electrophoresis was performed (Schagger 1987). Here the replacement of the tailing glycine ion by a faster tricine ion and the lower pH in the gel buffer results in a sharper band of the small chemokines.

Resolving gel:	16.5% acrylamide/Bis solution 49.5%:3%
	2.67 mL gel buffer
	12.5% glycerol
	0.1% (w/v) ammonium persulfate
	0.1% (v/v) TEMED
Stacking gel:	6% (w/v) acrylamide/Bis solution 49.5%:3%
	1.65 mL gel buffer
	0.1% (w/v) ammonium persulfate
	0.1% (v/v) TEMED
Gel buffer:	3.0 M Tris/HCl pH 8.45
	0.3% (w/v) SDS
Cathode buffer (10x):	1 M Tris/HCl pH 8.25
	1 M Tricine
	1% SDS
Anode buffer (10x):	2 M Tris/HCl pH 8.9

### II.3.4 Coomassie blue staining

The coomassie blue staining of the gels was carried out with PageBlue Protein Staining Solution (MBI Fermentas, Ontario, Canada). They were subsequently destained with a 12.5% (v/v) isopropanol, 30% (v/v) EtOH.

### II.3.5 Silver staining

Silver gel staining was adapted from Blum (Blum 1987). First of all, the proteins in the gel are fixed with solution A at least for 1 h. Then, after 3 x 20 sec washing (solution B) the gel was sensitized for 1 min (solution C). After that the gels were stained for 20 min with solution D containing AgNO<sub>3</sub>. Then the gels were treated with the developing solution E. At the end the reduction reaction is stopped with solution F.

Solution A	50% methanol 12% acetic acid 0.05% formalin
Solution B	50% methanol
Solution C	0.02% (w/v) Na <sub>2</sub> S <sub>2</sub> O <sub>3</sub> x 5 H <sub>2</sub> O
Solution D	0.02% AgNO <sub>3</sub> 0.076% formalin
Solution E	6% Na <sub>2</sub> CO <sub>3</sub> 0.0004% Na <sub>2</sub> S <sub>2</sub> O <sub>3</sub> x 5 H <sub>2</sub> O 0.05% formalin
Solution F	50% methanol 12% acetic acid

### II.3.6 Western blot analysis

Separated proteins from a SDS-PAGE (II.3.2, II.3.3) were transferred to a nitrocellulose membrane and detected using specific primary antibodies and HRP-conjugated secondary antibodies. The proteins were transferred from the gel to the nitrocellulose Hybond membrane (Amersham/GE Healthcare, Uppsala, Sweden), at 90 V for 1 hour in ice-cold blotting buffer. Nonspecific binding sites on the membrane were blocked with 5% (w/v) nonfat milk in TBS for 1 hour at rt. Thereafter, the membrane was incubated with a

primary antibody diluted in blocking buffer for 1 hour at rt or overnight at 4°C. After 3 times washing with TBS/0.05% (v/v) Tween, the membrane was incubated with a HRP-conjugated secondary antibody diluted in TBS for 1 hour at rt or overnight at 4°C. In the presence of hydrogen peroxide (H<sub>2</sub>O<sub>2</sub>) the protein-bound HRP converts luminol to an excited intermediate dianion, which emits light on return to its ground state. This light can be captured by a detector (LAS 3000 Image Reader, Fujifilm, Düsseldorf, Germany).

Blotting buffer (1x)	25 mM Tris base
	192 mM glycine
	10% (v/v) methanol
	0.005% (w/v) SDS

TBS (1x)	25 mM Tris-HCl, pH 7.4
	2.7 mM KCl
	137 mM NaCl

### II.3.7 Dot blot

This technique was used to identify the presence of the proteins in the fractions purified by FPLC in a more rapid approach than a western blot. Fractions were spotted on a nitrocellulose membrane and after drying it was advanced like a western blot after blotting (II.3.6).

### II.3.8 Primary antibody

CXCL4	anti-human-CXCL4 monoclonal antibody, clone MAB7951 (R&D Systems, Minneapolis, USA)
CXCL4L1	anti-CXCL4L1 monoclonal antibody lacking Fc tail, AbD07088.1 (AbD Serotec, Martinsried, Germany) AbD07089.1 AbD07090.1
CXCL4L1-b	AbD07088.1 biotinylated

	AbD07089.1 biotinylated
	AbD07090.1 biotinylated
CCL5	mouse Anti-Human Rantes VL1, RANT100 (Caltag, Burlingame, USA)
CD11b-PE-Cy7	rat anti-mouse mAb, PE-Cy7-conjugated, DC and monocyte marker (clone M1/70, BD Pharmingen)
CD45-APC-Cy7	rat anti-mouse mAb, APC-Cy7-conjugated, leukocyte marker (clone 30-F11, BD Pharmingen)
CD115-PE	rat anti-mouse mAb, PE conjugated, monocyte marker (clone AFS98, eBiosciences)
F4/80-APC	rat anti-mouse mAb, APC-conjugated, mature macrophage marker (clone A3-1, Serotec)
Gr-1-PerCP	rat anti-mouse mAb, PerCP-conjugated, mature granulocyte marker (clone RB6-8C5, BD Pharmingen)

### II.3.9 Secondary antibody

goat-anti-mouse-IgG-HRP	horseradish peroxidase (HRP)-conjugated, sc-2031 (Santa Cruz Biotech, Santa Cruz, USA)
goat-anti-human-IgG-F(ab') <sub>2</sub> -HRP	horseradish peroxidase (HRP)-conjugated anti-F(ab') <sub>2</sub> antibody, Code 0500-0099 (AbD Serotec, Martinsried, Germany)
Streptavidine-HRP	horseradish peroxidase (HRP)-conjugated, 016-030-084 (Jackson ImmunoResearch, West Grove, USA)

## II.4 Protein expression and purification

### II.4.1 CCL5 expression and purification

The CCL5 was expressed as inclusion bodies in the strain *E. coli* Rosetta (DE3)-pLysS using the pET32a+ vector (Novagen/ Merck Bioscience, Darmstadt, Germany). This vector permits the alignment of the desired protein as a fusion protein with thioredoxin, which facilitates the correct folding of the protein and enhances the formation of disulfides in the cytoplasm. The bacteria were grown either in LB or in Spectra-9N medium (Cambridge Isotope Labs, New Jersey, USA) containing <sup>15</sup>N enriched isotope for better metabolic



labeling. In detail, the bacteria were transferred from an overnight plate to 2x 1L prewarmed medium (LB or Spectra-9N) containing 100  $\mu\text{g}/\text{mL}$  carbenicillin as an ampicillin derivate and 40  $\mu\text{g}/\text{mL}$  chloramphenicol. The bacteria were cultivated with shaking at 37°C. At an  $\text{OD}_{600}$  0.6 the CCL5 expression was induced overnight by 1mM IPTG (isopropyl- $\beta$ -D-thiogalactopyranoside).

The bacteria were harvested by centrifugation at 5000 rpm for 10 min. The pellet including the target protein as inclusion bodies was frozen at -20°C until usage.

After thawing the pellet was resuspended in 5 mL/g wet cell weight BugBuster<sup>®</sup> Protein Extraction Reagent (Novagen/Merck Biosciences, Darmstadt, Germany) containing the Benzonase<sup>®</sup> nuclease. Additionally the mixture was sonicated at 50 W for 3x 30 sec until a homogenous lysate was formed. The inclusion bodies were washed 2x with PBS (PAA, Pasching, Austria) to remove membrane debris and detergents. Then the aggregated proteins were denatured in 6 M guanidine hydrochloride (Gnd-HCl) containing 1 mM DTT for about 1 h at 60°C or overnight at room temperature. After denaturation and disaggregation of the inclusion bodies, the protein was purified by several steps using the ÄKTA FPLC System (fast protein liquid chromatography).

## **II.4.2 CCL5 FPLC (fast protein liquid chromatography)**

### ***Sephacryl S-100HR***

The first step of the CCL5 purification involved the gel filtration column Sephacryl S-100HR (Amersham/GE Healthcare, Uppsala, Sweden). The denatured fusion proteins were loaded onto the column and separated according to their masses in 6 M Gnd-HCl, 50 mM Tris pH 8, 1 mM DTT. After verifying the presence of the CCL5/thioredoxin fusion protein in the collected samples (5 mL) by dot blotting, the next step was the refolding in 6x diluted 50 mM Tris pH 8 in presence of 6 mM cysteine and 8 mM cystine as redox partners overnight at 4°C. Then the HiTrap chelating HP loaded with  $\text{Ni}^{2+}$  was used to purify the refolded fusion protein.

### ***HiTrap chelating HP***

The HiTrap chelating HP (Amersham/GE Healthcare, Uppsala, Sweden) column was loaded with  $\text{Ni}^{2+}$  as according the manufacturer's instruction. Before loading the solution onto the column, the precipitations and other non soluble particles were removed by centrifugation (20.000g 30 min) and filtration (0.22  $\mu\text{m}$ , Millipore, Billerica, USA). The protein was

loaded with binding buffer at 2 mL/min and eluted for 10 min with a linear 0-100 % gradient imidazole. 2-3 mL fractions were collected and all protein containing samples were pooled for the enterokinase digestion. The thioredoxin tag was removed from CCL5 by digestion with 1 u per 50  $\mu$ g enterokinase (Novagen/ Merck Bioscience, Darmstadt, Germany) overnight at rt.

Binding buffer	20 mM Tris pH 8
	2 M Urea
Elution buffer	20 mM Tris pH 8
	2 M Urea
	250 mM Imidazole

***MonoS<sup>TM</sup> 5/50 GL***

After digestion, the CCL5 was separated from the thioredoxin tag by the strong cationic MonoS<sup>TM</sup> 5/50 GL column (Amersham/ GE Healthcare, Uppsala, Sweden). The CCL5 was eluted at 1 mL/min using a linear gradient from 0-50% elution buffer and collected at 0.5 mL fractions. The correct size was verified by SDS-PAGE and dot blots.

Binding buffer	50 mM NaAc pH 5.5
	6 M Urea
Elution buffer	50 mM NaAc pH 5.5
	6 M Urea
	2M NaCl

***Resource<sup>TM</sup> Reverse Phase Chromatography (RPC)***

In a last step of the FPLC the desired digested protein was further purified using the RPC (Amersham/GE Healthcare, Uppsala, Sweden). Here CCL5 bound to the polystyrene matrix of the column through hydrophobic interaction and almost all the impurities were removed. The elution was performed with a linear gradient from 0-67% at 1 mL/min. Again 0.5 mL fractions were collected and samples containing the correct protein were

analyzed by SDS-PAGE and western blot.

Binding buffer	0.1% TFA (trifluoroacetic acid)
Elution buffer	0.1% TFA (trifluoroacetic acid)
	90% acetonitrile

### II.4.3 CCL5 HPLC (high performance liquid chromatography)

At the end (polishing step) the recombinant CCL5 was purified by reversed phase-HPLC using a preparative Grace Vydac C-8 column (250 x 10 mm, 5  $\mu$ m, Grace Davison Discovery Sciences, Deerfield, USA). HPLC is a mode of chromatography that involves the separation of a protein via stationary and mobile phases. The stationary phase consists of porous beads containing several adsorbents (here C8 octyl group, non polar), and the mobile phase consists of a binary polar eluent mixture (buffer composition like RPC, sec). The binding between the protein and the C residues of the column is also based on the hydrophobic interaction. Following program was used:

<b>Time (min)</b>	<b>Eluent A (%)</b>	<b>Eluent B (%)</b>	<b>Flow (mL/min)</b>
0	100	0	1
5	100	0	1
35	33	67	1
40	33	67	1
43	0	100	1
53	0	100	1
56	100		1

All collected peaks were frozen in liquid N<sub>2</sub> and lyophilized. The samples were resuspended in H<sub>2</sub>O and the correct size was verified by coomassie blue staining and western blot.

#### II.4.4 CXCL4 and CXCL4L1

The chemokines CXCL4 and CXCL4L1 were expressed in *E. coli* Rosetta (DE3)-pLysS periplasm in a modified hyperosmotic medium previously described by Barth (Barth 2000).

First the bacteria were grown in a preparatory 200 mL TB medium containing kanamycin (50  $\mu\text{g}/\text{mL}$ ), chloramphenicol (50  $\mu\text{g}/\text{mL}$ ) as antibiotics,  $\text{ZnSO}_4$  (0.5  $\mu\text{M}$ ) as protein stabilizer in the periplasm and 2% (w/v) glucose as carbon source at 26°C for 20 h. Then the bacteria were transferred in 2 L fresh TB medium as described above, except sorbitol (0.5 M) instead of glucose as carbon source, then 3% (w/v) NaCl as osmoticum, betaine (40 mM) and BMC (1,2-bis(2-mercaptoacetamido) cyclohexane) (10  $\mu\text{M}$ ) (Woycechowsky 1999) as catalyzers, oxidized glutathione (2 mM) and reduced glutathione (1 mM) as redox additives. After acclimatization in the hyperosmotic medium for 1-2 h the protein expression was induced by 1 mM IPTG (isopropyl- $\beta$ -D-thiogalactopyranoside) overnight at 26°C. Finally the cells were harvested and frozen at -20°C until protein purification.

For the purification of the proteins, the cells were lysed in 5 mL/g cell pellet 5 mM  $\text{MgSO}_4$  containing bacterial complete protease inhibitor cocktail tablets (Roche, Mannheim, Germany). After centrifugation for 30 min at 20.000g the supernatant containing the soluble protein was dialyzed against 50 mM NaAc pH 5.5 and the crude solution was purified by sequential steps using the ÄKTA FPLC System (fast protein liquid chromatography) and the HPLC (high performance liquid chromatography) Spectra System SCM.

#### II.4.5 CXCL4 and CXCL4L1 FPLC

##### *HiLoad 16/10 SP-Sepharose*<sup>TM</sup>

In a first step the cation exchanger column *HiLoad 16/10 SP-Sepharose*<sup>TM</sup> (Amersham/ GE Healthcare, Uppsala, Sweden) was used to remove undesired proteins and contaminants. The filtered (0.22  $\mu\text{m}$ , Millipore, Billerica, USA) protein was loaded at a flow rate of 1-2 mL/min, after about 15 mL of washing with binding buffer the protein was eluted with a linear gradient of 0-100% elution buffer for 20 min. Each fraction was collected in 5 mL.

Binding buffer	50mM NaAc pH 5.5
Elution buffer	50mM NaAc pH 5.5
	2M NaCl

***MonoS™ 5/50 GL or Capto™ S***

In a second step, the protein containing fractions, determined by dot blotting were pooled and the desired protein was dialyzed in the binding buffer of the next column prior to loading for further purification using the stronger cation exchanger MonoS™ 5/50 GL or Capto™ S (Amersham/ GE Healthcare, Uppsala, Sweden). Proteins were filtered again through a 0.22  $\mu\text{m}$  filter to avoid clogging of the column by precipitates and loaded at the flow rate of 1 mL/min and eluted using a gradient 0-100% for 20 min. Each eluted sample was fractionated in 0.5 mL.

Binding buffer	50mM NaAc pH 4.5 or pH 5 for Capto™S
Elution buffer	50mM NaAc pH 4.5 or pH 5 for Capto™S
	2M NaCl

***Resource™ RPC***

After verification of the fractions containing the correct protein by dot blot and SDS-PAGE, the desired fractions were dialyzed 2 x against 1% acetic acid and 1 x against 0.1% TFA. Then in the third step the Resource™ RPC column was used. Here, proteins were bound to the column according to their hydrophobicity and elution was carried out with a linear increase of elution buffer containing the organic solvent acetonitrile in a 0-67 % gradient for 15 min. Each eluted sample was fractionated in 0.5 mL.

Binding buffer	0.1% TFA (trifluoroacetic acid)
Elution buffer	0.1% TFA (trifluoroacetic acid)
	90% acetonitrile

**II.4.6 CXCL4 and CXCL4L1 HPLC**

In a final polishing step the reversed phase-HPLC was performed to purify and enrich the protein. HPLC is a mode of chromatography that involves separation techniques of a protein between stationary and mobile phases. The stationary phase consist of porous beads containing several adsorbents (here C18, octadecyl, non polar), and the mobile phase consists of a binary eluent mixture (here H<sub>2</sub>O and acetonitrile, polar). For this purpose Hypersil Gold column (Thermo Fisher, Waltham, USA) was used. This silica-based column provides C18 like selectivity for separation of hydrophobic as well as ionic

interaction. This dual character enables an excellent peak shape and therefore greater sensitivity. Following elutes for the binary mobile phase and gradient were used:

Buffer

Eluent A 0.1% TFA (trifluoroacetic acid)

Eluent B 0.1% TFA (trifluoroacetic acid)

90% acetonitrile

**Program:**

<b>Time (min)</b>	<b>Eluent A (%)</b>	<b>Eluent B (%)</b>	<b>Flow (mL/min)</b>
0	100	0	1
5	100	0	1
15	65	35	1
25	65	35	1
35	33	67	1
45	33	67	1
50	0	100	1
55	0	100	1
60	100	0	1

#### **II.4.7 Chemical synthesis of CXCL4L1**

##### *Peptide synthesis and native chemical ligation*

The chemical synthesis of CXCL4L1 was carried out in the lab of Prof Tilman Hackeng (Department of Biochemistry, CARIM, Maastricht University) using the so called solid-phase peptide synthesis (SPPS) method. SPPS was invented by R.B. Merrifield in 1963. Here the protein is manually polymerized beginning from the carboxyl terminus (C) of the amino acid to the amino terminus (N). First the C-terminal amino acid is attached

covalently via a linker to solid beads (resin), so that the growing peptide cannot be washed away during coupling steps. Then one side and the reactive side chains of the amino acids have to be protected to prevent self assembly or unwanted branched chains forming. Before assembly of the next amino acid, the N-terminus of the attached amino acid and the C-terminus of the joining amino acid have to be deprotected without affecting the side chain protection. After coupling of the second amino acid to the growing chain the next round of assembly can begin. There are two different groups of side chain protection, Fmoc and t-Boc.

Fmoc stands for 9-Fluorenylmethoxycarbonyl and was introduced by R.C. Sheppard in 1971. Under basic conditions this group is removed from a growing peptide chain (usually 20% piperidine in DMF). Removal of side-chain protecting groups and peptide from the resin is achieved by incubating in TFA.

t-Boc (or Boc) stands for tert-Butyloxycarbonyl. To remove t-Boc from a growing peptide chain, acidic conditions are used (usually TFA). Removal of side-chain protecting groups and the peptide from the resin at the end of the synthesis is achieved by incubating in hydrofluoric acid. For this reason the t-Boc method is generally disfavored.

CXCL4L1 was synthesized by manual solid-phase peptide synthesis using the t-Boc method (Schnolzer 1992) and native chemical ligation (Dawson 1994). Since the SPPS method is limited up to a length of 40-60 residues and the mature CXCL4L1 has a length of 70 amino acids, the synthesis was carried out in two separate steps, N-terminal peptide (1-35 residues) on MPA-L-MBHA resin (mercaptopropionic acid-leucine-methylbenzhydrylamine, Penninsular Lab, Bellemont, USA) and C-terminal peptide (35-70 residues) on MBHA resin (Fig.II.1).

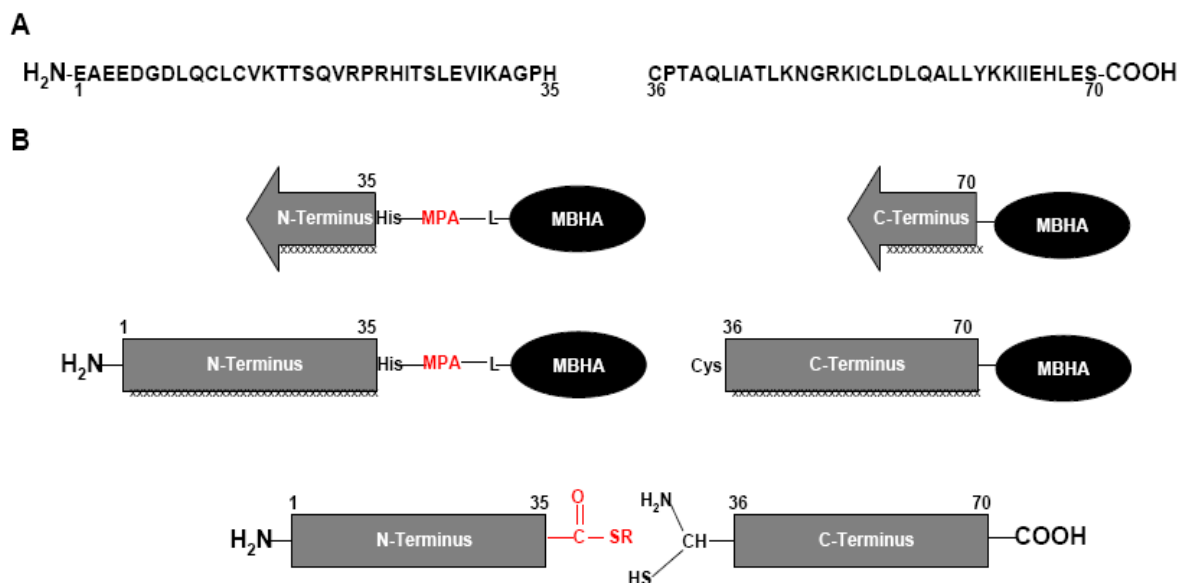


**Fig.II.1: Strategy for the chemical synthesis of human CXCL4L1.** (A) Amino acid sequence of hCXCL4L1 with the native chemical ligation site at His-35 and Cys-36. (B) Stepwise solid phase synthesis of the N-terminal and C-terminal peptides using the t-Boc method. The thioester group derived from MPA (mercaptopropionic acid) is indicated in red.

After that cleavage of both peptides from the resin by 10 mL HF (hydrofluoric acid) and deprotection of the side chains by 4% para-cresol were carried out. Then the peptides were purified by preparative HPLC (II.1) and lyophilized. The peptides were dissolved in 0.1% TFA at an end concentration of 20 mg/mL and the native chemical ligation was performed in presence of 10  $\mu$ L/mL benzylmercaptan and 10  $\mu$ L/mL thiophenol as catalyzers. The native chemical ligation is based on the chemoselective reaction between two unprotected peptides in which the C-terminal thioester undergoes a thiol exchange with the sulfhydryl side chain of the N-terminal cysteine. Thus after 24h incubation at 37°C a rapid, intramolecular rearrangement results in a native peptide bond at the site of the ligation (Fig.II.2).



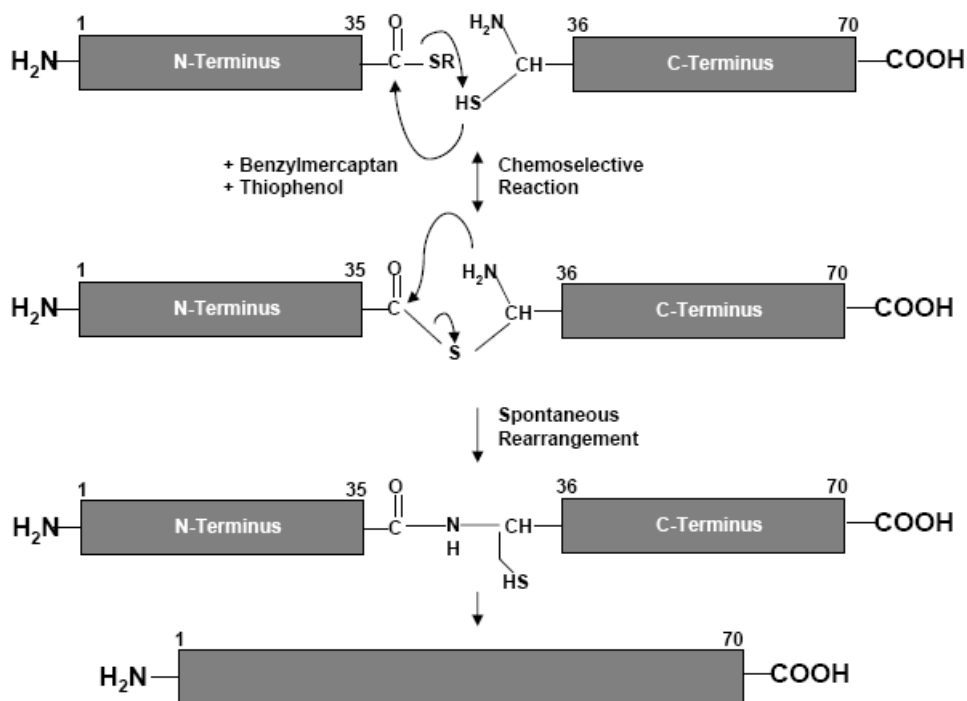


**Fig.II.2:** Native chemical ligation of the two unprotected peptide segments results in a formation of an amide bond. The two segments are initially joined by thioester formation. COSR of the N-terminus undergoes nucleophilic attack by the side chain of Cys-36 of the C-terminus; subsequent spontaneous rapid rearrangement forms a native peptide bond at the ligation site.

The final product was purified by preparative HPLC using a gradient from 0-100 % for 3 h. Each peak collected was controlled by mass spectroscopy for the presence of the protein and lyophilized. Then the protein was refolded at a concentration of 0.1-0.2 mg/mL in 1 M Gnd-HCL pH 8 supplemented with 8 mM cysteine and 1 mM cystine for 24 h at 4°C. At the end the refolded protein was purified again by preparative HPLC.

## II.5 Biochemical analysis of the CCL5-CXCL4 heterodimer

The biochemical analysis was performed in the lab of Dr. Kevin Mayo (Department of Biochemistry, University of Minnesota) and Prof Dr. Andreas Kungl (Department of Pharmaceutical Chemistry, University of Graz). The heterodimerization was characterized by the <sup>15</sup>N-<sup>1</sup>H heteronuclear single quantum coherence (HSQC) nuclear magnetic resonance (NMR) method using <sup>15</sup>N enriched CCL5.

<sup>15</sup>N-CCL5 was dissolved at a concentration of 0.3 mM in 50 mM sodium phosphate buffer made using a 95% H<sub>2</sub>O/ 5% D<sub>2</sub>O mixture, and pH was adjusted to 3.4. This solution of CCL5 was mixed with CXCL4 chemokine. All NMR experiments were carried out at 40 °C on a Varian Unity Inova 600-MHz spectrometer equipped with an H/C/N triple-

resonance probe and *x/y/z* triple-axis pulse field gradient unit. A gradient sensitivity-enhanced version of two-dimensional  $^1\text{H}$ - $^{15}\text{N}$  HSQC was applied with 256 (*t*<sub>1</sub>) × 2048 (*t*<sub>2</sub>) complex data points in nitrogen and proton dimensions, respectively. Raw data were converted, processed and analyzed by using NMRPipe and NMRview. The chemical-shift differences were averaged according to equation 1 and assignments were made based on those reported for CCL5 (Chung 1995; Duma 2007):

$$\delta\text{NH} = ((\Delta\delta(1\text{H}))^2 + 0.25(\Delta\delta(15\text{N}))^2)^{1/2}$$

### II.5.1 Molecular dynamics simulations

The NMR or x-ray structures of CCL5 and CXCL4 were taken from the Protein Data Bank, (1RTO for CCL5 and 1RHP for CXCL4). Heterodimers were built by manually replacing one monomer subunit in a homodimer with a monomer subunit from another homodimer using Insight-II software (Biosym Technologies Inc., San Diego, CA). Molecular dynamics simulations were performed for homodimers of CCL5, CXCL4 and CC-type and CXC type heterodimers of CCL5/CXCL4 using the c29b2 version of CHARMM33. A one nanosecond trajectory was simulated for each hetero- and homodimer. All dimers were simulated in a 74 × 68 × 63 Å<sup>3</sup> explicitly solvated periodic box. To make the box neutral, Cl<sup>-</sup> ions were added. Simulations were carried out using the version 22 all-hydrogen force field with a dielectric constant of 1.0. Each simulation was initialized with 2000 steps of steepest descent minimization, followed by gradual heating to 300 K and 5000 steps of system equilibration. The temperature during simulations was maintained at 300 K.

### II.5.2 Differential scanning calorimetry

A high-sensitivity differential scanning calorimeter MicroCal VP-DSC (MicroCal, Inc., Northampton, USA) was used at a heating rate of 60 °C h<sup>-1</sup>. Cells were pressurized to about 28 psi to prevent loss of solvent by evaporation and the appearance of bubbles upon heating. Solvent buffer (PBS) was used to fill the reference cell and to obtain the instrumental baseline. Excess heat-capacity functions were obtained after baseline adjustment and normalization to protein concentration (CCL5-CXCL4 0.5 mg each). The heat capacity profiles were fitted applying a non-two-state model using MicroCal's Origin software resulting in calorimetric ( $\Delta H_{\text{cal}}$ ) and van't Hoff ( $\Delta H_{\text{v}}$ ) enthalpy values.

Temperature of protein unfolding ( $T_{\text{unfold}}$ ) is taken as temperature of maximum heat capacity. Subsequent cooling and heating scans at  $60^{\circ}\text{C h}^{-1}$  were performed to gain information on the reversibility of protein unfolding.

### II.5.3 Interaction of CXCL4 or CXCL4L1 with CCL5

#### *Ligand blot*

1.5  $\mu\text{g}$  of the respective chemokine was applied onto a Hybond nitrocellulose membrane and dried at room temperature and blocked with 3% non-fat milk in Tris-buffered saline. CXCL4 (1  $\mu\text{g}/\text{mL}$ ) binding reaction was performed in the same buffer, detected with the monoclonal anti-CXCL4 antibody and subsequent corresponding secondary antibody coupled to horseradish peroxidase and visualized with the Fujifilm LAS imager 3000.

#### *Isothermal fluorescence titration*

In the isothermal fluorescence titrations, emission spectra of 200 nM CCL5 solutions in PBS were recorded over a range of 300–400 nm at 100 nm/min. The maximum of excitation was determined at a wavelength of 282 nm (tryptophan at position 57). The ligand-induced fluorescence quenching was followed by adding aliquots of 50 nM until saturation was achieved. After each addition a period of 30 seconds was kept to allow the system to equilibrate by constantly stirring the solution. A coupled external water bath maintained the temperature in the samples during the measurements at  $22^{\circ}\text{C}$  to ensure same conditions for all titrations. The slit widths were set at 5 nm and 10 nm for excitation and emission. Further a 290 nm cut-off filter was inserted in the emission path to avoid stray light. After background correction of the spectra the mean values of the fluorescence intensity ( $-\Delta F/F_0$ ), were plotted against the volume corrected concentration of the respective ligands (CXCL4 or CXCL4L1). The resulting binding isotherms were analysed by nonlinear regression using the programme GraphPad Prism 4.0 to the equation describing a bimolecular association reaction:

$$F = Fi + Fmax \left[ \frac{K_d + [\text{CCL5}] + [\text{L}] - \sqrt{(K_d + [\text{CCL5}] + [\text{L}])^2 - 4 * [\text{CCL5}] * [\text{L}]}{2 * [\text{CCL5}]} \right]$$

where  $Fi$  is the initial and  $Fmax$  is the maximum fluorescence value,  $K_d$  is the dissociation constant, and  $[\text{CCL5}]$  and  $[\text{L}]$  are the total concentrations of CCL5 and CXCL4 or CXCL4L1 ligand, respectively. The fitted parameters were  $Fmax$  and  $K_d$ . This equation is

based on the general solution for a bimolecular association reaction, as published (Goger 2002).

## **II.6 Cell culture**

### **II.6.1 General**

Cells were maintained in exponential growth in TS-25 or TS-75 (Greiner Bio-one, Frickenhausen, Germany) in a humidified 5% CO<sub>2</sub> atmosphere incubator at 37°C. All media and solutions used for cell culture were from Gibco (Gibco/Invitrogen, Karlsruhe, Germany) or PAA (Pasching, Austria) if not stated otherwise and purchased sterile or sterilized through a 0.22 µm filter. The VenorGeM Mycoplasma detection kit™ (Minerva Biolabs, Berlin, Germany) was regulatory used for detection of any contamination of the cell lines with mycoplasmas.

### **II.6.2 Cell lines**

The endothelial cell lines Human Umbilical Vein Endothelial Cells (HUVEC) and Human dermal microvascular endothelial cells (HDMEC) were purchased from PromoCell (Heidelberg, Germany) and were grown in Endothelial Cell Growth Medium and Endothelial Cell Growth Medium MV (PromoCell, Heidelberg, Germany) containing 50 µg/mL gentamycine to avoid contamination with bacteria. The cells were used for experiments until passage number 6.

The human monocytic cell line Mono Mac 6 (MM6) has been established from the peripheral blood of a patient with acute monocytic leukemia and was obtained from ATCC (Manassas, USA). MM6 cells were propagated in RPMI 1640 medium supplemented with 10% (v/v) FCS, 0.1 U/l penicillin, 100 µg/mL streptomycin, 1x MEM non-essential amino acid solution, 9 µg/mL insulin, 1 mM oxalacetate and 1 mM pyruvate. Cells were maintained in 24-well plates at a density between  $2 \times 10^5 - 10^6$  cells/mL.

### **II.6.3 Culturing of adherent cell monolayers**

Adherent cell lines were grown until confluence and then passaged by using the cell detachment solution Accutase™. The monolayer was first washed with phosphate buffered saline (PBS) (PAA, Pasching, Austria) and then incubated 5-10 min with 0.25% (v/v) Accutase™ at 37°C. After detachment of the monolayer, Accutase™ was inactivated by

the addition of medium. For subculturing, cells were harvested by centrifugation (5 min, 200 g, at room temperature) and then split with a ratio of 1:3.

#### **II.6.4 Culturing of cells in suspension**

Cells growing in suspension were cultured at a density of  $10^5$  -  $10^6$  cells/mL. Cells were harvested by centrifugation (5 min, 200 g, rt) and passaged with a ratio of 1:3-1:5.

#### **II.6.5 Freezing and thawing of cells**

Freeze stocks of cell lines were stored in 1.8 mL cryovials in liquid nitrogen. Cells were first harvested and then resuspended at a concentration of  $10^6$  -  $10^7$  cells/mL in complete medium containing 13% (v/v) dimethylsulfoxide (DMSO). The cryovials were placed overnight (o.n.) at  $-80^\circ\text{C}$  in a cryocontainer to assure slow cooling and then transferred to liquid nitrogen for long-term storage. For thawing of cells, cryovials were rapidly thawed in a  $37^\circ\text{C}$  water bath. Cells were slowly added to 4 mL warm corresponding growth medium, centrifuged and resuspended again in growth medium.

### **II.7 Functional assays**

#### **II.7.1 Angiogenesis *in vitro***

Tube formation assay was performed as previously described (Nicosia 1990). The matrigel (BD, Heidelberg, Germany) was diluted 1 to 3 with Endothelial Cell Growth Medium MV2 (Promocell, Heidelberg, Germany), transferred into a 24-well plate including 5  $\mu\text{g/mL}$  of each CXCL4 chemokine variant and allowed to solidify at  $37^\circ\text{C}$ . HDMECs (10.000/well) were plated in ECGF MV2 medium with or without 5  $\mu\text{g/mL}$  of each CXCL4 chemokine. After 20 hours pictures were taken using an Olympus IX81 microscope and tube formation was analyzed by the web based S.CORE Online Image Analysis software (S.CO LifeScience, Munich, Germany).

#### **II.7.2 Endothelial migration**

##### ***Transwell assay***

HDMECs were labeled with 1mM calcein-AM (Invitrogen, Karlsruhe, Germany) and seeded in 200  $\mu\text{L}$  RPMI-1640 containing 1% HSA into the Falcon-HTS Fluoroblocks inserts (BD Falcon, Germany, 8.0  $\mu\text{m}$  pore size) at a concentration of  $1 \times 10^5$  cells/mL.

The inserts were placed in a 24-well plate with 300  $\mu\text{L}$  RPMI-1640 and 1% HSA containing 300 ng/mL CXCL4 or CXCL4L1, or medium as control. After 3 hours the migrated cells were determined by measuring the fluorescence at 485 nm excitation and 535 nm emission with the microplate reader (see section II.1). The same assay was also performed with different concentrations of CXCL4L1 (0; 50; 100; 300; 750 and 1500 ng/mL).

### ***The $\mu$ -Slide Chemotaxis chamber***

The  $\mu$ -Slide Chemotaxis chamber, purchased from ibidi GmbH (Munich, Germany), was used to distinguish between chemokinesis and chemotaxis. CXCL4 and CXCL4L1 were used at a concentration of 300 ng/mL. The assay was prepared according to the manuals of the company. Cell movement was observed with time-lapse microscopy at 37°C in a 30 second interval for 3 hours using an inverted Olympus IX81 microscope. The data was analyzed with 'Manual Tracking' and 'Chemotaxis and Migration Tool V1.01' based on ImageJ (<http://rsb.info.nih.gov/ij>) as recommended by ibidi GmbH (Munich, Germany).

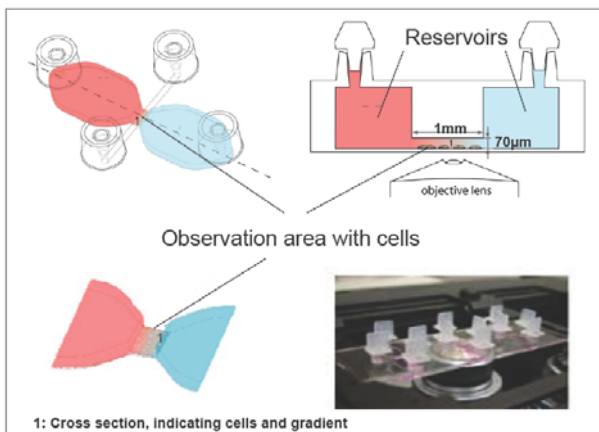


**Fig.II.3:  $\mu$ -Slide Chemotaxis chamber.** The  $\mu$ -Slide Chemotaxis is a tool for observing chemotactical responses of migrating cells over extended periods of time. Two large reservoirs (40  $\mu\text{L}$ ) for medium are connected by a narrow observation area, where the cells are seeded. The chemoattractant is added into one of the reservoirs (red) and the cells in the observation area become super-imposed by a linear and time-stable gradient.

### **II.7.3 Endothelial cell proliferation**

HDMECs (3.000 cells/well) were seeded in collagen-G coated 48-well plate with Endothelial Cell Basal Medium MV2 (PromoCell, Heidelberg, Germany) without and with 10  $\mu\text{g}/\text{mL}$  CXCL4 or CXCL4L1. After 0; 24; 48 and 72 hours the inhibition of the proliferation of the endothelial cells was determined using the CyQuant Cell Proliferation Kit Assay purchased from Invitrogen. The protocol was performed according to the

manual's instructions and the data were normalized against the control. A dose-response curve was generated from 0-50  $\mu\text{g/ml}$  chemokine and a time course established at 0; 24; 48 and 72 hours. The inhibition of endothelial cell proliferation was calculated as follows: For time 0, medium was discarded and the plate frozen. Analysis was performed together with the plate containing cells after 72 hours of proliferation. A proliferation factor was calculated by dividing the actual fluorescence intensity by values obtained at time 0. The proliferation index was calculated by dividing the proliferation factor for medium alone by the value obtained for each chemokine concentration. Curves were fitted by non-linear regression analysis to determine the  $\text{IC}_{50}$  (GraphPad Prism 4.0).

## II.7.4 Monocyte recruitment

### *In vitro*

A flow chamber adhesion assay was used to investigate cell arrest under physiological flow conditions. MM6 cells ( $10^5$  cells/mL) were pretreated for 10 min with each of the chemokine CCL5, CXCL4, CXCL4L1, or in combination CCL5 + CXCL4, CCL5 + CXCL4L1 (all 1  $\mu\text{g/mL}$ ) or only with PBS as control in 2 mL HH assay buffer (10 mM HEPES, 1x HBSS, 0.5% BSA) and 1 mM  $\text{Ca}^{2+}/\text{Mg}^{2+}$ . Then the monocytes were perfused at 1.5 dyne/cm over pre-activated (with 10 ng/mL IL  $\beta$ -1 for 6-12 hours) HDMECs. The number of monocytes firmly adherent by primary interaction with endothelium after 5 minutes of accumulation was quantified in multiple fields by analysis of images recorded with a JVC 3CCD video camera and recorder (JVC, Yokohama, Japan).

### *In vivo*

*In vivo* peritoneal recruitment of monocytes was determined in C57BL/6 (Charles River, Wilmington, USA) mice which were injected i.p. (intraperitoneal) with sterile PBS, 5  $\mu\text{g}$  CCL5 alone or in conjunction with either 5  $\mu\text{g}$  CXCL4 or CXCL4L1. After 4 h, the inflammatory infiltrate was harvested by intraperitoneal lavage with ice-cold HBSS containing 5 mM EDTA and stained with anti-CD45, -CD115, -Gr1, -F4/80 (eBiosciences, San Diego, USA), and analyzed by FACS. The absolute number was determined by CountBright absolute counting beads (Invitrogen, Karlsruhe, Germany). Inflammatory monocytes were determined as  $\text{F4/80}^-$ ,  $\text{Gr1}^+$  and  $\text{CD115}^+$  cells.

### **II.7.5 Heparin neutralization**

For analyzing the binding and neutralizing the effect of heparin the activated partial thromboplastin time (aPTT) test was conducted with and without CXCL4 or CXCL4L1. Pooled human plasma in Na citrate (Dunn Labortechnik, Germany) was mixed with the Dade<sup>®</sup> Actin<sup>®</sup> FS reagent (Dade-Behring, Germany) including 12  $\mu$ U heparin (Ratiopharm, Germany) in presence and absence of various concentration of CXCL4 or CXCL4L1 (0; 1; 2.5; 5; 7.5; 10; 15  $\mu$ g/mL) and the aPTT was determined in a KC 10 coagulometer (Amelung, Germany) according to the manufacturer's instruction.

### **II.7.6 Protein C activation**

Protein C activation by thrombin/thrombomodulin was measured as described (Slungaard 1994). Rabbit thrombomodulin (5 nM) was preincubated with protein C (200 nM) and varying concentrations of recombinant CXCL4 or CXCL4L1 for 10 minutes at 37 °C in assay buffer (20 mM Tris pH 7.4, 100 mM NaCl, 0.1% BSA, 0.1% PEG-8000 and 0.1 mM CaCl<sub>2</sub>). Protein C activation was then initiated by the addition of 1 nM of thrombin and incubated for 30 minutes at 37 °C. The reaction was terminated by the addition of 100 nM hirudin, incubated for 5 minutes at 37 °C and APC amidolytic activity was measured at 405 nm using S2366 in the microtiter plate reader at 37 °C. The amount of APC generated was calculated from a calibration curve using purified APC and S2366. A negligible amount of APC was formed in the absence of thrombomodulin.

### **II.7.7 Data illustration and statistic analysis**

Graphs display results as mean  $\pm$  SEM of 3 to 10 independent experiments, if not indicated otherwise. To compare data, one-way analysis of variance (ANOVA) and Newman-Keuls post-hoc test or an unpaired Student's t-test with Welch's correction was performed using GraphPad Prism 4.0. Differences with at least  $P < 0.05$  were considered as statistical significant.



### III Results

#### III.1 Protein expression and purification

##### III.1.1 Expression and purification of recombinant CCL5

In order to characterize the interaction between CXCL4 and CCL5 and to develop a 3-dimensional model by NMR (nuclear magnetic resonance)-spectroscopy one of the binding partners had to be labeled with the stable isotope  $^{15}\text{N}$ , which considerably increases the resolution and sensitivity of the NMR spectra. Hence CCL5 was expressed in *E. coli* as inclusion bodies in enriched  $^{15}\text{N}$  media as a fusion protein with thioredoxin. The inclusion bodies were purified from the bacterial lysate as described in section II.4.1. Then the pure inclusion bodies were denatured in 50 mM Tris pH 8 containing 6 M guanidine-HCl and 1 mM DTT.

The purification of  $^{15}\text{N}$ -CCL5 was carried out as described in Fig.III.1.1 in accordance with the following purification steps: Capture phase, Intermediate phase and Polishing phase.

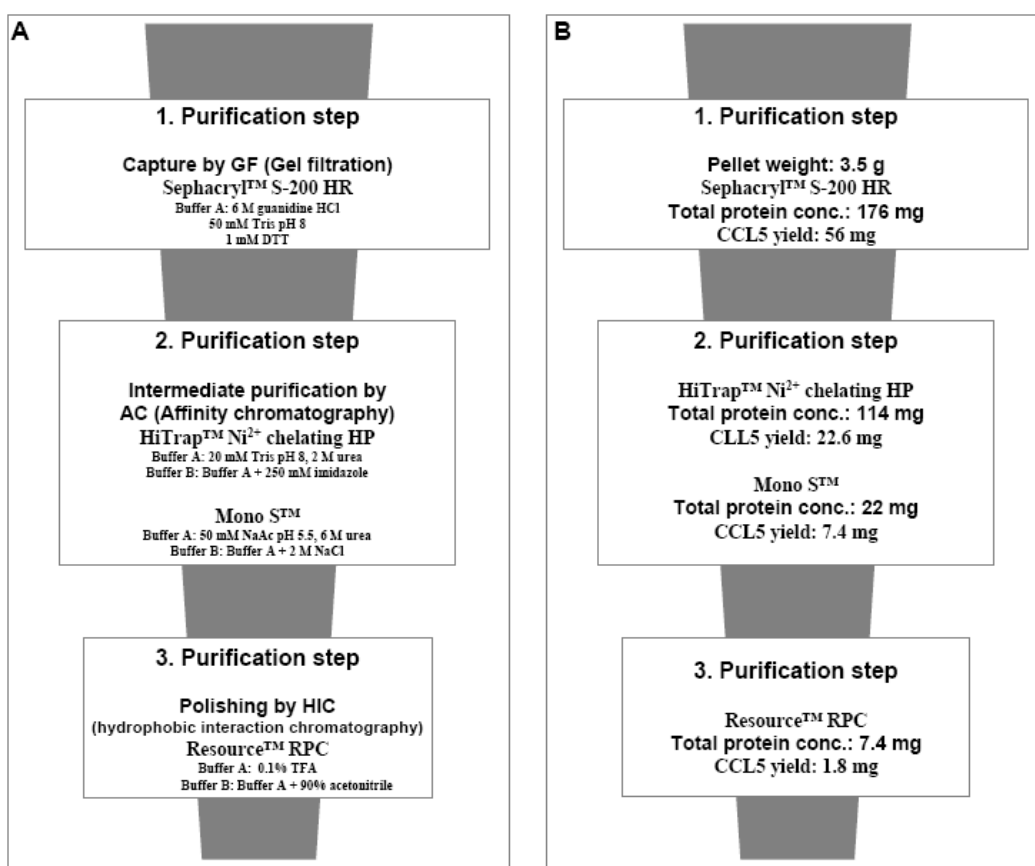


**Fig.III.1.1: (A) Purification strategy of  $^{15}\text{N}$ -CCL5 and (B) the average yield of the protein after each purification step.**

In the first FPLC purification step (capture phase), the solution was applied in 4 sequential steps onto the gel filtration column Sephacryl 200 HR (II.4.2). The column was run at a flow rate of 1 mL/min and 2.5 mL fractions were collected (Fig.III.1.2). The first opalescent fractions were discarded and the later fractions were pooled for refolding. The fusion proteins were refolded overnight at 4°C by a 6-fold dilution in a 50 mM Tris pH 8 buffer containing 6 mM cysteine and 8 mM cystine as redox additives.

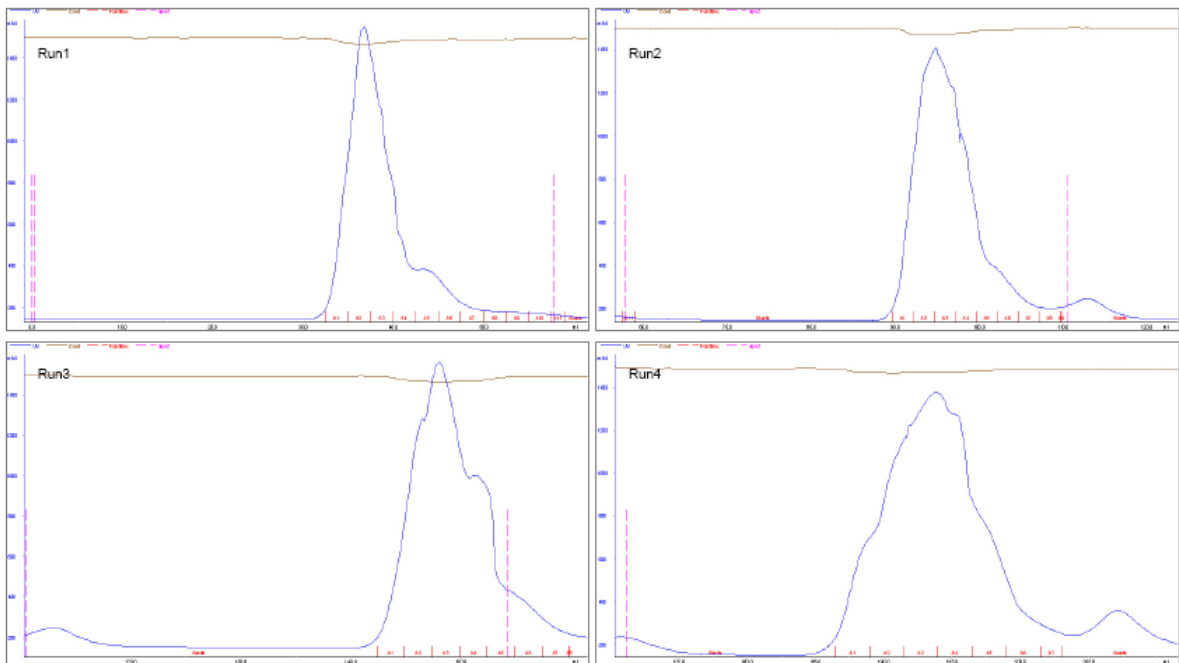


**Fig.III.1.2: Gel filtration chromatogram of  $^{15}\text{N}$ -CCL5 using a Sephacryl S-200HR column.**  $^{15}\text{N}$ -CCL5 fusion protein was eluted in 4 successively steps with 6 M Guanidine-HCl; 50 mM Tris; pH 8; 1 mM DTT. 5 mL fractions were collected and used for further purification.

Since thioredoxin is able to bind  $\text{Ni}^{2+}$  ions, the next purification step (intermediate phase) was an IMAC (immobilized metal affinity chromatography) using HiTrap  $\text{Ni}^{2+}$  chelating columns (Fig. III.1.3). The refolded fusion protein was loaded in two steps (Run1 and Run2) onto the column and eluted with 250 mM imidazole (II.4.2). All eluted proteins were pooled and dialyzed against 20 mM Tris pH 8 overnight at 4°C.

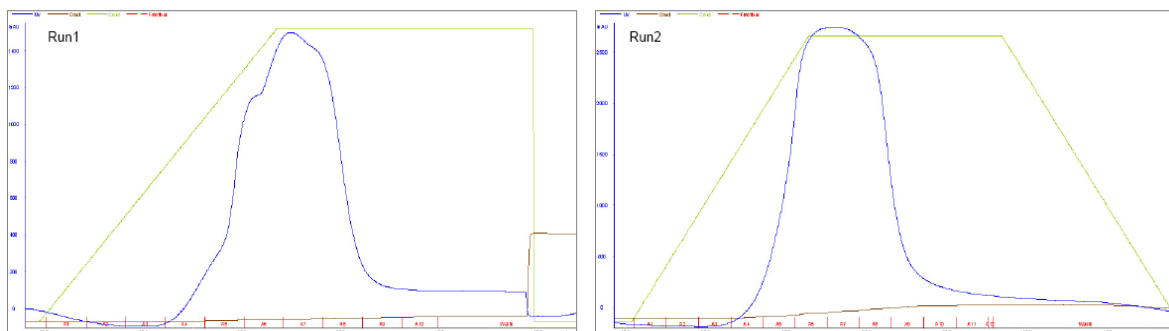


**Fig.III.1.3: FPLC chromatogram using the HiTrap Ni<sup>2+</sup> chelating column.** In the second purification step a Ni<sup>2+</sup> chelating column was applied. As binding buffer 20 mM Tris pH 8; 2 M Urea was used. Bound proteins were eluted with the same buffer supplemented with 250 mM imidazole at 1mL/min. 2 mL fractions were collected and used for further purification.

After buffer exchange the volume of the solution was decreased using the Macrosep<sup>®</sup> concentration tube. Subsequently a volume of 8-10 mL the thioredoxin tag was removed from <sup>15</sup>N-CCL5 by digestion with enterokinase (1U/ 50  $\mu$ g CCL5) for 16 hours at room temperature.

Since the enzymatically liberated <sup>15</sup>N-CCL5 formed an insoluble hetero-aggregate with the <sup>15</sup>N-CCL5/thioredoxin, the aggregate was pelleted by centrifugation for 30 min at 25 000 g and redissolved in a buffer containing 8 M Urea and 20 mM Tris pH 7.5.

The separation <sup>15</sup>N-CCL5 with thioredoxin was carried out by using the cation exchanger MonoS<sup>™</sup> column (II.4.2, intermediate phase II). First the pH of the solution was decreased to 5.5 to avoid aggregation and to enhance binding of <sup>15</sup>N-CCL5 onto the column. Then the solution was applied to the column previously equilibrated in 50 mM sodium acetate buffer pH 5.5 containing 6 M urea, which also supported the disaggregation. The absorbed protein was eluted with a linear 0-1 M NaCl gradient in the same buffer. The fractions containing only the cleaved CCL5 were pooled and dialyzed 2 x against acetic acid and 1 x against 0.1% TFA (Fig.III.1.4).

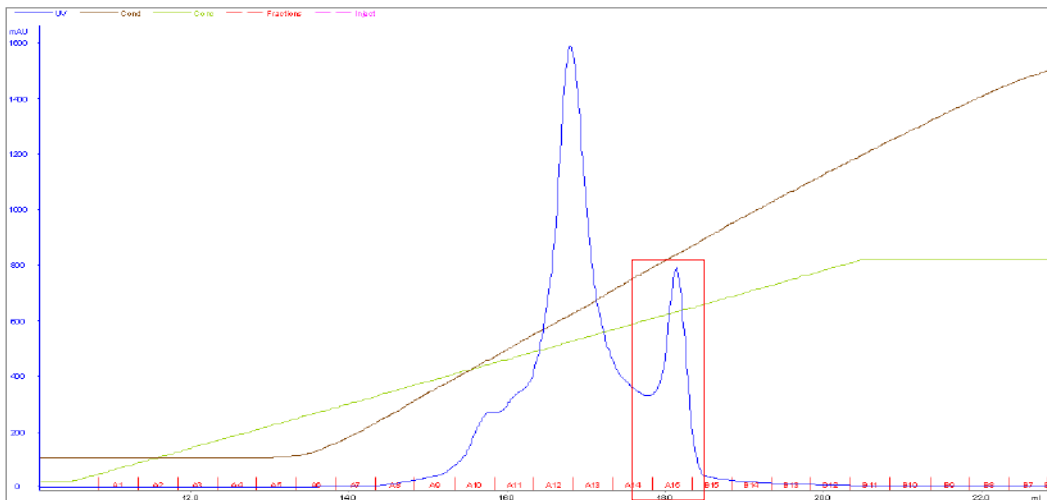


**Fig.III.1.4: FPLC chromatogram using the Mono S™.** After digestion of the fusion protein with enterokinase, pure <sup>15</sup>N-CCL5 (fraction A14+A15, red rectangle) was separated from the fusion protein (fraction A10-A13) by Mono S™ column using 50 mM Na-acetate; pH 5.5, 6 M Urea as binding buffer and 50 mM Na-acetate pH 5.5, 6 M Urea, 2M NaCl as elution buffer. Flow rate was 1 mL/min and 0.5 mL fractions were collected.

For the polishing step, the hydrophobic interaction chromatography (HIC) was performed using the reverse phase column Resource™ RPC (II.4.2). The dialyzed protein was loaded onto the column and bound protein was eluted with a linear 0-67% gradient using 0.1% TFA containing 90% acetonitrile. Each fraction was analyzed by SDS-PAGE and coomassie blue staining (Fig.III.1.5).

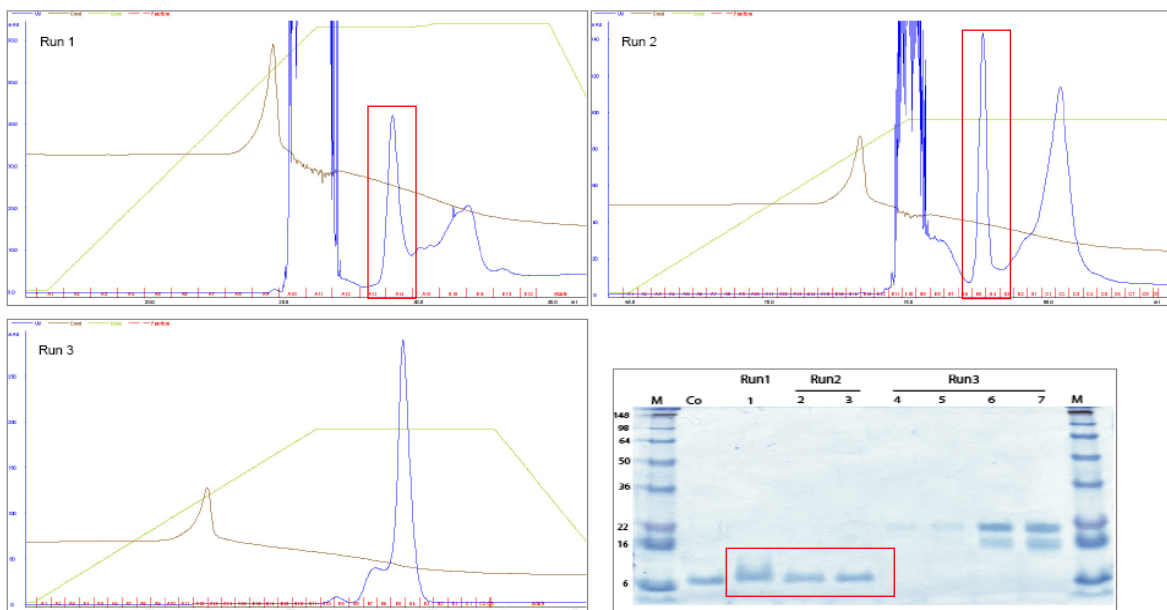


**Fig.III.1.5: FPLC RPC™ chromatogram.** Fractions from Mono S™ containing <sup>15</sup>N-CCL5 (A14+A15) were pooled and purified further by the RPC™ column in 3 successive runs. 0.1% TFA as binding buffer and 0.1% TFA containing 90% acetonitrile as elution buffer were used to purify <sup>15</sup>N-CCL5 from traces impurities. (bottom, right) All fractions were controlled for the presence of <sup>15</sup>N-CCL5 (red rectangle, Run1 1, Run2 2+3) by SDS-PAGE (12.5% gel) and coomassie blue staining.

At the end of the purification procedure 5  $\mu\text{L}$  aliquots from every of the purification steps were run on a 12.5% SDS polyacrylamide gel and analyzed either by coomassie blue staining (Fig.III.1.6 A) or by western blotting (Fig.III.1.6 B).

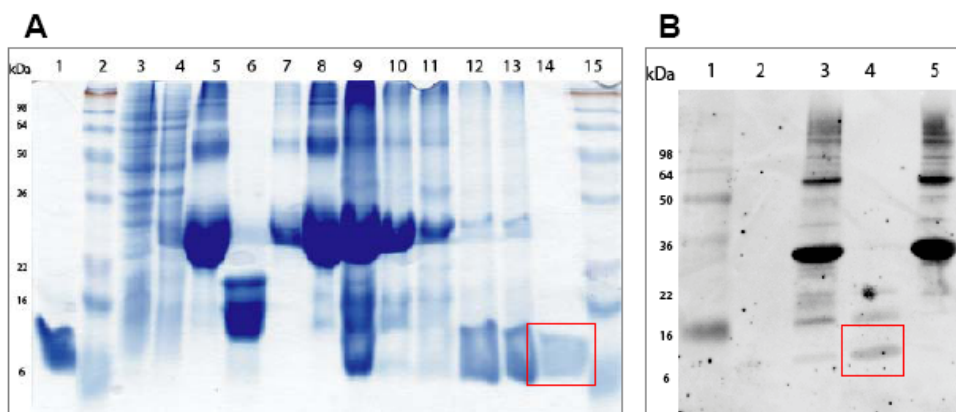


**Fig.III.1.6: Analysis of purification steps using SDS-PAGE after RPC™ purification.** 5  $\mu\text{L}$  aliquots of each purification step were loaded on a 12.5% acrylamide gel and stained with coomassie blue (A) or analyzed by western blot (B). (A) Coomassie staining: 1: CCL5 control, 2: SeeBlue® Plus2 marker, 3: before protein expression induction, 4: after induction, 5:  $\text{Ni}^{2+}$  pool, 6: supernatant of enterokinase digestion, 7+8: Macrosep concentration sample, 9: input Mono S™, 10+11: Mono S™ fusion protein fraction pool, 12: Mono S™  $^{15}\text{N}$ -CCL5 fraction pool, 13 input RPC™, 14: pure  $^{15}\text{N}$ -CCL5 (red rectangle), 15: SeeBlue® Plus2 marker. (B) Western blot: 1: SeeBlue® Plus2 marker, 2: CCL5 control, 3: input RPC™, 4: pure  $^{15}\text{N}$ -CCL5 pool (Run1 A14 + Run2 B5 and B4, red rectangle), 5: pool Run3 (B5+B4).

## III.2 NMR chemical shift mapping of CCL5-CXCL4 heterodimer

Since the cooperative effects of CXCL4 and CCL5 are explained by the direct interaction, we wanted to shed light on the structural basis of this interaction. The heterodimerization was characterized by the  $^{15}\text{N}$ - $^1\text{H}$  heteronuclear single quantum coherence (HSQC) nuclear magnetic resonance (NMR) technique in the lab of Dr. Kevin Mayo (Department of Biochemistry, University of Minnesota). Using this method, the chemical shift of the amino acids involved in the interaction of the monomers in comparison with the heteromers was measured. Titration of CXCL4 into a solution of uniformly labeled  $^{15}\text{N}$ -CCL5 induced a chemical-shift change and a decrease in CCL5 monomer signal intensities, consistent with interactions of CCL5 and CXCL4 (Fig.III.2.1). Maximal  $^{15}\text{N}$ - $^1\text{H}$  chemical shift changes in the heteromer formation were observed in the N-terminal residues which indicated a CC-type rather than a CXC-type interaction. In the other hand, minimal chemical shift changes were found from residues of the first  $\beta$ -strand that mediates CXC-type dimer formation.

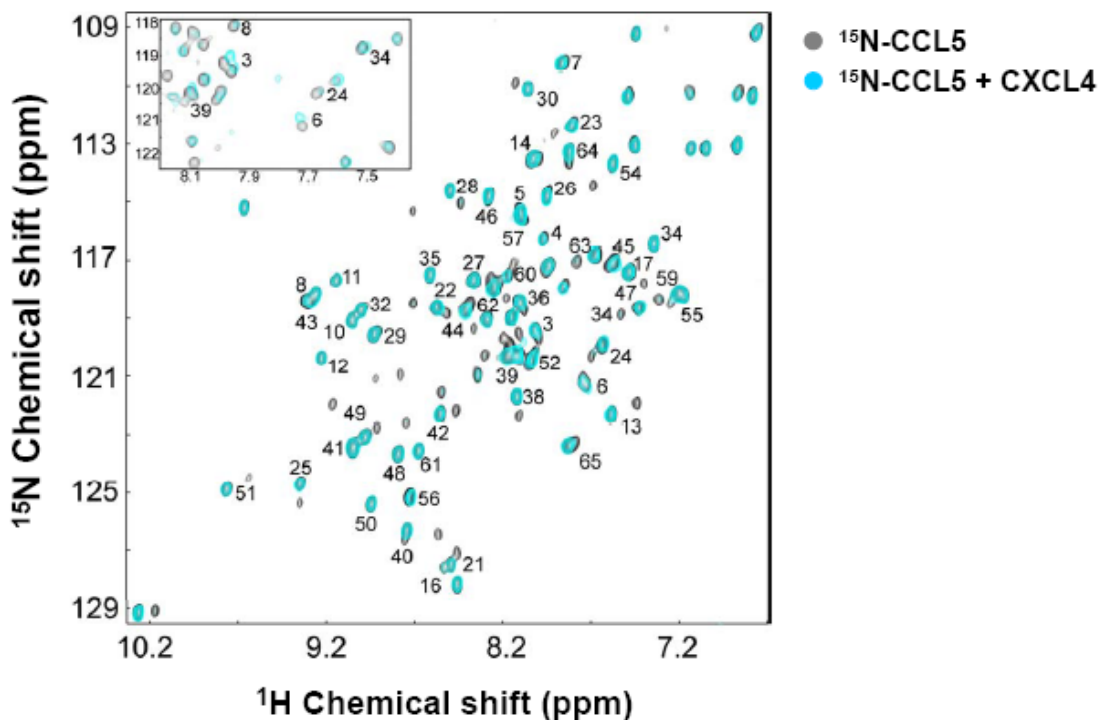


**Fig.III.2.1: Biophysical characterization of CCL5-CXCL4 interaction.** HSQC spectrum of  $^{15}\text{N}$ -CCL5 in the absence (gray cross-peaks) or presence (blue cross-peaks) of CXCL4 (molar ratio 1:1) with numbers representing respective CCL5 residues. Inset: Region from the HSQC spectrum of  $^{15}\text{N}$ -CCL5, exemplifying chemical shift changes caused by the addition of CXCL4 at the molar ratio of 1:16 (Koenen 2009).

In support of the CC-type heterodimerization, molecular dynamics simulations on docked CC-type and CXC-type CCL5-CXCL4 heterodimers revealed a more thermodynamically favorable CC-type heterodimer conformation, as shown in the Fig.III.2.2 for the calculated free energies.

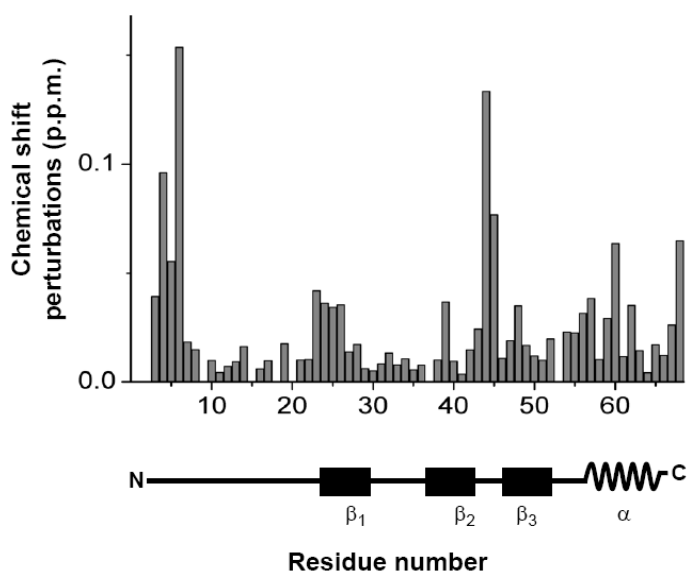


**Fig.III.2.2: Chemical shift perturbations analysis.** Changes in chemical shift of  $^{15}\text{N}$ -CCL5 backbone amides in p.p.m. caused by the addition of CXCL4 (molar ratio, 1:2). Bottom, schematic of the secondary structure of CCL5; black boxes and the wavy line,  $\beta$ -strands and an  $\alpha$ -helix, respectively (Koenen 2009).

Based on the molecular dynamics simulation a CCL5-CXCL4 heteromer structure could be calculated (Fig.III.2.3 A). There, the N-terminal CCL5 residues (3-6 aa) and the N-terminal CXCL4 residues (7-10 aa) showed a close proximity. As shown by the chemical shift mapping these residues displayed the greatest chemical shift changes in the presence of CXCL4, particularly at high concentrations of CXCL4 (Fig.III.2.1 inset). Also the highly negatively charged remainder of the CXCL4 N-terminus crosses the net positively charged first and second loops of CCL5 (Fig.III.2.3 A), which is observed in the chemical shift changes within the first (21-24) and second (44-46) loop of CCL5 (Fig.III.2.2). In line with chemical shift changes observed in residues 60 and 62 the N-terminus of CXCL4 is proximal to the C-terminus helix of CCL5. Differential scanning calorimetry indicated that CCL5-CXCL4 heterodimers are stable at temperatures up to 65 °C (Fig.III.2.3 B).

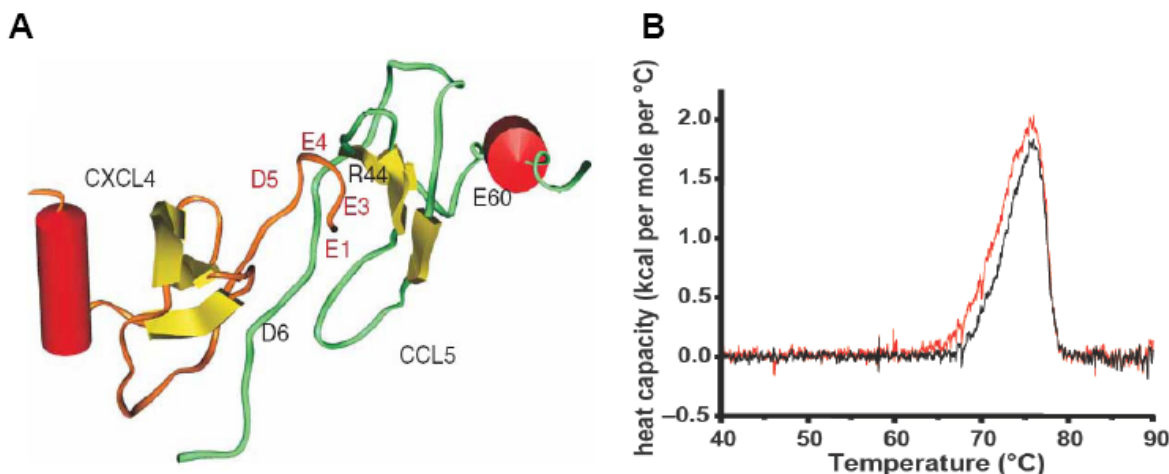


**Fig.III.2.3: Structural model of the CCL5-CXCL4 heterodimer.** (A) The most prominently involved residues are shown in red (CXCL4) and black (CCL5). The negatively charged N-terminus of CXCL4 extends over the net positively charged first and second loops of CCL5. (B) Differential scanning calorimeter analysis of the heteromer. Solvent-normalized heat capacity curves as a function of temperature obtained by heating of CCL5-CXCL4 complex in PBS. Black and red curves represent two separate experiments with calculated melting temperatures of CCL5-CXCL4 of 76 °C (Koenen 2009).

### III.3 CXCL4/CXCL4L1 Purification

CXCL4 and CXCL4L1 were expressed in the periplasm of *E. coli* strain Rosetta DE3-pLysS in TB medium and extracted from the bacteria as described in the section II.4.4. The recombinant proteins were separated from the bacterial lysate by centrifugation and purified sequentially using FPLC and HPLC step according to following purification steps: Capture phase, Intermediate phase, Polishing phase (Fig.III.3.1). In the following section, only the chromatographic purification steps of CXCL4L1 are described in detail, since for CXCL4, the purification procedure is identical. The correct size and the purity of the recombinant chemokines are summarized in Fig.III.3.6.

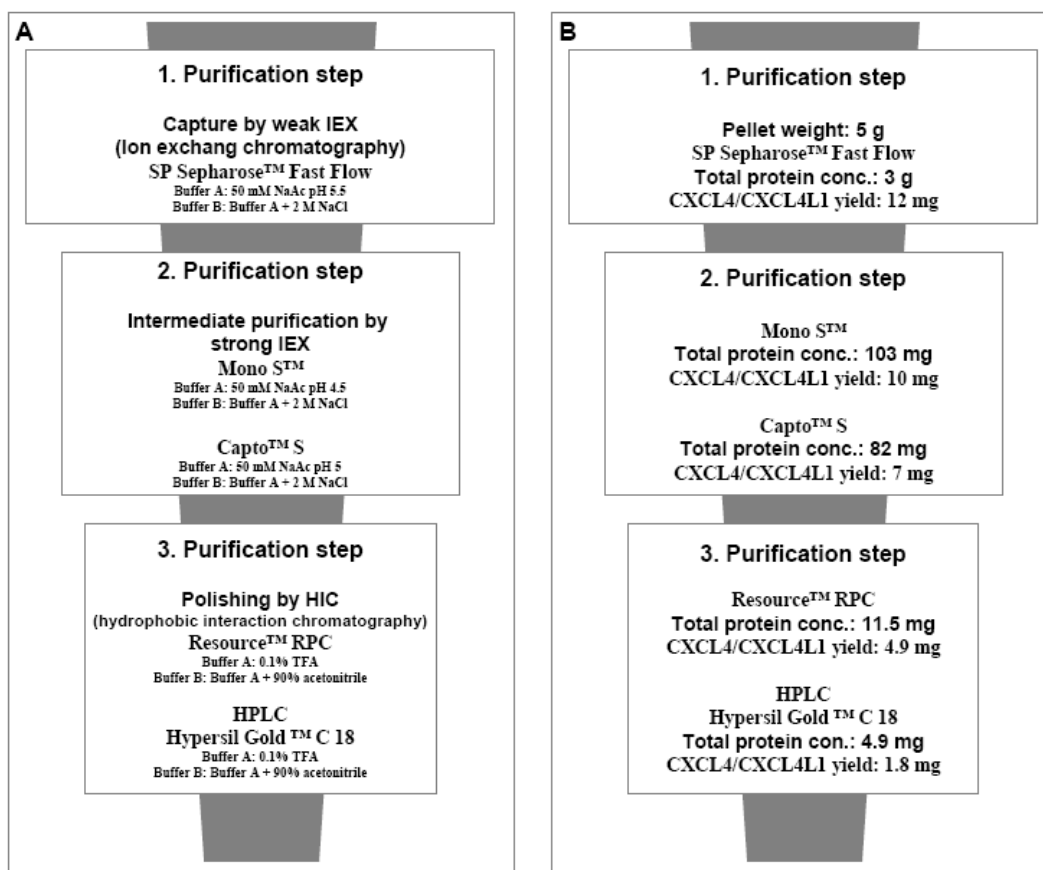


**Fig.III.3.1:** (A) Purification strategy of CXCL4 and CXCL4L1 and (B) the average yield of the protein after each purification step.

After dialysis of the bacterial periplasm solution against the binding buffer containing 50 mM NaAc pH 5.5 the first purification step (capture phase) was performed by FPLC using the SP Sepharose™ column (II.4.5). Bound proteins were eluted at 0.6 M NaCl using a gradient between 0-2 M (Fig.III.3.2, Run1). The flow through was collected and loaded



again onto the column and eluted also with the same gradient as in Run 1 (Fig.III.3.2, Run2). Each fraction was controlled for the desired protein by dot blot analysis (II.3.7) (Fig.III.3.2, bottom).

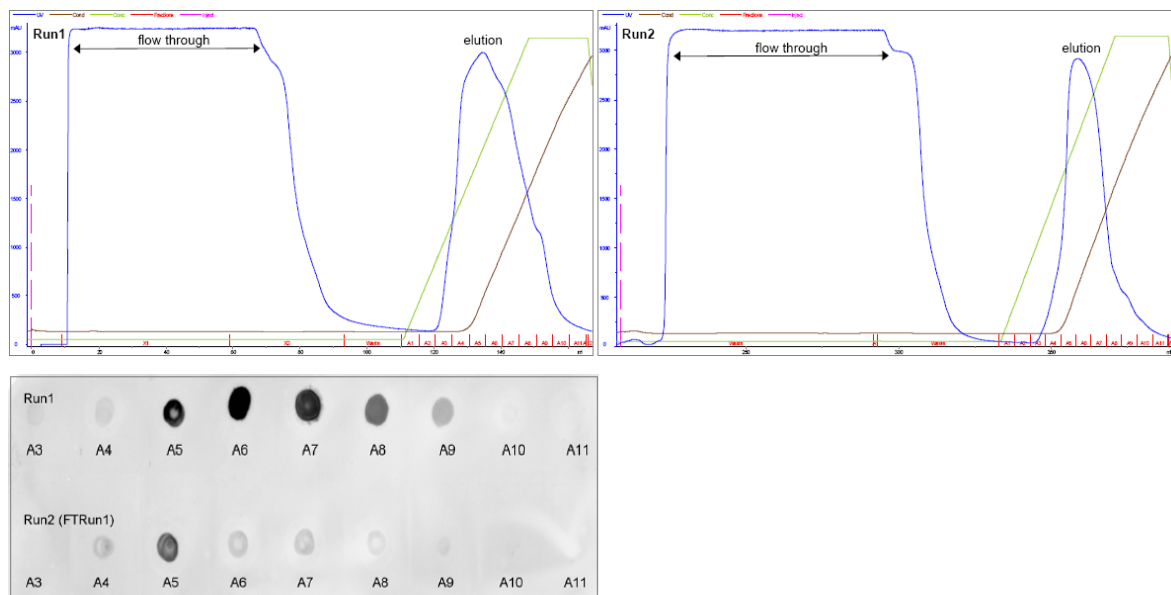


**Fig.III.3.2: FPLC chromatograms of the first step of purification of CXCL4L1.** Proteins were loaded on a HiLoad 16/10 SP-Sepharose<sup>™</sup> column using 50 mM NaAc pH 5.5. Elution of bound protein was carried on with a 0-2 M NaCl gradient. The flow through of the first run was again loaded on the column and eluted using the same gradient (run2). (bottom left) All eluted fractions were controlled for the CXCL4L1 protein by a dot blot using specific antibodies against CXCL4L1 (see II.3.7). Fractions containing the protein (Run1: A4-A9, Run2: A4-A7) were pooled and used for further purification. (Same procedure was done with CXCL4, data not shown).

After dialysis against 50 mM NaAc (pH 4.5 - 5) the protein was purified by the next FPLC step (intermediate phase) using a cation exchanger with a higher resolution capability (e.g. MonoS<sup>™</sup> 5/50 GL or HiTrap CantoS II.4.5). In both cases the bound protein was eluted with a linear 0-2 M NaCl gradient (Fig.III.3.3) and fractionized in 0.5 mL volumes. Since Mono S has a lower binding capacity but a high resolution the flow through was loaded again for a better yield (Fig.III.3.3, Run 2). Each fraction was again controlled via dot blot analysis for the recombinant protein (Fig.III.3.3, bottom right). Fractions containing the protein were pooled and prepared for the next purification step by dialyzing 2 x against 1 % acetic acid and 1 x against 0.1% TFA (trifluoroacetic acid) for at least 3 h.

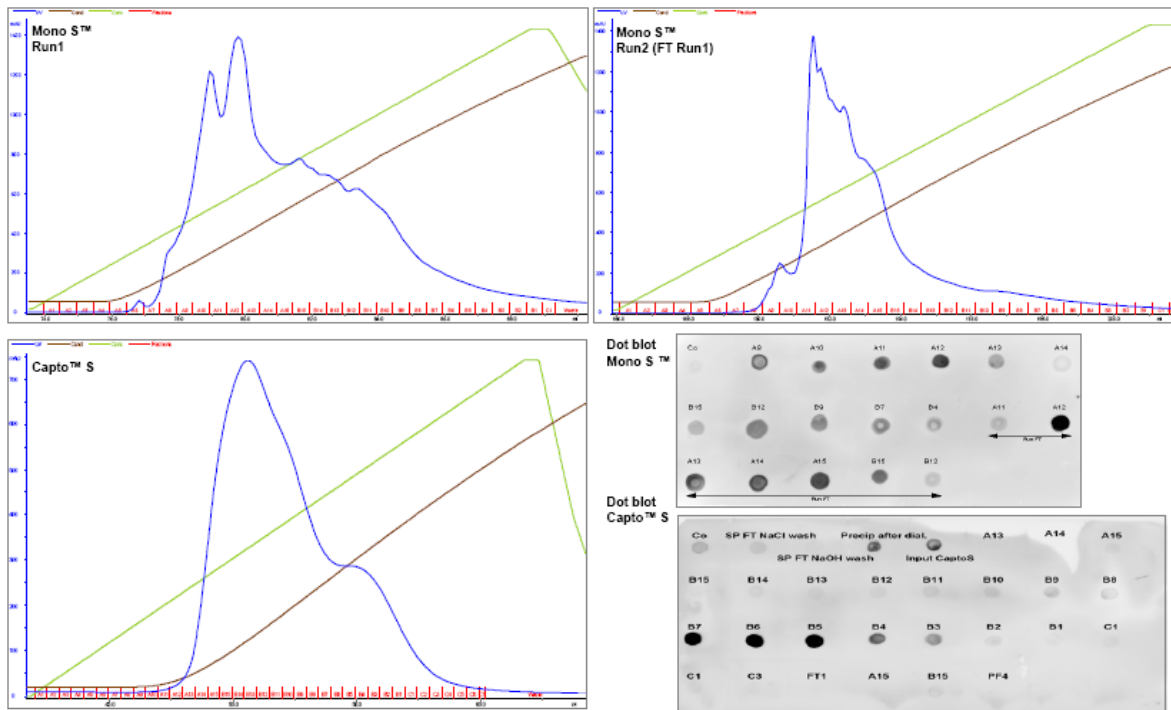


**Fig.III.3.3: Purification of CXCL4L1 using Mono S™ or Capto™ S cation exchanger columns.** For binding of the protein to the columns following buffer was used: 50 mM NaAc pH 4.5 (Mono S™, polystyrene-based matrix) or pH 5 (Capto™ S, agarose-based matrix). The elution was carried out with a 0-2 M NaCl linear gradient. In the case of Mono S™ flow through from Run1 (FTRun1) was applied again onto the column (Run2). All fractions were collected and controlled for the desired protein by dot blotting.

For the final removal of trace contaminants the reverse phase column RPC™ was chosen (polishing phase). The interaction of the protein with the resin of the column originated mainly through hydrophobic amino acid on the surface of the protein and the underivatized monodisperse polystyrene/ divinylbenzene beads.

After dialysis against 0.1% TFA, the protein solution was loaded on the column with 1 mL/ min flow rate and eluted with the organic solvent acetonitrile (90%) in 0.1% TFA using a 0-67% gradient (Fig.III.3.4). The eluted protein was collected in 0.5 mL fractions and the sizes were controlled by SDS-PAGE and coomassie staining (Fig.III.3.4, right). Fractions containing the correct size of the recombinant proteins were pooled and purified further by HPLC.

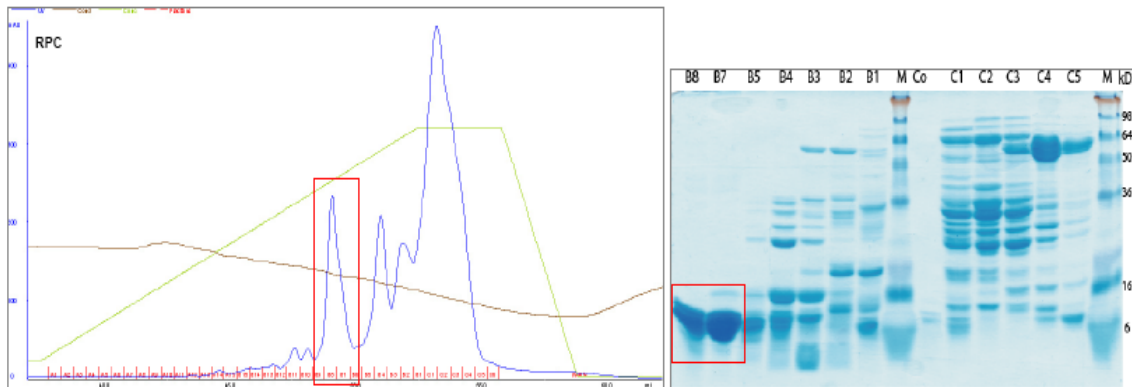


**Fig.III.3.4: Reverse phase chromatography (RPC) of the CXCL4L1 protein.** As a final purification step in the FPLC, proteins were loaded on a RPC column using 0.1% TFA as binding buffer and eluted using a linear 0-67% gradient with 0.1% TFA containing 90% acetonitrile (left). Fractions containing purified proteins (B8+B7, red rectangle) were analyzed by SDS-PAGE (12.5% gel) and coomassie staining (right).

To obtain a highly pure yield, pooled protein fractions were applied on a HPLC system with a Hypersil Gold C-18 column. Using the program described in section (II.4.6), the pure protein was eluted with the elution buffer containing 0.1% TFA and 90% acetonitrile (Fig.III.3.5). All peaks obtained from the HPLC run were collected and lyophilized to remove the TFA and acetonitrile traces. The lyophilized proteins were dissolved in sterile H<sub>2</sub>O. The purity and correct sizes were analyzed by SDS-PAGE silver gel staining, western blotting and mass spectroscopy (Fig.III.3.6).

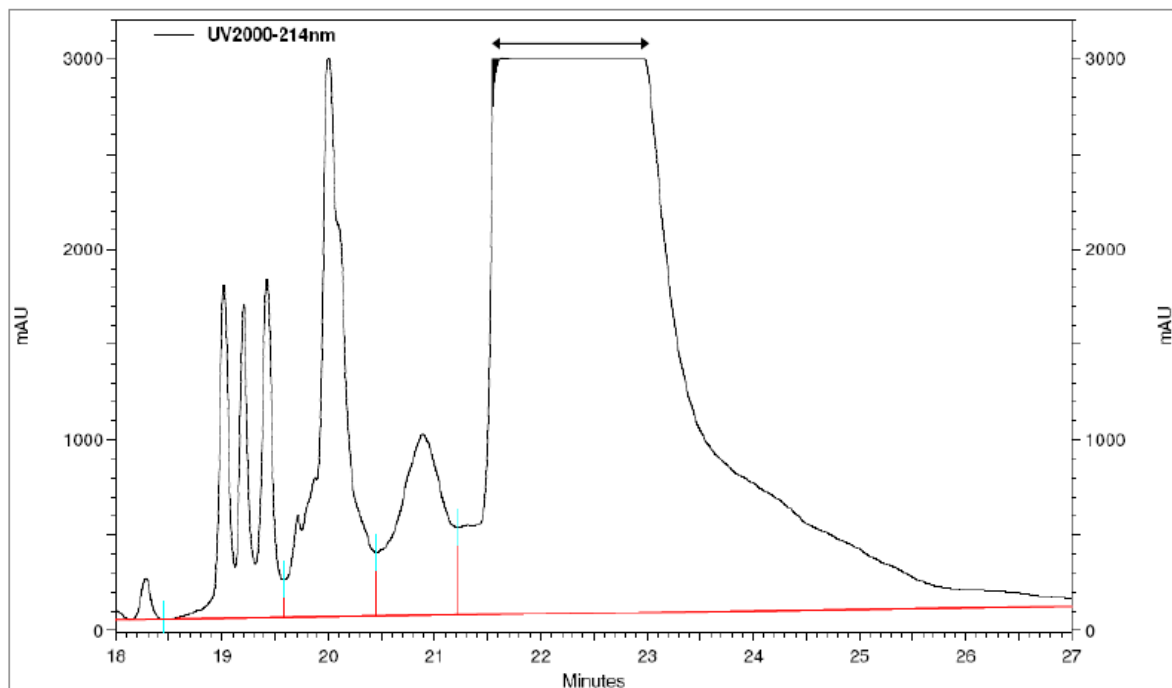


**Fig.III.3.5: HPLC chromatogram of CXCL4L1.** Using the program described in section II.4.6, CXCL4L1 was further purified from any other contaminants. Highly pure protein (see arrow, retention time: 21.5-23.5) was obtained and used for further characterizations.

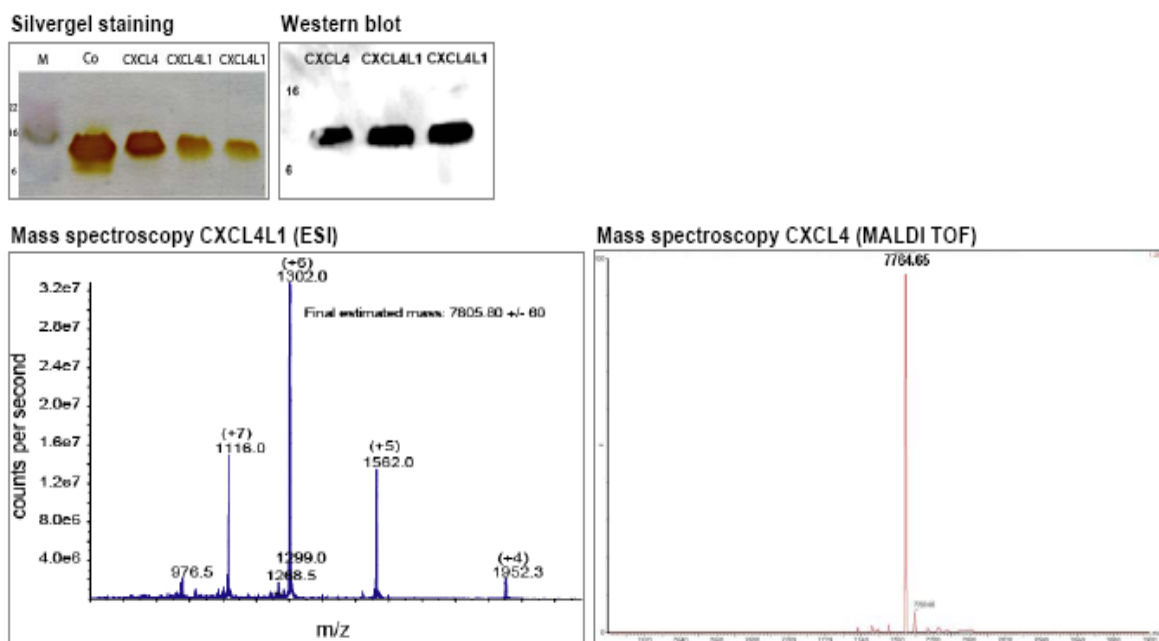


**Fig.III.3.6: Validation of the correct size and purity of CXCL4L1 and CXCL4.** Silver gel staining following a SDS-PAGE and western blotting using polyclonal antibodies against CXCL4 and CXCL4L1 were performed as reported in the section II.3.5 + 6 (Co: human CXCL4 form Chromatec (Greifswald, Germany), concentration of the proteins: 1  $\mu\text{g}/\text{mL}$ ). The correct masses were also determined by mass spectroscopy (7805.8 by electro spray ionization for CXCL4L1 and 7764.65 by MALDI TOF for CXCL4).

### III.4 Chemical synthesis of CXCL4L1

Solid-phase protein synthesis (SPPS) (Fig.III.4.1), invented by Bruce Merrifield in 1963, was used to synthesize CXCL4L1 in a more pure form compared to recombinant expression.

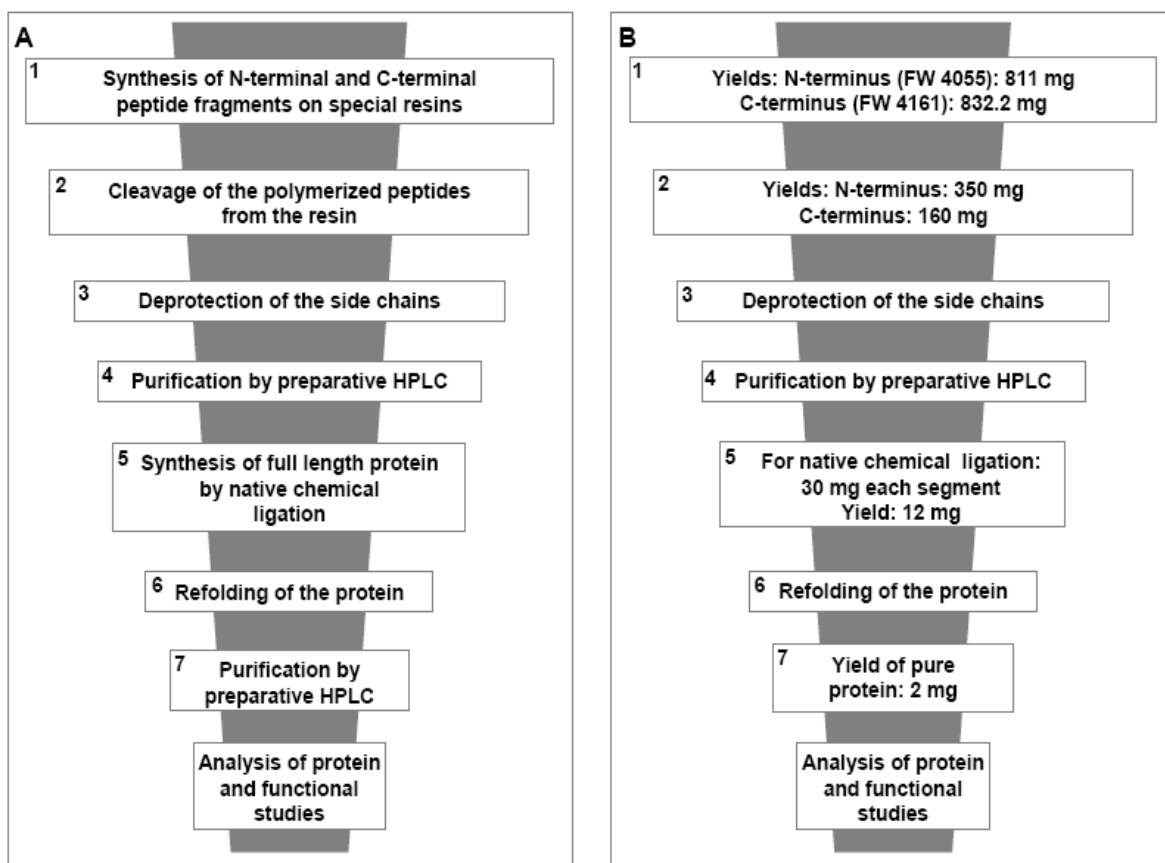


**Fig.III.4.1:** (A) Solid-phase protein synthesis (SPPS) strategy of CXCL4L1 and (B) the average yield of the protein after each purification step.

As described in the section II.4.7 CXCL4L1 chemical synthesis was carried on in 2 steps. First the N-terminal segment of CXCL4L1 ( $^1\text{E-H}^{35}$  aa) containing the thioester residue at position 35 was synthesized (yield: 811mg). Then the C-terminal segment ( $^{36}\text{C-S}^{70}$  aa) with the important cysteine at the N-terminus was synthesized (yield: 832.2 mg). The synthesis was controlled by analytical HPLC and mass spectroscopy (Fig.III.4.2).

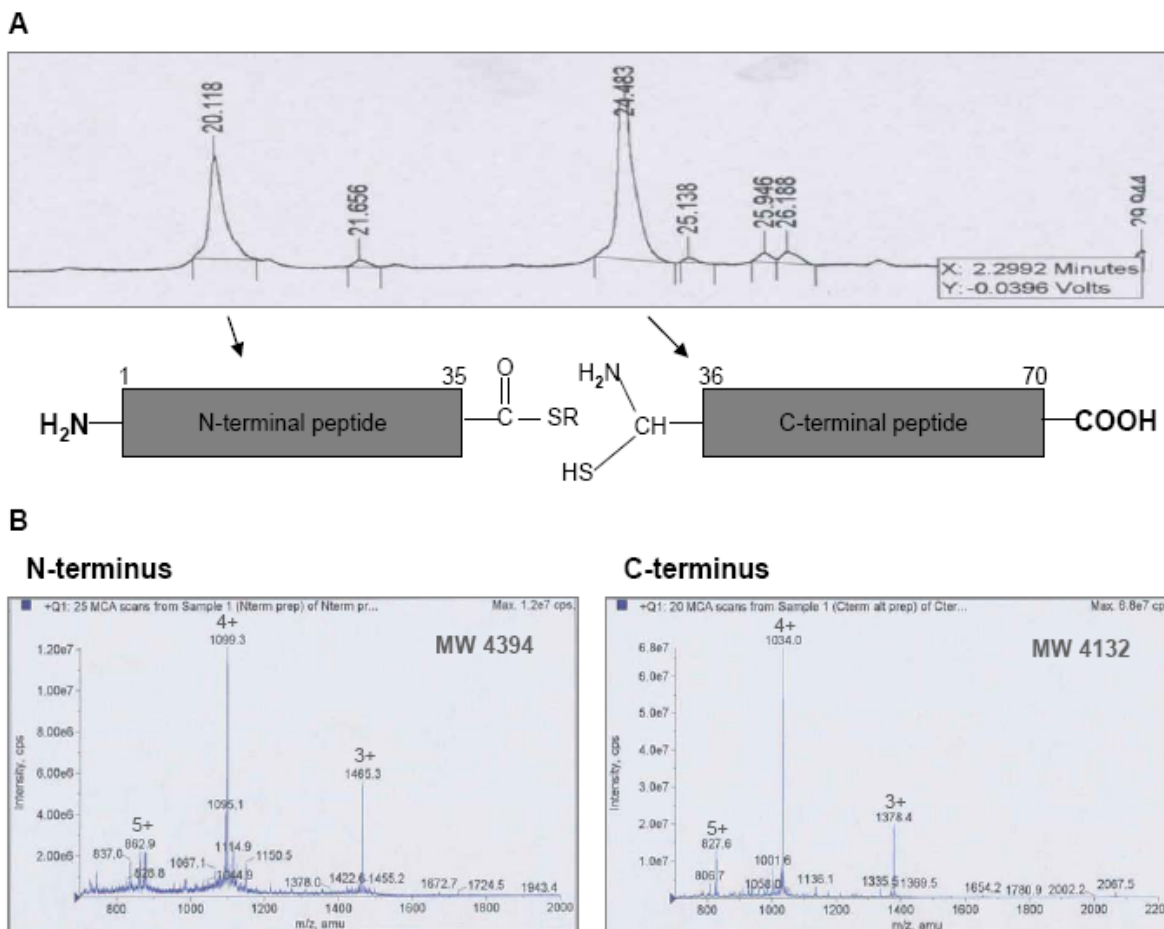


**Fig.III.4.2: Total chemical synthesis of CXCL4L1 N-terminal and C-terminal segments.** The 35-residue N-terminal peptide-thioester (COSR) fragment and the 35-residue C-terminal fragment of CXCL4L1 were synthesized by stepwise SPPS techniques using t-Boc chemistry protocols (II.4.7). The synthesis was monitored by analytical HPLC (A) (retention time of N-terminal segment at 20 min; retention time of C-terminal segment at 24.5 min) and by mass spectroscopy (ESI-MS) (B).

After cleavage of both segments from the resin and purification by preparative HPLC the yield resulted in 350 mg for crude N-terminal and 160 mg for crude C-terminal fragments. For the native chemical ligation 30 mg of each were used to assemble both segments for 24 h at 37°C in presence of 1% benzylmercaptan and 1% thiophenol as catalyzers. In the native chemical ligation procedure, the thioester bond at the ligation site spontaneously rearranges and gives via an intramolecular nucleophilic attack a native backbone amide bond joining the two polypeptide segments at  $^{35}\text{H-C}^{36}$  (II.4.7, Fig.II.2). The progress of the ligation was monitored by analytical HPLC (Fig.III.4.3). The single segments gradually disappeared and a new signal emerged containing the full length protein. The result was a complete native polypeptide chain that was obtained directly in its final sequence (dry yield after preparative HPLC: 12 mg).

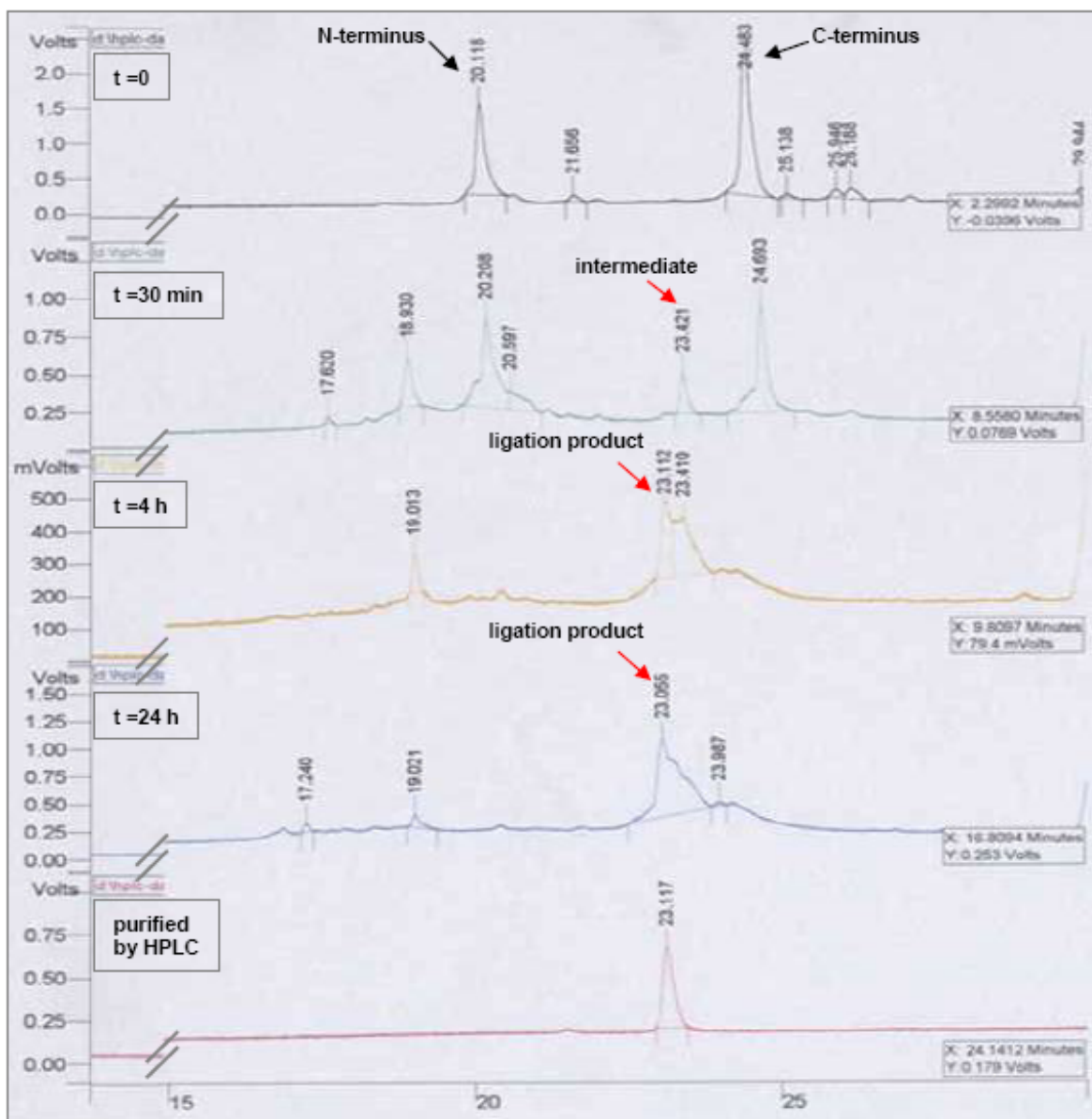


**Fig.III.4.3: Formation of CXCL4L1 by native chemical ligation.** As shown by HPLC chromatograms, N-terminal and C-terminal fragments were initially joined by thioester formation (as intermediate,  $t = 30$  min), and a subsequent spontaneous, rapid rearrangement resulted in the formation of a native peptide bond at the site of ligation (at  $t = 4$  h). Finally after 24 h ligation has been finished and pure protein was obtained after preparative HPLC purification (retention time at 23 min).

Since the synthesized protein was reduced and not folded correctly, the protein was refolded at a concentration of 0.1-0.2 mg/mL in 1M guanidine HCl pH 8 containing 8 mM cysteine and 1 mM cystine as redox additives for 24 hours at 4°C. The refolding (final yield: 2 mg) was observed by HPLC as shown in the decrease of the retention time of the refolded protein compared with the unfolded ligation product (Fig.III.4.4) due to disulfide bond formations (cysteine-10 with cysteine-36, cysteine-12 with cysteine-52), and by mass spectroscopy (Fig.III.4.5). The sizes and the purity were verified also by silver gel staining

(Fig.III.4.6 A) following the SDS-PAGE or by western blotting (Fig.III.4.6 B).

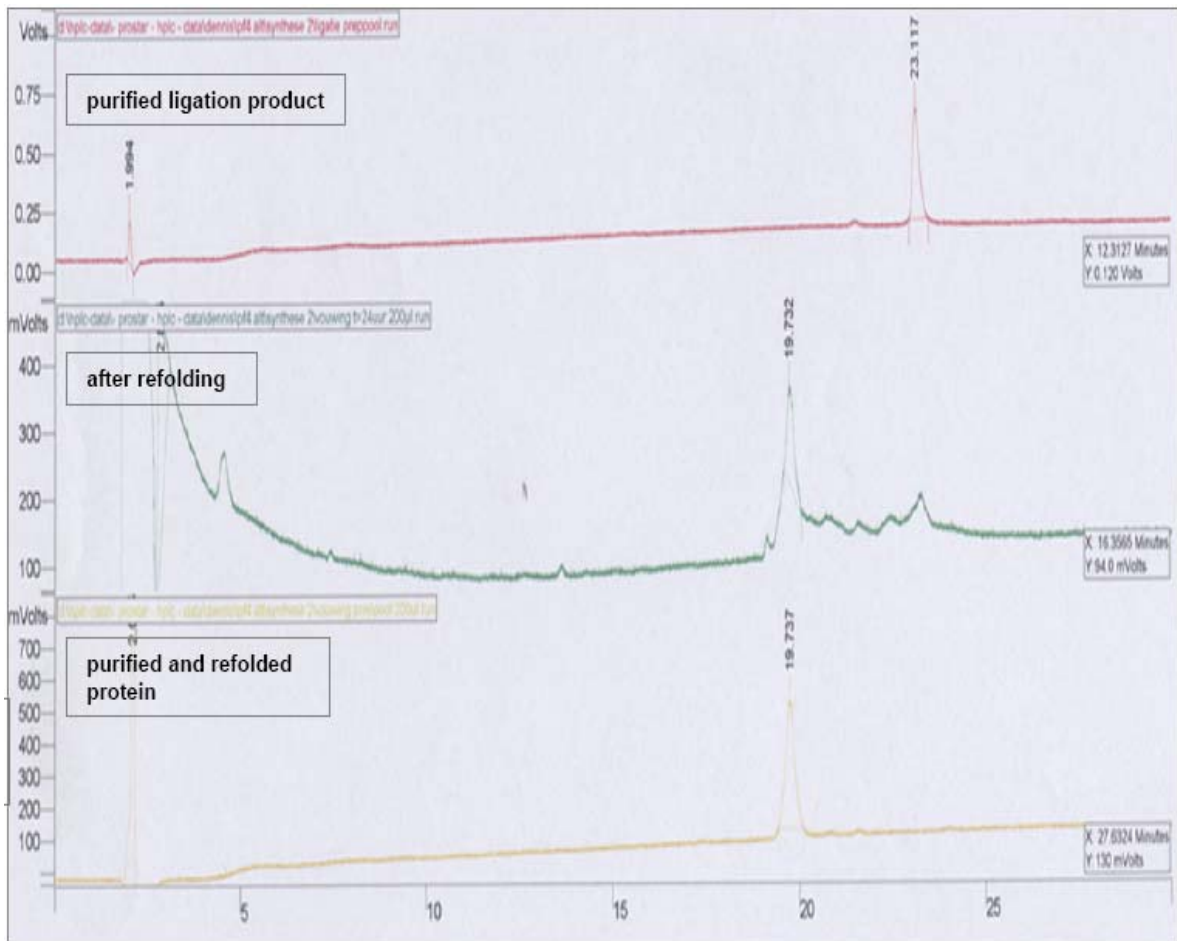


**Fig.III.4.4: Folding and disulfide formation of CXCL4L1.** HPLC chromatograms of the purified, reduced CXCL4L1 ligation product (top), the crude material after refolding (middle), and the purified final CXCL4L1 product (bottom).

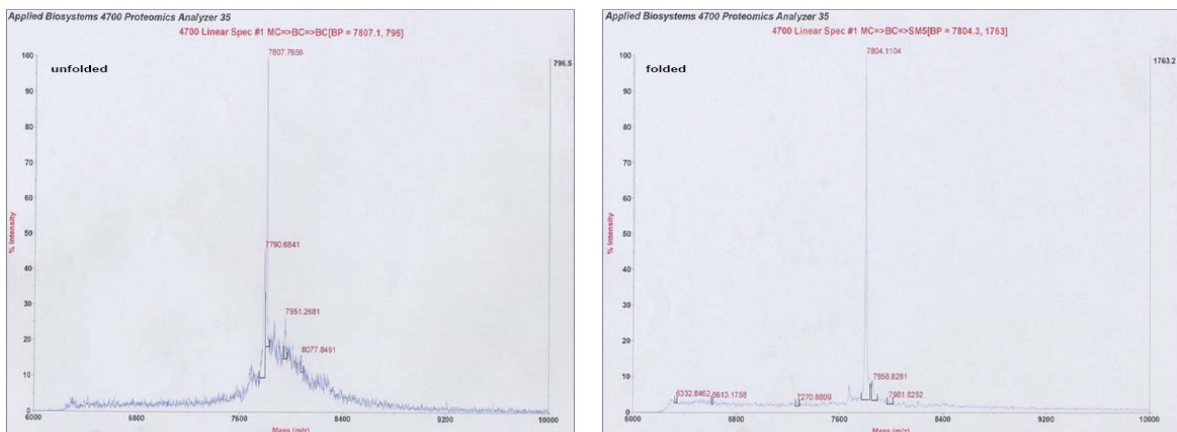


**Fig.III.4.5: Mass spectroscopy spectrums (MALDI TOF).** Unfolded and folded CXCL4L1 with a calculated mass of 7807.77 and 7804.11 Da (theoretical mass of CXCL4L1: 7805). The decrease of the mass indicates the loss of the H atoms due to disulfide bond formations.



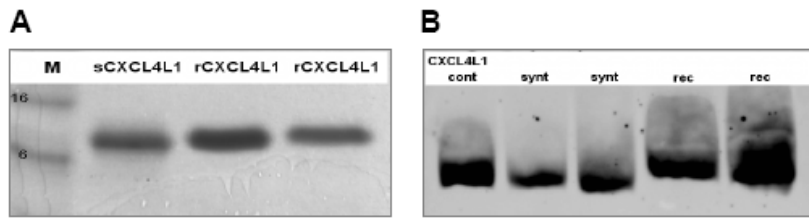


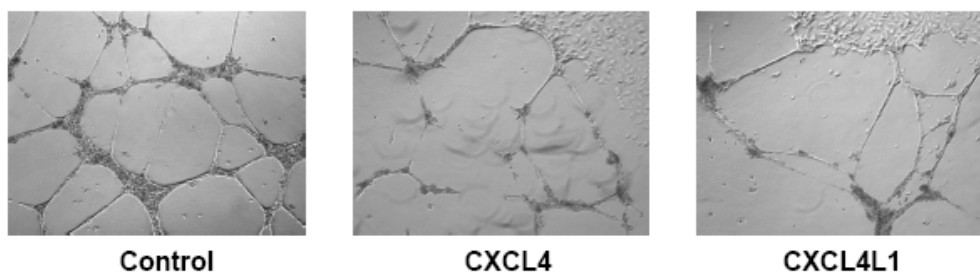
**Fig.III.4.6: Validation of the purity of the chemically synthesized CXCL4L1.** (A) SDS-PAGE silver gel staining showed the correct size of the synthesized protein (sCXCL4L1) compared to recombinant samples (rCXCL4L1). (B) The correct folding of the synthesized protein was also verified by a western blot using specific anti-CXCL4L1 antibodies. cont: CXCL4L1 control, synt: chemically synthesized CXCL4L1, rec: recombinant CXCL4L1.

## III.5 Functional analysis of CXCL4L1 and CXCL4

### III.5.1 CXCL4L1 and CXCL4 inhibit tube formation

Since CXCL4 had been well known for its angiostatic feature, we wanted to examine the effect of both CXCL4 variants in angiogenesis. We opted to assess the tube formation of microvascular endothelial cells (HDMEC) in matrigel as model. Matrigel was allowed to solidify with 5  $\mu\text{g}/\text{mL}$  of the respective chemokine or medium alone before culturing HDMECs for 20 hours (II.7.1). Tube length was analyzed by the web based S.CORE Online Image Analysis software and indicated in micrometers. As reported in the literature (Struyf 2004), CXCL4L1 significantly reduced tube length (Fig.III.5.1.1). On the other hand a difference between CXCL4L1 (142  $\mu\text{m}$ ) and CXCL4 (128  $\mu\text{m}$ ) with regards to the inhibition of endothelial tube formation could not be observed (control: 192  $\mu\text{m}$ ).

A



B

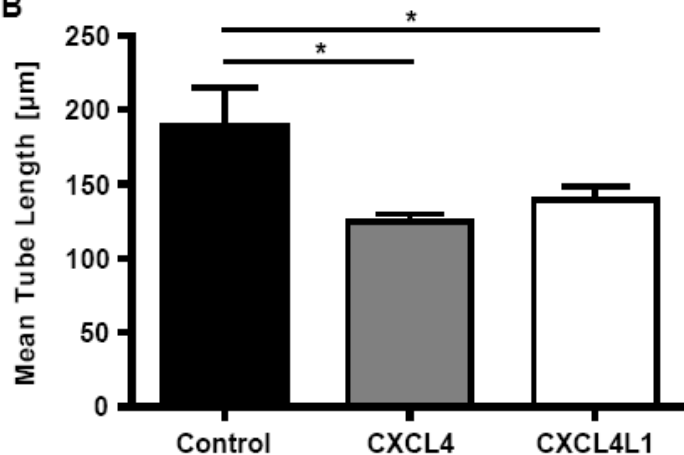


**Fig.III.5.1.1: CXCL4 and CXCL4L1 inhibit tube formation.** (A) HDMEC were seeded on matrigel with or without the indicated recombinant chemokine and allowed to form tubes for 20 hours. Shown are representative microscopic images, where compared to the control (medium) CXCL4 and CXCL4L1 inhibit continuous tube formation. (B) Tube length was analyzed by the online analysis program S.CORE (control: 192  $\mu\text{m}$ , CXCL4: 128  $\mu\text{m}$ , CXCL4L1: 142  $\mu\text{m}$ ). Statistical analysis was performed using the non-parametric Wilcoxon signed rank test (two-tailed;  $n = 5$  independent experiments; \*  $p < 0.05$ ). Images were recorded at 100x magnification.

### III.5.2 CXCL4L1 induces endothelial cell chemokinesis

Given the angiostatic effects of CXCL4 and CXCL4L1, we investigated the capacity of both chemokines to affect endothelial cell migration. HDMECs were labeled with calcein, and seeded into the upper well of a chemotaxis chamber. The migration of endothelial cells was quantified by determining the fluorescence intensity below the surface. HDMEC dose dependently migrated towards a CXCL4L1 gradient. Interestingly, endothelial cells migrated to a comparable extent significantly and dose-dependently even when the gradient of CXCL4L1 was disturbed by the addition of equal concentrations to the upper well (Fig.III.5.2.1 A). On the other hand, CXCL4 elicited only weak endothelial cell migration when applied with or without a gradient which did not reach statistical significance (Fig.III.5.2.1 B).

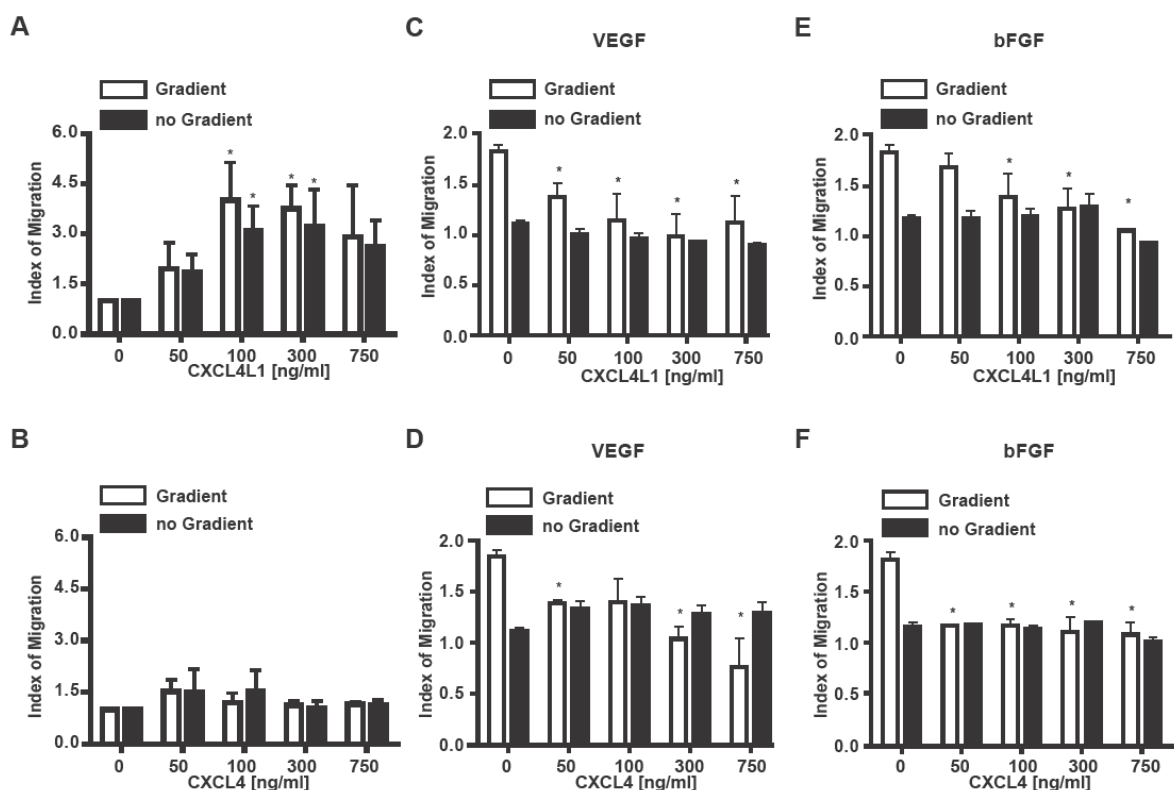


**Fig.III.5.2.1: Effect of CXCL4L1 and CXCL4 on endothelial cell migration.** Dose-dependent transmigration of calcein-labeled HDMEC with (empty bars) or without (filled bars) a gradient of recombinant CXCL4L1 (A) or CXCL4 (B) in combination with 20 ng/mL VEGF (C, D) or bFGF (E, F) was quantified by determining the fluorescence intensity in a modified Boyden chamber (Fluoroblok, Becton Dickinson) (n = 4-6 independent experiments, \* p<0.05 compared to control by ANOVA and post hoc analysis with Tukey's Multiple Comparison Test).

Accordingly, cell migration distance obtained by time-lapse video microscopy of HDMEC in a  $\mu$ -slide chemotaxis chamber (II.7.2) revealed that CXCL4L1 triggered the cells to

move a longer distance compared to CXCL4 (both 300ng/mL), which was significantly longer only compared to the control (Fig.III.5.2.2 A). Representative images of the migration paths of endothelial cells stimulated with the indicated chemokine or medium alone as control were selected (Fig.III.5.2.2 B).

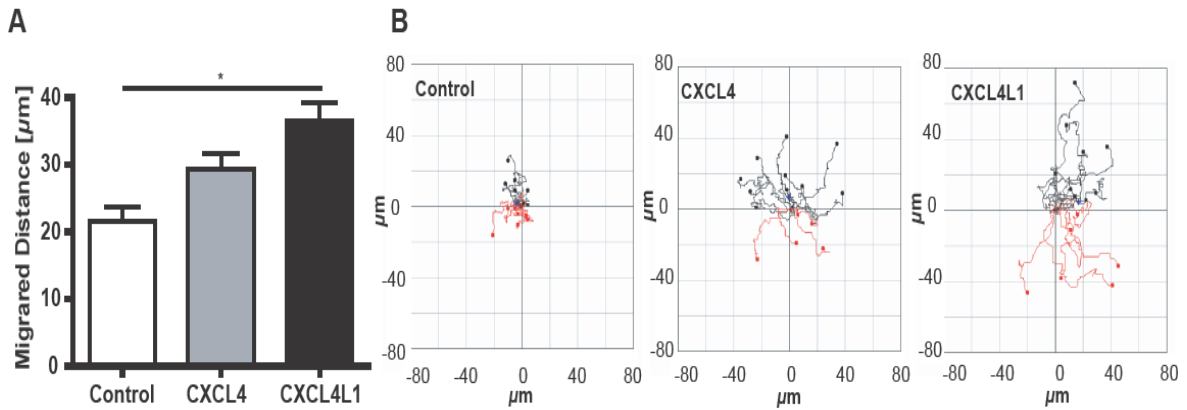


**Fig.III.5.2.2: Time lapse microscopy.** In a separate setup, the covered distance and direction were recorded online by video microscopy. (A) A stable gradient of CXCL4, CXCL4L1 or control medium alone was generated over firmly attached HDMEC in a  $\mu$ -slide chemotaxis chamber and cell tracks were recorded by video microscopy. The migrated distance in  $\mu\text{m}$  was determined ( $n = 45$  of 3 independent experiments). (B) Representative images of the migration pattern of HDMEC with the respective chemokine are shown (red lines indicate migration towards, black lines away from the stimulus).

### III.5.3 CXCL4L1 does not inhibit endothelial cell proliferation

The presence of CXCL4 inhibits the proliferation of different cell types including endothelial cells. This prompted us to compare the potential of CXCL4L1 and CXCL4 to inhibit HDMEC proliferation. To rule out contaminations during the isolation of the recombinant chemokines, we also studied the effects of synthesized chemokines side-by-side (II.4.7). Chemokines were added to HDMEC one hour after seeding to allow sufficient attachment, and proliferation was determined by analyzing the increase in DNA content using CyQuant<sup>®</sup> staining (II.7.3). Inhibition of cell proliferation was determined as percent inhibition compared to cells maintained in regular endothelial growth medium without chemokines. In general, no significant differences between recombinant and synthesized chemokines were observed. CXCL4 dose dependently inhibited endothelial cell proliferation (Fig.III.5.3.1 A). Using non-linear regression analysis, we calculated concentrations for half maximal inhibition of proliferation for recombinant (8.5  $\mu\text{g}/\text{mL}$ ), commercial-platelet-derived (6.9  $\mu\text{g}/\text{mL}$ ) and synthetic (6.7  $\mu\text{g}/\text{mL}$ ) CXCL4 (Table 2). In contrast to CXCL4, CXCL4L1 did not exert a measurable influence on the proliferation of endothelial cells. After 72 hours, recombinant CXCL4 at 10  $\mu\text{g}/\text{mL}$  inhibited endothelial cell proliferation by 44% versus 0% for CXCL4L1 (Fig.III.5.3.1 B, Table 2). Both,

recombinant as well as synthesized CXCL4L1, were unable to block proliferation.

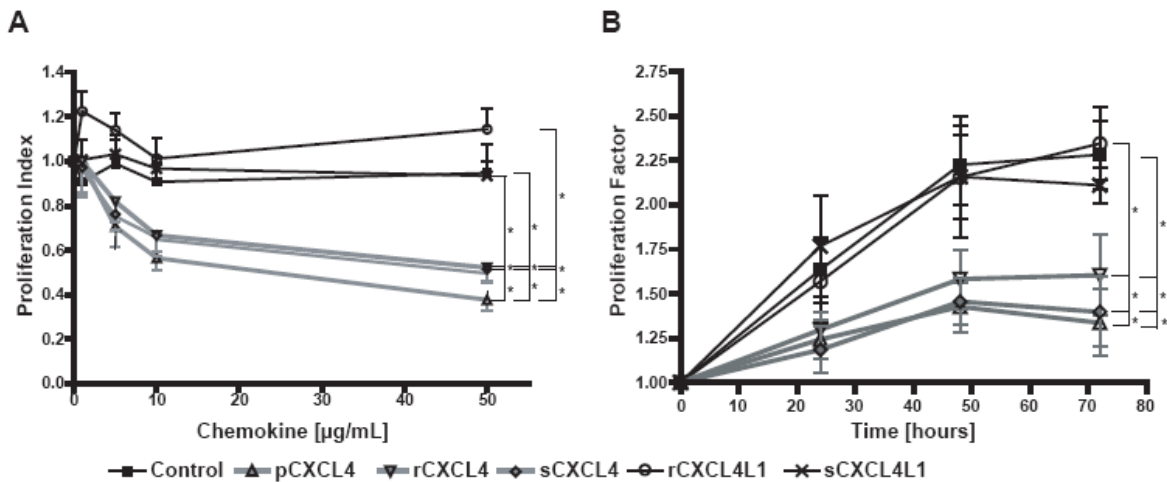


**Fig.III.5.3.1: CXCL4L1 and CXCL4 differentially affect endothelial cell proliferation.** (A) The HDMEC number was quantified by CyQuant®. Chemokines were added at increasing doses and compared to medium alone. The proliferation index was calculated from the increase in fluorescence after 72 hours of proliferation for medium alone divided by the increase obtained with a given chemokine concentration; (ANOVA was performed for 50 µg/mL; n = 4 independent experiments; \* p<0.05). (B) The time course was monitored for up to 72 hours with a constant chemokine concentration of 10 µg/mL (n = 4 independent experiments; ANOVA; \* p<0.05). Chemokines were used either as recombinant (prefix r), synthetic (prefix s) or purified protein from platelet packs (prefix p) as indicated.

	EC <sub>50</sub> µg/mL	Inhibition %
pCXCL4	6.91	68
rCXCL4	8.45	44
sCXCL4	6.69	61
rCXCL4L1	>70	0
sCXCL4L1	>70	15

**Table 2: Inhibition of endothelial cell proliferation by chemokines.** After non-linear regression analysis, the half-maximal effective inhibitory concentration (EC<sub>50</sub>) of CXCL4 and CXCL4L1 (prefixes: p = platelet-derived, r = recombinant, s = synthetic) for inhibition of HDMEC proliferation was calculated, and the inhibition of HDMEC proliferation with indicated chemokines at a concentration of 10 µg/mL after 72 hours is given as percentage of control.

### III.5.4 Hetero- and homooligomerization differ in CXCL4L1 and CXCL4

Since growth factors like bFGF and VEGF are the driving force for proliferation of endothelial cells and the inhibitory activity of CXCL4 on proliferation has been associated with direct binding of these factors, we semiquantitatively compared the interaction of VEGF, bFGF, and CCL5 using ligand blots (II.5.3). Incubation of CXCL4L1 with the immobilized proteins resulted in a measurable retention on immobilized VEGF, bFGF and CCL5, which was comparable to that of CXCL4 (Fig.III.5.4.1. A). Newly developed anti-CXCL4L1 bivalent Fab-miniantibody (II.3.8) was used for specific detection of CXCL4L1 (Fig.III.5.4.1. B). We also analyzed the affinity of CCL5 for CXCL4 and

CXCL4L1 by isothermal fluorescence titration (II.5.3) and observed a moderately reduced affinity of CXCL4L1 compared to CXCL4 (Fig.III.5.4.1. C). The titration of CXCL4L1, and CXCL4 respectively, into 200 nM CCL5 resulted in a significantly lower dissociation constant of  $26 \pm 1.2$  nM for CXCL4 compared to  $38 \pm 8.8$  nM for CXCL4L1. Thus a functional difference of CXCL4L1 may be explained by the reduced formation of pro-adhesive CCL5 heterodimers.

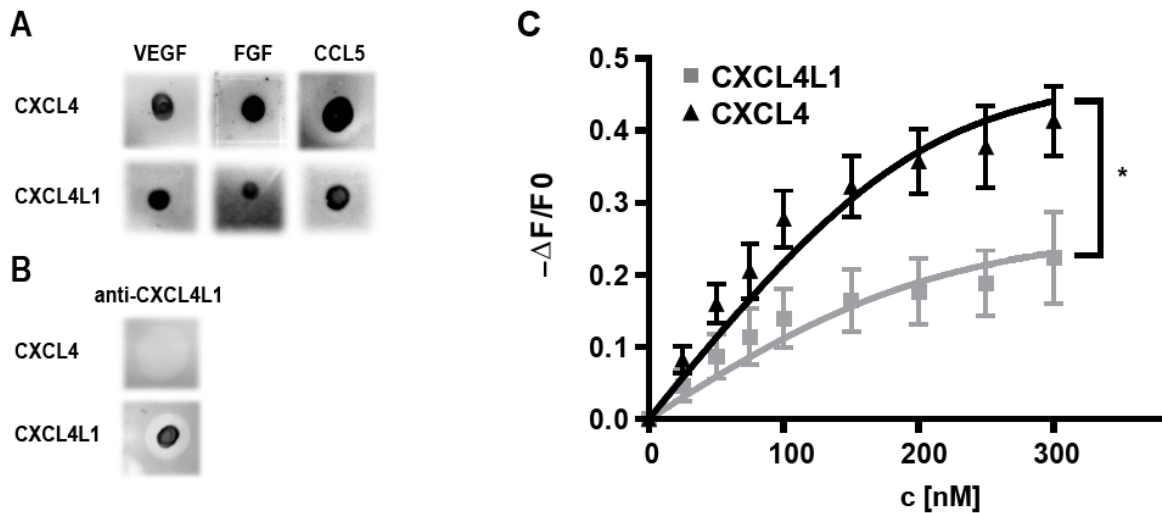


**Fig.III.5.4.1: Heterooligomerization of CXCL4 and CXCL4L1.** (A) CXCL4 or CXCL4L1 were incubated with immobilized VEGF, bFGF, and CCL5 ( $1.5 \mu\text{g}/\text{spot}$ ). Direct binding was determined by incubating either CXCL4 or CXCL4L1 ( $1 \mu\text{g}/\text{mL}$ ) and detection with anti-CXCL4L1 Fab-fragments and CXCL4 antibodies (representative of 3 independent experiments). (B) Specificity of the CXCL4L1 Fab-fragments ( $0.5 \mu\text{g}/\text{mL}$ ) is shown. (C) Fluorescence binding isotherms of the interaction of CCL5 with CXCL4 or CXCL4L1. The changes of endogenous fluorescence were plotted as the normalized fluorescence intensity changes ( $-\Delta F/F_0$ , where  $F_0$  is the initial fluorescence intensity). The dissociation constant  $K_d$  was derived from the isotherms which were fitted by non-linear regression ( $n = 4$  CXCL4 and CXCL4L1, Mann-Whitney test, \*  $p < 0.05$ ).

Since distinct oligomer formation might explain differential functional characteristics, recombinant CXCL4 and CXCL4L1 were crosslinked or left untreated before being separated by SDS-PAGE under non-reducing conditions. Untreated chemokines showed a visible monomer, dimer and trimer band. Addition of the crosslinker DSS revealed the existence of tetramers and aggregate formation of both chemokines (Fig.III.5.4.2. A). Thus an apparent difference in oligomeric state of CXCL4L1 could not be observed. We subjected CXCL4 and CXCL4L1 to gel filtration in order to quantify the different oligomeric states more accurately (Fig.III.5.4.2. B). Compared to inert molecular weights standards, both CXCL4 and CXCL4L1 eluted at a later time point than expected. This might be explained by an interaction with the column hampering an unequivocal allocation of the peaks to tetramer, dimer or monomer state. After injection at  $2 \text{ mg}/\text{ml}$ , CXCL4

eluted in three peaks consisting of 73 %, 19 % and 8 % area under the curve (AUC) of the total peak area in line with the known distribution of predominantly tetramers. Interestingly, the elution profile of CXCL4L1 was composed of only two peaks (60 % and 40 % of total protein), which eluted simultaneously with the putative CXCL4 dimers and monomers.

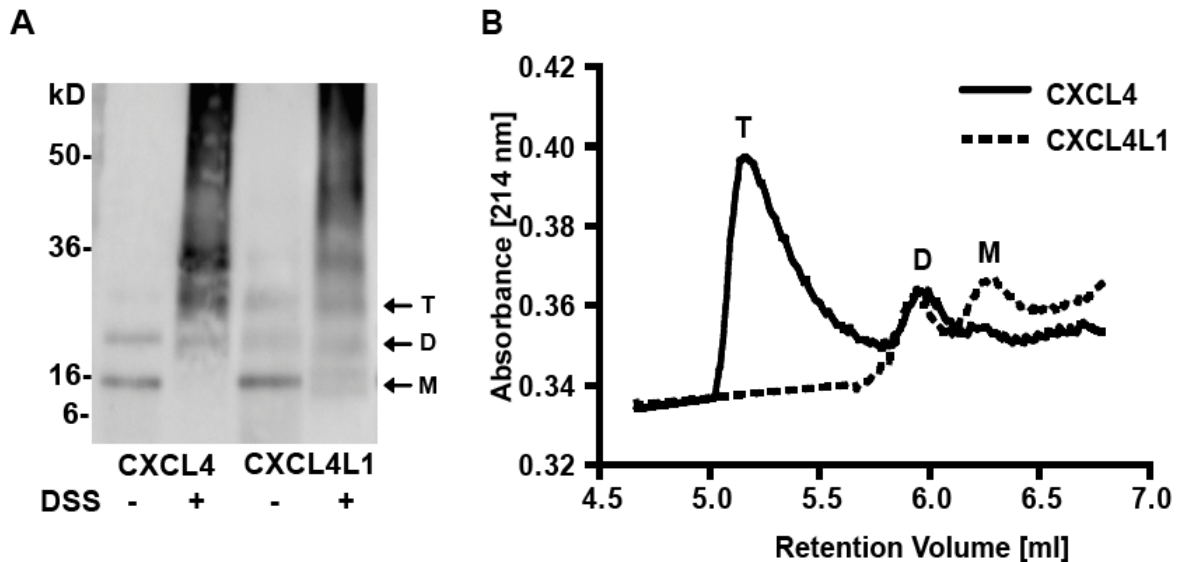


**Fig.III.5.4.2: Homooligomerization of CXCL4 and CXCL4L1.** (A) CXCL4L1 and CXCL4 were crosslinked (DSS) or left untreated and separated by SDS-PAGE under non-reducing conditions (representative of 3 independent experiments). (B) Homooligomerization was quantified by gel filtration of CXCL4 and CXCL4L1 on a Super-SW 2000 TSK column (1 mg/mL in 500 mM NaCl, 0.2% Tween, pH 7.0). The peaks of the putative tetramers, dimers and monomers are designated as T, D, and M.

### III.5.5 CXCL4L1 interaction with CCL5 does not enhance CCL5-triggered monocyte arrest

The functional relevance of the high-affinity interaction between CXCL4 and CCL5 has been shown previously (von Hundelshausen 2005). The formation of CCL5/CXCL4 heteromers enhanced the recruitment ability of CCL5 for monocytes arrest into the vascular wall. Here, we wanted to know if CXCL4L1 attained the same effect. Monocytic Mono Mac 6 cells pre-incubated with CCL5 or its combination with CXCL4 or CXCL4L1 were perfused on a monolayer of HUVECs. The coincubation of CCL5 with CXCL4 resulted in a significant enhancement of firm monocyte arrest, whereas CXCL4L1 failed to increase CCL5-triggered monocyte adhesion significantly (Fig.III.5.5.1 A).

These findings were supported by an *in vivo* assay demonstrating the robust recruitment of inflammatory monocytes into the peritoneal cavity after intraperitoneal injection of 5  $\mu$ g of CCL5. Addition of 5  $\mu$ g CXCL4 to CCL5 led to a further enhanced monocyte migration,

whereas injection of 5  $\mu\text{g}$  CXCL4L1 instead of CXCL4 did not enhance CCL5-induced monocyte recruitment (Fig.III.5.5.1 B).

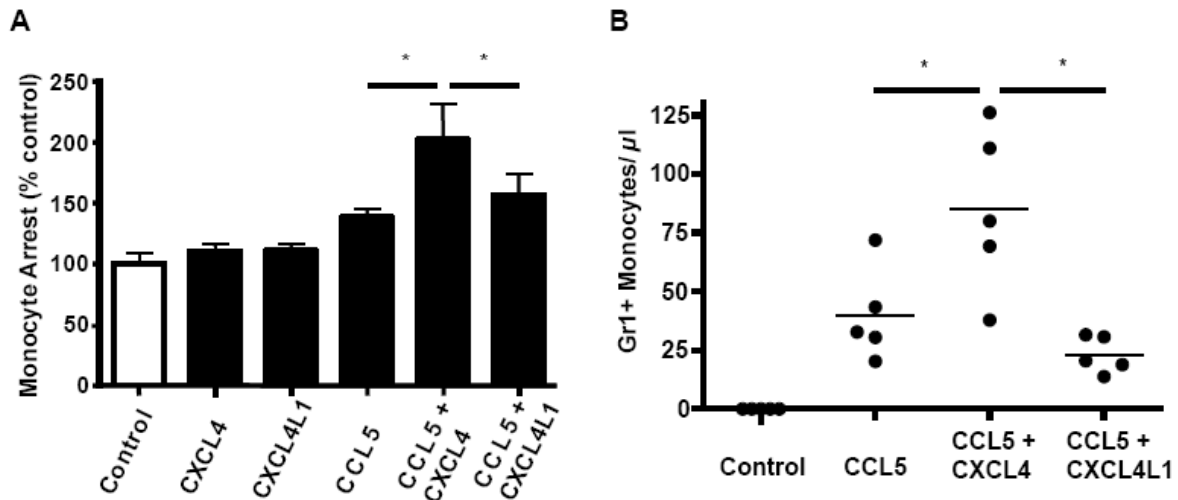


**Fig.III.5.5.1: Interaction of CXCL4 and CXCL4L1 with CCL5.** (A) The arrest stimulating activity of CXCL4 and CXCL4L1 on CCL5 (all recombinant) activated monocytic Mono-Mac-6 cells was investigated under flow conditions. Cells were pulsed with the indicated chemokine (300 ng/mL) and the number of firmly adherent monocytes was determined after accumulation for 5 minutes. Data represent SEM of 4 independent experiments (\*  $p < 0.05$ ). (B) Monocyte recruitment *in vivo*. The ability of recombinant CCL5, CXCL4, and CXCL4L1 (5  $\mu\text{g}$ ) to recruit cells were tested by i.p. (intraperitoneal) injection. After 4 hours, the inflammatory infiltrate was harvested and monocytes were discriminated by the markers F4/80, Gr-1, and CD115 by flow cytometry ( $n = 5$ , \*  $p < 0.05$  by Kruskal-Wallis test).

### III.5.6 Influence of CXCL4L1 on heparin neutralization and APC generation

CXCL4 prevents inhibition of blood coagulation proteases by heparin at least in part independent of antithrombin by forming an inhibitory ternary heparin-fXa-CXCL4 complex (Fiore 2009). The heparin-neutralizing activity of CXCL4 is well known and depends on positively charged amino acids, particularly lysine and arginine (Mayo 1995). We investigated differences in the heparin-neutralizing affinity by analyzing the aPTT (activated partial thromboplastin time, II.7.5) after adding heparin to pooled human normal plasma (Fig.III.5.6.1 A). In line with previous findings, the prolonged aPTT was reversed by adding CXCL4. Especially in the range of lower concentrations, CXCL4L1 less effectively neutralized the effect of heparin. The half-maximal concentration was achieved at 2  $\mu\text{g}/\text{mL}$  of CXCL4L1 compared to 1  $\mu\text{g}/\text{mL}$  of CXCL4.

Conversely, heparin reverses the APC-generating activity of CXCL4 (Slungaard 1994). APC is a potent anticoagulant by proteolytically inactivating factors Va and VIIIa and is



generated in the presence of thrombin and thrombomodulin by proteolytic cleavage of protein C. As it has been reported, CXCL4 binds and induces conformational changes in protein C and enhances APC generation (Dudek 1997). We compared the capacity of CXCL4 and CXCL4L1 to generate APC (II.7.6). After incubation of protein C with its cofactor thrombomodulin and the chemokines, the reaction was started with thrombin, stopped with hirudin, APC concentrations were derived from the amidolytic activity relative to a calibration curve. Again, CXCL4L1 exhibited a less pronounced effect on APC generation, as compared to CXCL4 (Fig.III.5.6.1 B).

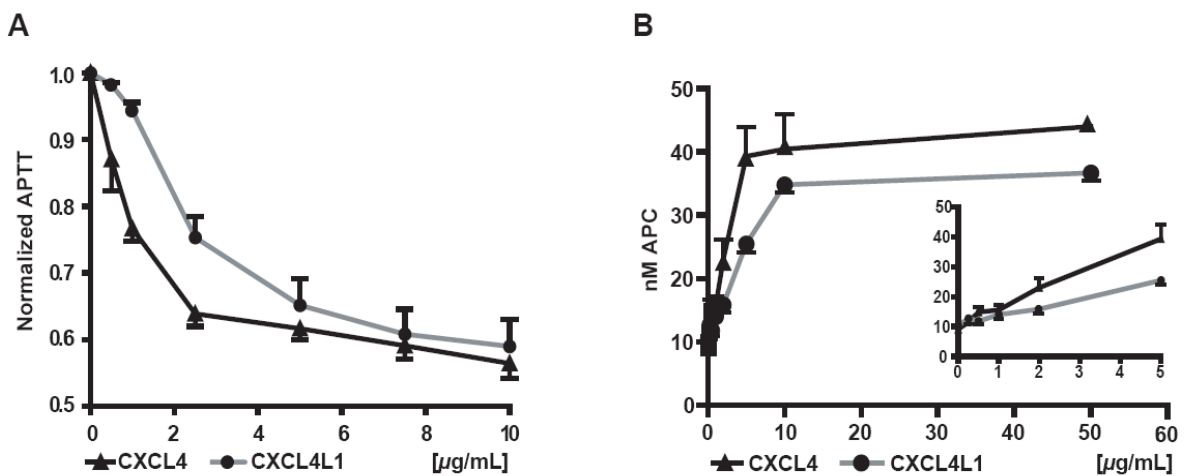


**Fig.III.5.6.1: Effects of CXCL4 and CXCL4L1 on heparin activity and APC generation.** (A) Heparin activity was measured by analyzing the activated partial thromboplastin time (aPTT) in heparinized pooled human plasma in the presence and absence of increasing concentrations of CXCL4 or CXCL4L1 (0 to 10  $\mu\text{g/mL}$ ). The clotting time was normalized to the time measured in the absence of additional CXCL4 and CXCL4L1 ( $n = 4$ ). (B) The concentration of APC after thrombin stimulation of thrombomodulin and protein C was determined by measuring the absorbance after cleavage of the chromogenic substrate S2366 ( $n = 4$ ). Since the lower concentrations appear to overlap in the graph an inset is depicted to more clearly demonstrate the difference of the curves.

## IV Discussion

### IV.1 Different expression strategies for obtaining the CCL5, CXCL4 and CXCL4L1

For the characterization and comparative studies, the chemokines CCL5, CXCL4 and CXCL4L1 were recombinantly expressed in a bacterial system using *E. coli* (II.2.2) in LB or <sup>15</sup>N-enriched medium (CCL5) and TB medium (CXCL4/CXCL4L1). Since these small proteins did not need any post-translational modifications, like e.g. glycosylation, the prokaryotic system seemed to be adequate. Two different approaches for the expression of these chemokines were used. CCL5 was expressed in the cytoplasm as inclusion bodies, whereas CXCL4 and CXCL4L1 were expressed as soluble, active proteins in the periplasm. For the expression of both chemokines the pET vector system (II.2.3) was used, where recombinant protein expression was under the control of the IPTG inducible T7lac promoter. Additionally the CXCL4L1 chemokine was also synthesized chemically using the solid phase peptide synthesis method (II.4.7).

CCL5 fused with thioredoxin was expressed using the pET-32a vector system. Although it has been reported that the thioredoxin tag would be beneficial for obtaining highly soluble protein in the cytoplasm (LaVallie 1993), the main batch of the recombinant CCL5 was expressed as insoluble inclusion bodies. As a disadvantage, expression of proteins as inclusion bodies required a solubilization and refolding step *in vitro* to obtain the protein in an active conformation. Critical steps were the choice of solubilizing agents, e.g. guanidine-HCl, where a monomolecular dispersion was essential and also the conditions for the refolding of the protein, where parameters like pH, presence of redox reagents, the speed of denaturant removal were important. Nevertheless inclusion bodies harbored also some advantages, e.g. they were easily isolated by centrifugation to yield highly concentrated homogenous protein and also proteolytic attacks were diminished by formation of inclusion bodies.

Although expression of recombinant protein as inclusion bodies included some additional effort, the received yield of fully active recombinant CCL5 was satisfactory for further characterization of CCL5. Furthermore, by incubating the expressing bacteria in <sup>15</sup>N-enriched medium, it was possible to produce recombinant <sup>15</sup>N-CCL5, which enabled an increased resolution in the structural determination of the heterodimerization of CCL5 with

CXCL4 (III.2).

For the expression of CXCL4 and CXCL4L1 the pET-26+ vector was chosen. The expression product of this vector was transported in the periplasmic space under hyperosmotic condition supplemented with compatible solutes such as betaine or glycerol (III.3). The pelB signal sequence of the pET-26+ vector allowed the secretion of the recombinant protein into the periplasm, where the pelB signal sequence was cleaved off from the recombinant protein by the bacterial enzymes at the cytoplasmic membrane resulting in an active protein without any additional tags. The periplasmic space with its oxidizing milieu (Bardwell 1993) also supported the disulfide bond formation and therefore the correct folding of the recombinant protein.

As already described for the expression of the immunotoxin in the periplasmic space (Barth 2000), low temperature (20-26°C), hyperosmotic conditions (4% NaCl) and at the same time protection of the recombinant proteins by compatible solubles (or osmolytes) supported formation of highly pure and correctly folded protein, although the yield was low. Beside the low yield the most challenging factor was the ineffective cleavage of the pelB signal sequence from the recombinant protein. A reason for this could be the overall positive net charge of the CXCL4 and CXCL4L1, since it has been reported that hydrophobic and positively charged amino acid residues can block the export of proteins into the periplasmic space when introduced after the pelB signal sequence (Kajava 2000). Nevertheless the compatible solute-supported periplasmic expression offered an alternative method for expression of soluble, active and correctly folded recombinant proteins, without involving an *in vitro* refolding step.

As already mentioned, CXCL4L1 was also synthesized chemically by the SPPS method to obtain highly purified protein. Since the SPPS method is limited to 40-60 amino acid residues, the CXCL4L1 was synthesized in two peptide parts (N-terminal and C-terminal) and assembled by native chemical ligation (Fig.II.2). The synthesis of each peptide part started with the C-terminal amino acid and ended with the N-terminal amino acid (Fig.II.1), where the amino acids were connected sequentially step-by-step. To prevent a misfolding and undesired polymerization the side chains of the growing polypeptide were protected by a t-Boc group. Removal of the protecting group and the peptide from the resin was achieved by treatment with the highly toxic HF (hydrofluoric acid). The ligation of the unprotected peptide segments was performed as described in section II.4.7 which resulted in a fully functional active CXCL4L1. The correct formation of the disulfide bonds was

also proven by a shortened retention time of the folded CXCL4L1 compared to the unfolded extended byproducts by RP-HPLC (Fig.III.4.4), because of the more polar surface area. The refolding was also demonstrated by ESI-MS, where a shift from a higher  $m/z$  state (unfold) to a lower  $m/z$  state (folded) was observed (Fig.III.4.5), due to less potential residues for carrying a charge on native, folded proteins under ESI-MS ionization conditions compared to unfolded.

Taken together, synthesizing CXCL4L1 by the SPPS method resulted in the generation of highly pure protein with a higher yield compared to recombinant techniques.

## **IV.2 Structural differences between CXCL4 and CXCL4L1**

The amino acid changes in mature CXCL4L1 (proline-58 to leucine, lysine-66 to glutamic acid, leucine-67 to histidine) may cause significant alterations in the secondary structure of the protein. All three residues are conserved in human (Walz 1977), rat (Doi 1987), and bovine (Ciaglowski 1981) CXCL4. Therefore, the differences in CXCL4L1 are not likely caused by CXCL4 gene duplication. The proline-58 to leucine change could have a major effect on the secondary structure of the protein because the carboxy-terminal helix of CXCL4 starts at proline-58. Since proline is a helix breaker, the change to leucine could extend the helix in the amino-terminal direction and alter the turn at positions 55 to 57 that links the helix to the third strand of the  $\beta$ -sheet. Due to the lysine-66 to glutamic acid change, the carboxy-terminal region of CXCL4L1 would be less positively charged than that of CXCL4, which could also explain the reduced interaction with the anionic heparin. The leucine-67 to histidine change could also significantly alter the characteristics of the carboxy-terminal helix. Leucine-67, which is between the helix and the hydrophobic surface of the  $\beta$ -sheet, is buried and surrounded by hydrophobic residues. Histidine at this position, especially if it is protonated, would weaken the packing of the helix against the sheet (Green 1989).

The leader sequence of the CXCL4L1 gene showed the greatest change from that of CXCL4. Albeit only 15 of the 93 nucleotides were different, except for a three-codon insert in the middle of the sequence. However, these differences resulted in an increased net positive charge of the CXCL4L1 leader sequence resulting from five arginine residues compared with only one for CXCL4. This may imply a difference in the tissue or cell type in which CXCL4L1 is expressed or a difference in its mode of secretion (Lasagni 2007).

Interestingly CXCL4 in combination with CXCL8, which is also present in platelets,

showed an inhibitory effect by blocking CXCL8 mediated activation of hematopoietic stem cells (Dudek 2003) and increased anti-proliferative effects from CXCL4 on endothelial cells in culture (Nesmelova 2005).

The conserved monomer structure of all of the CXC and CC chemokines generally allows heterodimerization. The interaction of specific pairs of amino acid residues at the dimer interface of individual monomers seems to dictate the nature of thermodynamic stability and selection of dimer type (CXC or CC). This applies especially for CXC-CC mixed heterodimers, where placement of specific amino acid residues (positively/ negatively charged, polar, or hydrophobic) within the  $\beta$ -strand 1 and/or within the N-terminus determines selection of CXC-type or CC-type heterodimers. It has been shown that for CXCL4 the homodimerization is thermodynamically unfavorable because of the repulsion of the positively charged amino acids at their dimerization site, whereas in a tetramer formation these amino acids do not repel each other. Moreover, in a CXCL4-CXCL8 interaction, CXCL8 is responsible for the dissociation of the CXCL4 tetramer and supports the formation of CXCL4-CXCL8 heterodimers. In general, heterodimerization is mediated primarily by non-electrostatic interactions, with the exception of CXCL8 and CCL5 where electrostatic forces contribute significantly to the binding free energy (Nesmelova 2008).

### **IV.3 CXCL4-CXCL4L1 functional comparison**

Platelets play a crucial role in the manifestation of atherosclerosis. They either act directly by rolling and adhering to the endothelial cells or indirectly by releasing stimulatory mediators (e.g. chemokines). Upon activation, platelets secrete chemokines from their  $\alpha$ -granules, which are deposited onto endothelial cells and participate in the progression of atherosclerosis. It has been shown that injection of activated platelets in *ApoE*<sup>-/-</sup> mice exacerbates atherosclerotic lesion formation and delivers chemokines, such as CCL5 and CXCL4 onto atherosclerotic endothelium led to an increased monocyte arrest recruitment and followed by transmigration of the endothelium (Huo 2003).

In chronic inflammatory processes such as atherosclerosis, CXCL4 plays a proatherogenic role which is not yet fully understood (von Hundelshausen 2007). A potential mechanism resides in its enhancing effects on the subintimal recruitment of monocytes by CCL5. It has been shown that CCL5-induced monocyte arrest can be enhanced by high-affinity interaction with CXCL4, which has a considerable impact on the development of atherosclerotic lesions in the mouse. Moreover, using pulsed field gradient NMR self-

diffusion experiments demonstrated that CCL5 induced dissociation of CXCL4 tetramers, which were normally formed in solution (Mayo 1989; Koenen 2009) and promoted formation of CCL5-CXCL4 heterodimers in a CC-type configuration. Furthermore, this synergistic enhancement of the monocyte-recruiting function of CCL5 could be blocked by peptides disrupting the interaction of CXCL4 and CCL5, which expanded the therapeutic potential of anti-atherosclerotic treatment. A synthetic cyclic peptide, named CKEY2, based on CCL5 residues 24-44 ( $\beta$ 1 and  $\beta$ 2 strands), competed with CXCL4 for binding to the N-terminus of CCL5 ( $K_d = 100$  nM). Through introduction of the murine peptide orthologue, MKEY, into hyperlipidemic mice on high fat diet, the inhibition of the enhancement of CCL5-induced monocyte arrest by CXCL4 was verified also *in vivo*. The progression of atherosclerosis and the monocyte accumulation in the plaque were significantly reduced compared to a scrambled control peptide. Unlike the treatment with the CCL5 antagonist Met-CCL5, where the T-cell proliferation and the virus clearance were impaired (Sorensen 2004), immunological side effects and hampered normal CCL5-related survival signals had not been observed by treatment with MKEY (Koenen 2009).

Other than CXCL4, CXCL4L1 failed to enhance CCL5 induced monocyte arrest which might be explained by the reduced affinity to CCL5. Nevertheless the substitutions of the 3 amino acids in the C-terminal helix of CXCL4L1 seem to influence the structure of the protein at such rate that different physiological effects occur. The remaining affinity of CXCL4L1 to CCL5 is probably due to the N-terminal interaction as observed for the CC-type of the CXCL4-CCL5 heterodimer.

In the course of evolution, a possible duplication of the CXCL4 gene might have occurred quite recently, because an orthologue gene sequence was not identified in the mouse genome (Eisman 1990). The absence of the CXCL4L1 gene in rodents suggests that it may not have a critical role in platelet function. Nevertheless it has been reported that CXCL4L1 in humans exerts a more effective angiostatic activity than CXCL4.

Since a direct comparison of CXCL4 and CXCL4L1 has not yet been performed so far, we were prompted to uncover biological differences between these proteins, which might lead to a better understanding of their role in the physiology and pathophysiology of blood and vascular diseases. Although exact mechanisms are not yet fully elucidated, CXCL4 and CXCL4L1 both exert angiostatic effects (Struyf 2004). Angiogenesis is a finely regulated process requiring multiple stimulatory and inhibitory molecular cues and is dependent on both, the proliferation and/or the recruitment/migration of endothelial or endothelial

progenitor cells and their correct assembly (Carmeliet 2005). Thus, the directed migration of endothelial cells is crucial for the development of a prevascular structure. Relevant chemotactic properties for different leukocyte populations, which have initially been ascribed to CXCL4 in the 1980s, could not be reproduced and might therefore have been due to concomitantly isolated chemokines during protein purification from platelets. However, recent findings indicate chemotactic properties of CXCL4 in activated T cells (Mueller 2008). Our finding that endothelial cell migration is rather weakly induced by CXCL4 and much more potently induced by CXCL4L1 in a transwell-filter assay is only at first sight contradictory to findings by Struyf et al., who found CXCL4L1 to be a potent inhibitor of bFGF- and CXCL8-mediated endothelial cell migration in a similar chemotaxis assay. The migration pattern of endothelial cells in the  $\mu$ -slide chamber, which permits analyzing the direction and length of the covered distance, reveals that CXCL4L1 primarily stimulates endothelial cell motility and increases migration length but does not influence the direction of cell movement. These experiments as well as checker-board analysis indicate that CXCL4L1 induces random migration that lacks directionality (chemokinesis) rather than enhanced-rate locomotion with a gradient-imposed, unidirectional migration (chemotaxis) of endothelial cells. Of note VEGFA, a highly potent angiogenic factor elicits chemotaxis and simultaneously reduces chemokinesis emphasizing the importance of the directed endothelial migration for angiogenesis (Barkefors 2008). Our experiments confirm these observations, since both VEGF and bFGF were chemotactic yet able to block CXCL4L1 induced chemokinesis. Although endothelial cells in culture are adjusted to similar conditions such as growth factor supplement and lack of shear stress, their provenience leaves site-specific properties which are epigenetically programmed (Aird 2007). Thus, for instance microvascular endothelial cells of dermal or pulmonary origin may deviate in their phenotype which may lead to differences in experimental results. The angiostatic mechanism of CXCL4 has been proposed to depend on specific inhibition or competition of growth factor-stimulated endothelial cell proliferation e.g. bFGF and VEGF (Maione 1990; Gengrinovitch 1995). The effects of CXCL4L1 on undirected endothelial migration may be also mediated by a replacement of other growth factors or by direct activation of CXCR3 and thus, may provide an alternative explanation for angiostatic effects.

In line with these results, CXCL4 inhibited endothelial cell proliferation, whereas surprisingly, CXCL4L1 had no effect. We found the required concentration of CXCL4 to

exert a half maximal inhibition of endothelial cell proliferation at a micromolar level and thus orders of magnitude higher than the concentration of pro-inflammatory CCL5 being biologically effective at nanomolar levels which is in line with previous results (Gentilini 1999). CXCL4L1 exerted endothelial chemokinesis, reflecting potential receptor binding and signaling differences. Plasma concentrations of CCL5 being much lower than those of CXCL4 reflect these distinct mechanisms since CCL5-driven chemotaxis is exerted via high affinity binding to G-protein coupled receptors while the mechanisms of the biologic effects of CXCL4 and CXCL4L1 are still incompletely understood and can not be entirely explained by the existence of CXCR3A and CXCR3B (von Hundelshausen 2007; Mueller 2008). It has been shown that endothelial survival and proliferation is dependent on heparin-binding growth factors, most prominently VEGF which needs heparin-like/decorated molecules for its receptor stimulating activity. The anti-VEGF activity of CXCL4 has been explained by direct binding to VEGF and its high affinity to heparin may competitively displace VEGF from cell surface heparan sulfates and VEGF receptors (Gengrinovitch 1995). The difference in the anti-proliferative activity between CXCL4 and CXCL4L1 might be explained by the absence of direct binding of CXCL4L1 to bFGF and VEGF. However, CXCL4 and CXCL4L1 behave similarly in this regard, as demonstrated by semiquantitative ligand blots. The affinity of CXCL4 to heparin-like molecules results in a gaugeable prolongation of the clotting time (Fiore 2003). The distinct oligomer distribution of CXCL4L1 and CXCL4 may be important for their distinct affinities for CCL5 and glycosaminoglycans. It has been shown that under physiologic pH and salt conditions, CXCL4 predominantly forms tetramers, which in turn form complexes with heparin (Rauova 2005). It is conceivable that the reduced tetramer formation of CXCL4L1 may be one of the reasons for a decreased GAG-affinity, besides charge differences. In this study, CXCL4L1 showed a lower heparin-neutralizing activity as compared to CXCL4, indicating a lower affinity to heparin which can explain to some extent the abolished effect on endothelial cell proliferation by inactivating less VEGF. However, the differences in the primary amino acid sequence affect only the C-terminal  $\alpha$ -helix. Initially, it was thought that this region, especially the lysine residues are responsible for the interaction with heparin (Loscalzo 1985). However, later performed NMR studies point to a minor role of this region (Mayo 1995) and favor arginine residues, which are located in the loops between the three-stranded anti-parallel  $\beta$ -sheet. This is in accordance with our data, since heparin neutralization by CXCL4L1 is still well detectable. Although CXCL4L1 exhibits



lower heparin neutralizing affinity than CXCL4 and has no proliferation blocking effect, it has a comparative effect on inhibiting angiogenesis, as determined by endothelial tube formation. Animal *in vivo* studies have shown an even stronger angiostatic activity of CXCL4L1 as compared to CXCL4 in a tumor model (Struyf 2007).

Our results that CXCL4L1 less potently enhances APC generation may be due to the decreased affinity of CXCL4L1 to glycosaminoglycans, since this activity depends partly on the presence of a sulfated chondroitin moiety on thrombomodulin (Dudek 1997). Thus, the positive influence of CXCL4 in acute inflammatory syndromes like sepsis might not be exerted by CXCL4L1.

In chronic inflammatory processes such as atherosclerosis, CXCL4 plays a proatherogenic role which is not yet fully understood (von Hundelshausen 2007). A potential mechanism resides in its enhancing effects on the subintimal recruitment of monocytes by CCL5. Previously, it has been shown that CCL5 induced monocyte arrest can be enhanced by high-affinity interaction with CXCL4, which has a considerable impact on the development of atherosclerotic lesions in the mouse and can be blocked by peptides disrupting the interaction of CXCL4 and CCL5 (von Hundelshausen 2005; Koenen 2009). Unlike CXCL4, CXCL4L1 failed to enhance CCL5-induced monocyte arrest which might be explained by the reduced affinity to CCL5. The remaining affinity of CXCL4L1 to CCL5 is probably due to a N-terminal interaction as observed for the CC-type of the CXCL4-CCL5 heterodimer (Koenen 2009). Our finding that monocyte recruitment into the peritoneal cavity in mice was likewise enhanced following injection of CXCL4 but not of CXCL4L1 indicates a minor role for CXCR3B, which does not exist in mice.

Taken together, we identified that CXCL4L1 elicits in contrast to CXCL4 no anti-proliferative activity on endothelial cells and neutralizes to a lesser extent heparin and generates less APC. However, angiostatic activity is still noted and may be explained by the induction of chemokinesis, impeding the correct assembly of endothelial cells in the process of tube formation.

Moreover, our finding that CXCL4L1, compared to CXCL4 has a reduced affinity for CCL5 and heparin, may have implications for understanding of the equilibrium of both chemokines. CXCL4L1 may act as a homeostatic chemokine primarily as a weak antagonist of CXCL4 with angiostatic effects inducing random endothelial migration, whereas CXCL4 is the more pro-inflammatory chemokine.

## V Summary

Chemokines play an important role in the development of inflammation and in the recruitment of leukocytes from the vessel into the inflamed tissue. Activated platelets serve as a rich source of chemokines, e.g. CCL5, CXCL4 and its closely related variant CXCL4L1. The pro-inflammatory CCL5 is a known potent chemoattractant for monocytes and also responsible for its arrest on inflamed endothelium. Since this arrest is enhanced by the interaction of CCL5 with CXCL4, we aimed to determine the structural interaction of this CCL5-CXCL4 heterodimer in the first part of this thesis.

For this purpose, CCL5, CXCL4 and CXCL4L1 were expressed recombinantly in *E. coli* by different techniques, CCL5 as inclusion bodies in the cytoplasm, CXCL4 and CXCL4L1 as soluble proteins in the periplasmic space. For structural analysis of the heterodimerization of the CCL5-CXCL4 complex, <sup>15</sup>N-enriched CCL5 was expressed. Additionally, CXCL4L1 was chemically synthesized by the solid-phase peptide synthesis method. All generated proteins were purified by sequential steps with chromatographic methods using FPLC and HPLC.

Chemical shift mapping of the <sup>15</sup>N-CCL5 by the <sup>15</sup>N-<sup>1</sup>H heteronuclear single quantum coherence (HSQC) nuclear magnetic resonance (NMR) and 3D modeling revealed that the N-termini were responsible for the formation of the CCL5-CXCL4 heterodimer.

In the second part of this dissertation, a functional comparison between CXCL4 and CXCL4L1 was carried out to evaluate the differences of these closely related chemokines. This comparison revealed that the angiogenesis, as assessed by endothelial tube formation, was inhibited by CXCL4 as well as CXCL4L1, but only CXCL4L1 triggered undirected locomotion of endothelial cells (chemokinesis). The chemotactic response towards the growth factors VEGF and bFGF was attenuated by both variants but only CXCL4L1-induced chemokinesis was blocked by bFGF or VEGF. Endothelial cell proliferation was inhibited by CXCL4 but not by CXCL4L1, while both chemokines bound directly to VEGF and bFGF. Moreover, CXCL4 enhanced CCL5-induced monocyte arrest *in vitro* and as well *in vivo*, whereas CXCL4L1 had no effect. CXCL4L1 revealed lower affinity for CCL5 than CXCL4 as quantified by isothermal fluorescence titration. As evidenced by the reduction of the activated partial thromboplastin time, CXCL4L1 exhibited less heparin-neutralizing activity than CXCL4. In addition, activation of protein C by

thrombin/thrombomodulin was less effectively accelerated by CXCL4L1 compared with CXCL4. It was also discovered that the C-terminal natural changes in CXCL4L1 compared to CXCL4 determine a different quaternary structure since CXCL4 predominantly exists as tetramer and CXCL4L1 as dimer under physiological conditions despite a comparable general positive charge. These structural differences are closely related to the different biological effects most prominently exemplified by the distinct effects in monocyte recruitment and angiogenesis.

Summing up, CXCL4L1 may act angiostatically by causing random endothelial cell locomotion, disturbing directed migration towards angiogenic chemokines, serving as a homeostatic chemokine with a moderate structural distinction yet different functional profile from CXCL4.

## VI Zusammenfassung

Chemokine spielen eine wichtige Rolle bei der Entstehung von Entzündungsprozessen und bei der Rekrutierung von Leukozyten aus dem Gefäß in das entzündete Gewebe. Aktivierte Blutplättchen stellen eine wichtige Quelle für Chemokine dar, z.B. CCL5, CXCL4 und dessen eng verwandte Variante CXCL4L1. Das proinflammatorische Chemokin CCL5 ist ein auf Monozyten stark chemotaktisch wirkender Lockstoff, welcher auch deren Arrest auf entzündetem Endothel vermittelt. Da dieser Arrest durch die Interaktion von CCL5 mit CXCL4 verstärkt wird, war das Ziel im ersten Teil der Studie die strukturelle Wechselwirkung des CCL5-CXCL4 Heteromers aufzuklären.

Zu diesem Zweck wurden CCL5, CXCL4 und CXCL4L1 mithilfe von unterschiedlichen Methoden in *E. coli* rekombinant exprimiert, CCL5 als Einschlusskörperchen im Cytoplasma, CXCL4 und CXCL4L1 als lösliche Proteine im periplasmatischen Raum. Zur strukturellen Analyse der CCL5-CXCL4 Heteromerisierung, wurde <sup>15</sup>N-angereichertes CCL5 exprimiert.

Des Weiteren wurde CXCL4L1 mit Hilfe der Festphasensynthese chemisch erzeugt. Alle so gewonnenen Proteine wurden in sequenziell aufeinanderfolgenden Schritten chromatographisch, mittels FPLC und HPLC, weiter aufgereinigt.

Die chemische Verschiebung von <sup>15</sup>N-CCL5, welche durch die HSQC-Kernresonanzspektroskopie ermittelt wurde, und die Erstellung eines 3D Modells, machten die zentrale Bedeutung der N-terminalen Domänen bei der Heteromerisierung der Chemokine CCL5-CXCL4 deutlich.

Im zweiten Teil dieser Arbeit wurde ein funktioneller Vergleich zwischen CXCL4 und CXCL4L1 durchgeführt, um die Unterschiede der eng miteinander verwandten Proteine zu analysieren. Dieser Vergleich zeigte, dass sowohl CXCL4 als auch CXCL4L1 die Angiogenese, gezeigt durch die Fähigkeit von Endothelzellen gefäßähnliche Strukturen auszubilden, inhibierten. Aber nur CXCL4L1 war in der Lage eine ungerichtete Migration der Endothelzellen (Chemokinese) auszulösen. Die chemotaktische Reaktion auf die Wachstumsfaktoren VEGF und bFGF wurde zwar durch beide Proteinvarianten vermindert, aber nur die CXCL4L1 bedingte Chemokinese konnte durch bFGF oder VEGF geblockt werden. Während beide Chemokinvarianten in der Lage waren an VEGF und bFGF direkt zu binden, inhibierte nur CXCL4 die Proliferation der Endothelzellen.

Darüber hinaus konnte sowohl *in vitro* als auch *in vivo* gezeigt werden, dass nur CXCL4 den CCL5-induzierten Monozytenarrest vermittelt.

Mittels der isothermalen Fluoreszenztitration wurde für CXCL4L1 eine geringere Affinität als für CXCL4 zu CCL5 nachgewiesen. Wie durch die Abnahme der aktivierten partiellen Thromboplastinzeit gezeigt werden konnte, weist CXCL4L1 eine schwächere Aktivität der Heparin-Neutralisierung als CXCL4 auf. Auch die Aktivierung von Protein C durch Thrombin/Thrombomodulin wurde im Vergleich zu CXCL4 durch CXCL4L1 weniger beschleunigt. Es konnte weiter gezeigt werden, dass die unterschiedlichen C-terminalen Enden auch die quartäre Struktur der beiden Proteine beeinflussen, da trotz der gleichen Ladung der Proteine, CXCL4 unter physiologischen Bedingungen überwiegend als Tetramer, aber CXCL4L1 mehrheitlich als Dimer vorhanden ist. Diese strukturellen Unterschiede könnten auch für die unterschiedlichen biologischen Wirkungen der Proteinvarianten verantwortlich sein, z.B. in der Monozytenrekrutierung und der Angiogenese.

Zusammenfassend kann man vermuten, dass CXCL4L1 angiostatisch wirkt, indem es eine ungerichtete Lokomotion der Endothelzellen auslöst und dadurch die gerichtete Migration entlang eines angiogenen Chemokingradienten beeinträchtigt. Darüber hinaus stellt CXCL4L1 im Vergleich zu CXCL4 ein homeostatisches Chemokin mit einer leichten strukturellen Abweichung und dadurch veränderten funktionellen Eigenschaften dar.

## VII Acknowledgement

I would like to thank Prof. Dr. Christian Weber for the possibility to work in his institute on an interesting topic and for his scientific support.

I am also very grateful to Prof. Dr. Rainer Fischer for reviewing my thesis and helpful discussions during this work.

Special thanks to my supervisor Dr. Rory Koenen and Dr. Philipp von Hundelshausen for the help and guidance through these years in the lab, good discussions and collaboration.

Thank you very much to Birgit, Sabine and Jolanta, for the help and support in the lab and for giving me moral uplift, when every time needed. Thank you to Svenja, Yvonne, Maik, Martin S, Delia, Oli, Susanne, Michael, Martin H and of course Regina for the wonderful atmosphere in and also out of the lab, particularly in the poker evenings and afterwards.

I would also like to thank all the other colleagues from the IMCAR lab for the nice and cheerful time, especially during the ‘discussion rounds’ at the kicker table.

I also thank Tilman Hackeng and Denis Suylen from CARIM for good collaborations.

Last but not least, I would like to thank my family and friends for their support and distraction from the daily routine.

**VIII      References**

Aidoudi, S., K. Bujakowska, et al. (2008). "The CXC-chemokine CXCL4 interacts with integrins implicated in angiogenesis." *PLoS One* **3**(7): e2657.

Aird, W. C. (2007). "Phenotypic heterogeneity of the endothelium: I. Structure, function, and mechanisms." *Circ Res* **100**(2): 158-73.

Baltus, T., P. von Hundelshausen, et al. (2005). "Differential and additive effects of platelet-derived chemokines on monocyte arrest on inflamed endothelium under flow conditions." *J Leukoc Biol* **78**(2): 435-41.

Bardwell, J. C., J. O. Lee, et al. (1993). "A pathway for disulfide bond formation in vivo." *Proc Natl Acad Sci U S A* **90**(3): 1038-42.

Barkefors, I., S. Le Jan, et al. (2008). "Endothelial cell migration in stable gradients of vascular endothelial growth factor A and fibroblast growth factor 2: effects on chemotaxis and chemokinesis." *J Biol Chem* **283**(20): 13905-12.

Barth, S., M. Huhn, et al. (2000). "Compatible-solute-supported periplasmic expression of functional recombinant proteins under stress conditions." *Appl Environ Microbiol* **66**(4): 1572-9.

Bello, L., C. Giussani, et al. (2002). "Suppression of malignant glioma recurrence in a newly developed animal model by endogenous inhibitors." *Clin Cancer Res* **8**(11): 3539-48.

Blum, H., H. Beier, et al. (1987). "Improved silverstaining of plant proteins, RNA and DNA in polyacrylamide gels." *Electrophoresis* **8**: 93-99.

Brandt, E., A. Ludwig, et al. (2000). "Platelet-derived CXC chemokines: old players in new games." *Immunol Rev* **177**: 204-16.

Carmeliet, P. (2005). "Angiogenesis in life, disease and medicine." *Nature* **438**(7070): 932-6.

Chang, T. L., C. J. Gordon, et al. (2002). "Interaction of the CC-chemokine RANTES with glycosaminoglycans activates a p44/p42 mitogen-activated protein kinase-dependent signaling pathway and enhances human immunodeficiency virus type 1 infectivity." *J Virol* **76**(5): 2245-54.

Charo, I. F. and M. B. Taubman (2004). "Chemokines in the pathogenesis of vascular disease." *Circ Res* **95**(9): 858-66.

Chung, C. W., R. M. Cooke, et al. (1995). "The three-dimensional solution structure of RANTES." *Biochemistry* **34**(29): 9307-14.

Ciaglowski, R. E., J. W. Snow, et al. (1981). "Bovine platelet antiheparin protein: platelet factor 4." *Ann N Y Acad Sci* **370**: 668-79.

- Clore, G. M. and A. M. Gronenborn (1995). "Three-dimensional structures of alpha and beta chemokines." Faseb J **9**(1): 57-62.
- Combadiere, C., S. K. Ahuja, et al. (1995). "Cloning and functional expression of a human eosinophil CC chemokine receptor." J Biol Chem **270**(28): 16491-4.
- Davi, G. and C. Patrono (2007). "Platelet activation and atherothrombosis." N Engl J Med **357**(24): 2482-94.
- Dawson, P. E., T. W. Muir, et al. (1994). "Synthesis of proteins by native chemical ligation." Science **266**(5186): 776-9.
- Deuel, T. F., P. S. Keim, et al. (1977). "Amino acid sequence of human platelet factor 4." Proc Natl Acad Sci U S A **74**(6): 2256-8.
- Doi, T., S. M. Greenberg, et al. (1987). "Structure of the rat platelet factor 4 gene: a marker for megakaryocyte differentiation." Mol Cell Biol **7**(2): 898-904.
- Dorsam, R. T. and J. S. Gutkind (2007). "G-protein-coupled receptors and cancer." Nat Rev Cancer **7**(2): 79-94.
- Dudek, A. Z., I. Nesmelova, et al. (2003). "Platelet factor 4 promotes adhesion of hematopoietic progenitor cells and binds IL-8: novel mechanisms for modulation of hematopoiesis." Blood **101**(12): 4687-94.
- Dudek, A. Z., C. A. Pennell, et al. (1997). "Platelet factor 4 binds to glycanated forms of thrombomodulin and to protein C. A potential mechanism for enhancing generation of activated protein C." J Biol Chem **272**(50): 31785-92.
- Duma, L., D. Haussinger, et al. (2007). "Recognition of RANTES by extracellular parts of the CCR5 receptor." J Mol Biol **365**(4): 1063-75.
- Eisman, R., S. Surrey, et al. (1990). "Structural and functional comparison of the genes for human platelet factor 4 and PF4alt." Blood **76**(2): 336-44.
- Eslin, D. E., C. Zhang, et al. (2004). "Transgenic mice studies demonstrate a role for platelet factor 4 in thrombosis: dissociation between anticoagulant and antithrombotic effect of heparin." Blood **104**(10): 3173-80.
- Fernandez, E. J. and E. Lolis (2002). "Structure, function, and inhibition of chemokines." Annu Rev Pharmacol Toxicol **42**: 469-99.
- Fiore, M. M. and V. V. Kakkar (2003). "Platelet factor 4 neutralizes heparan sulfate-enhanced antithrombin inactivation of factor Xa by preventing interaction(s) of enzyme with polysaccharide." Biochem Biophys Res Commun **311**(1): 71-6.
- Fiore, M. M. and I. J. Mackie (2009). "Dual effect of Platelet Factor 4 on the activities of Factor Xa." Biochem Biophys Res Commun **379**(4): 1072-5.
- Gengrinovitch, S., S. M. Greenberg, et al. (1995). "Platelet factor-4 inhibits the mitogenic activity of VEGF121 and VEGF165 using several concurrent mechanisms." J Biol Chem **270**(25): 15059-65.



- Gentilini, G., N. E. Kirschbaum, et al. (1999). "Inhibition of human umbilical vein endothelial cell proliferation by the CXC chemokine, platelet factor 4 (PF4), is associated with impaired downregulation of p21(Cip1/WAF1)." Blood **93**(1): 25-33.
- Gerard, C. and B. J. Rollins (2001). "Chemokines and disease." Nat Immunol **2**(2): 108-15.
- Goger, B., Y. Halden, et al. (2002). "Different affinities of glycosaminoglycan oligosaccharides for monomeric and dimeric interleukin-8: a model for chemokine regulation at inflammatory sites." Biochemistry **41**(5): 1640-6.
- Green, C. J., R. S. Charles, et al. (1989). "Identification and characterization of PF4var1, a human gene variant of platelet factor 4." Mol Cell Biol **9**(4): 1445-51.
- Guan, E., J. Wang, et al. (2001). "Identification of human macrophage inflammatory proteins 1alpha and 1beta as a native secreted heterodimer." J Biol Chem **276**(15): 12404-9.
- Hagedorn, M., L. Zilberberg, et al. (2001). "A short peptide domain of platelet factor 4 blocks angiogenic key events induced by FGF-2." Faseb J **15**(3): 550-2.
- Handel, T. M., Z. Johnson, et al. (2005). "Regulation of protein function by glycosaminoglycans--as exemplified by chemokines." Annu Rev Biochem **74**: 385-410.
- Hansson, G. K. and P. Libby (2006). "The immune response in atherosclerosis: a double-edged sword." Nat Rev Immunol **6**(7): 508-19.
- Hoogewerf, A. J., G. S. Kuschert, et al. (1997). "Glycosaminoglycans mediate cell surface oligomerization of chemokines." Biochemistry **36**(44): 13570-8.
- Huo, Y., A. Schober, et al. (2003). "Circulating activated platelets exacerbate atherosclerosis in mice deficient in apolipoprotein E." Nat Med **9**(1): 61-7.
- Jennings, L. K. (2009). "Mechanisms of platelet activation: need for new strategies to protect against platelet-mediated atherothrombosis." Thromb Haemost **102**(2): 248-57.
- Jouan, V., X. Canron, et al. (1999). "Inhibition of in vitro angiogenesis by platelet factor-4-derived peptides and mechanism of action." Blood **94**(3): 984-93.
- Kajava, A. V., S. N. Zolov, et al. (2000). "The net charge of the first 18 residues of the mature sequence affects protein translocation across the cytoplasmic membrane of gram-negative bacteria." J Bacteriol **182**(8): 2163-9.
- Kameyoshi, Y., A. Dorschner, et al. (1992). "Cytokine RANTES released by thrombin-stimulated platelets is a potent attractant for human eosinophils." J Exp Med **176**(2): 587-92.
- Kelner, G. S., J. Kennedy, et al. (1994). "Lymphotactin: a cytokine that represents a new class of chemokine." Science **266**(5189): 1395-9.
- Klinger, M. H., D. Wilhelm, et al. (1995). "Immunocytochemical localization of the chemokines RANTES and MIP-1 alpha within human platelets and their release during

storage." Int Arch Allergy Immunol **107**(4): 541-6.

Kobayashi, Y. (2006). "Neutrophil infiltration and chemokines." Crit Rev Immunol **26**(4): 307-16.

Koenen, R. R. and P. von Hundelshausen (2008). "The Chemokine system as therapeutic target in cardiovascular disease." Drug Discovery Today: Disease Mechanisms **5**(3-4): 285-292.

Koenen, R. R., P. von Hundelshausen, et al. (2009). "Disrupting functional interactions between platelet chemokines inhibits atherosclerosis in hyperlipidemic mice." Nat Med **15**(1): 97-103.

Kuschert, G. S., F. Coulin, et al. (1999). "Glycosaminoglycans interact selectively with chemokines and modulate receptor binding and cellular responses." Biochemistry **38**(39): 12959-68.

Laemmli, U. K. (1970). "Cleavage of structural proteins during the assembly of the head of bacteriophage T4." Nature **227**(5259): 680-5.

Lambert, M. P., Y. Wang, et al. (2009). "Platelet factor 4 regulates megakaryopoiesis through low-density lipoprotein receptor-related protein 1 (LRP1) on megakaryocytes." Blood **114**(11): 2290-8.

Lasagni, L., M. Francalanci, et al. (2003). "An alternatively spliced variant of CXCR3 mediates the inhibition of endothelial cell growth induced by IP-10, Mig, and I-TAC, and acts as functional receptor for platelet factor 4." J Exp Med **197**(11): 1537-49.

Lasagni, L., R. Grepin, et al. (2007). "PF-4/CXCL4 and CXCL4L1 exhibit distinct subcellular localization and a differentially regulated mechanism of secretion." Blood **109**(10): 4127-34.

LaVallie, E. R., E. A. DiBlasio, et al. (1993). "A thioredoxin gene fusion expression system that circumvents inclusion body formation in the E. coli cytoplasm." Biotechnology (N Y) **11**(2): 187-93.

Loscalzo, J., B. Melnick, et al. (1985). "The interaction of platelet factor four and glycosaminoglycans." Arch Biochem Biophys **240**(1): 446-55.

Lowry, O. H., N. J. Rosebrough, et al. (1951). "Protein measurement with the Folin phenol reagent." J Biol Chem **193**(1): 265-75.

Maione, T. E., G. S. Gray, et al. (1990). "Inhibition of angiogenesis by recombinant human platelet factor-4 and related peptides." Science **247**(4938): 77-9.

Martin, L., C. Blanpain, et al. (2001). "Structural and functional analysis of the RANTES-glycosaminoglycans interactions." Biochemistry **40**(21): 6303-18.

Mayo, K. H. and M. J. Chen (1989). "Human platelet factor 4 monomer-dimer-tetramer equilibria investigated by 1H NMR spectroscopy." Biochemistry **28**(24): 9469-78.

Mayo, K. H., E. Ilyina, et al. (1995). "Heparin binding to platelet factor-4. An NMR and

site-directed mutagenesis study: arginine residues are crucial for binding." Biochem J **312** ( Pt 2): 357-65.

Moser, B., M. Wolf, et al. (2004). "Chemokines: multiple levels of leukocyte migration control." Trends Immunol **25**(2): 75-84.

Mueller, A., A. Meiser, et al. (2008). "CXCL4-induced migration of activated T lymphocytes is mediated by the chemokine receptor CXCR3." J Leukoc Biol **83**(4): 875-82.

Murdoch, C. and A. Finn (2000). "Chemokine receptors and their role in inflammation and infectious diseases." Blood **95**(10): 3032-43.

Murdoch, C. and A. Finn (2000). "Chemokine receptors and their role in vascular biology." J Vasc Res **37**(1): 1-7.

Murphy, P. M., M. Baggiolini, et al. (2000). "International union of pharmacology. XXII. Nomenclature for chemokine receptors." Pharmacol Rev **52**(1): 145-76.

Nassar, T., B. S. Sachais, et al. (2003). "Platelet factor 4 enhances the binding of oxidized low-density lipoprotein to vascular wall cells." J Biol Chem **278**(8): 6187-93.

Neote, K., D. DiGregorio, et al. (1993). "Molecular cloning, functional expression, and signaling characteristics of a C-C chemokine receptor." Cell **72**(3): 415-25.

Nesmelova, I. V., Y. Sham, et al. (2005). "Platelet factor 4 and interleukin-8 CXC chemokine heterodimer formation modulates function at the quaternary structural level." J Biol Chem **280**(6): 4948-58.

Nesmelova, I. V., Y. Sham, et al. (2008). "CXC and CC chemokines form mixed heterodimers: association free energies from molecular dynamics simulations and experimental correlations." J Biol Chem **283**(35): 24155-66.

Nicosia, R. F. and A. Ottinetti (1990). "Growth of microvessels in serum-free matrix culture of rat aorta. A quantitative assay of angiogenesis in vitro." Lab Invest **63**(1): 115-22.

Offermanns, S. (2006). "Activation of platelet function through G protein-coupled receptors." Circ Res **99**(12): 1293-304.

Paoletti, S., V. Petkovic, et al. (2005). "A rich chemokine environment strongly enhances leukocyte migration and activities." Blood **105**(9): 3405-12.

Perollet, C., Z. C. Han, et al. (1998). "Platelet factor 4 modulates fibroblast growth factor 2 (FGF-2) activity and inhibits FGF-2 dimerization." Blood **91**(9): 3289-99.

Petersen, F., L. Bock, et al. (1998). "A chondroitin sulfate proteoglycan on human neutrophils specifically binds platelet factor 4 and is involved in cell activation." J Immunol **161**(8): 4347-55.

Pitsilos, S., J. Hunt, et al. (2003). "Platelet factor 4 localization in carotid atherosclerotic plaques: correlation with clinical parameters." Thromb Haemost **90**(6): 1112-20.

- Preston, R. J., S. Tran, et al. (2009). "Platelet factor 4 impairs the anticoagulant activity of activated protein C." J Biol Chem.
- Proudfoot, A. E. (2006). "The biological relevance of chemokine-proteoglycan interactions." Biochem Soc Trans **34**(Pt 3): 422-6.
- Proudfoot, A. E., S. Fritchley, et al. (2001). "The BBXB motif of RANTES is the principal site for heparin binding and controls receptor selectivity." J Biol Chem **276**(14): 10620-6.
- Proudfoot, A. E., T. M. Handel, et al. (2003). "Glycosaminoglycan binding and oligomerization are essential for the in vivo activity of certain chemokines." Proc Natl Acad Sci U S A **100**(4): 1885-90.
- Ragona, L., S. Tomaselli, et al. (2009). "New insights into the molecular interaction of the C-terminal sequence of CXCL4 with fibroblast growth factor-2." Biochem Biophys Res Commun **382**(1): 26-9.
- Rajagopalan, L. and K. Rajarathnam (2006). "Structural basis of chemokine receptor function--a model for binding affinity and ligand selectivity." Biosci Rep **26**(5): 325-39.
- Raport, C. J., J. Gosling, et al. (1996). "Molecular cloning and functional characterization of a novel human CC chemokine receptor (CCR5) for RANTES, MIP-1beta, and MIP-1alpha." J Biol Chem **271**(29): 17161-6.
- Rodríguez-Frade, J. M., M. Mellado, et al. (2001). "Chemokine receptor dimerization: two are better than one." Trends in Immunology **22**(11): 612-617.
- Roscic-Mrkic, B., M. Fischer, et al. (2003). "RANTES (CCL5) uses the proteoglycan CD44 as an auxiliary receptor to mediate cellular activation signals and HIV-1 enhancement." Blood **102**(4): 1169-77.
- Rossi, D. and A. Zlotnik (2000). "The biology of chemokines and their receptors." Annu Rev Immunol **18**: 217-42.
- Rot, A. and U. H. von Andrian (2004). "Chemokines in innate and adaptive host defense: basic chemokines grammar for immune cells." Annu Rev Immunol **22**: 891-928.
- Sachais, B. S., A. A. Higazi, et al. (2004). "Interactions of platelet factor 4 with the vessel wall." Semin Thromb Hemost **30**(3): 351-8.
- Sachais, B. S., A. Kuo, et al. (2002). "Platelet factor 4 binds to low-density lipoprotein receptors and disrupts the endocytic machinery, resulting in retention of low-density lipoprotein on the cell surface." Blood **99**(10): 3613-22.
- Sachais, B. S., T. Turrentine, et al. (2007). "Elimination of platelet factor 4 (PF4) from platelets reduces atherosclerosis in C57Bl/6 and apoE<sup>-/-</sup> mice." Thromb Haemost **98**(5): 1108-13.
- Saiki, R. K., D. H. Gelfand, et al. (1988). "Primer-directed enzymatic amplification of DNA with a thermostable DNA polymerase." Science **239**(4839): 487-91.

Sambrook, J. and D. Russell (2001). "Molecular cloning."

Sambrook, J. and D. W. Russell (2001 ). "Molecular cloning : a laboratory manual." Cold Spring Harbor: Cold Spring Harbor Laboratory Press.

Schagger, H. and G. von Jagow (1987). "Tricine-sodium dodecyl sulfate-polyacrylamide gel electrophoresis for the separation of proteins in the range from 1 to 100 kDa." Anal Biochem **166**(2): 368-79.

Schall, T. J., K. Bacon, et al. (1990). "Selective attraction of monocytes and T lymphocytes of the memory phenotype by cytokine RANTES." Nature **347**(6294): 669-71.

Schall, T. J., J. Jongstra, et al. (1988). "A human T cell-specific molecule is a member of a new gene family." J Immunol **141**(3): 1018-25.

Schnolzer, M., P. Alewood, et al. (1992). "In situ neutralization in Boc-chemistry solid phase peptide synthesis. Rapid, high yield assembly of difficult sequences." Int J Pept Protein Res **40**(3-4): 180-93.

Slungaard, A., J. A. Fernandez, et al. (2003). "Platelet factor 4 enhances generation of activated protein C in vitro and in vivo." Blood **102**(1): 146-51.

Slungaard, A. and N. S. Key (1994). "Platelet factor 4 stimulates thrombomodulin protein C-activating cofactor activity. A structure-function analysis." J Biol Chem **269**(41): 25549-56.

Sorensen, L. N. and S. R. Paludan (2004). "Blocking CC chemokine receptor (CCR) 1 and CCR5 during herpes simplex virus type 2 infection in vivo impairs host defence and perturbs the cytokine response." Scand J Immunol **59**(3): 321-33.

Sticht, H., S. E. Escher, et al. (1999). "Solution structure of the human CC chemokine 2: A monomeric representative of the CC chemokine subtype." Biochemistry **38**(19): 5995-6002.

Strieter, R. M., P. J. Polverini, et al. (1995). "The functional role of the ELR motif in CXC chemokine-mediated angiogenesis." J Biol Chem **270**(45): 27348-57.

Struyf, S., M. D. Burdick, et al. (2007). "Platelet factor-4 variant chemokine CXCL4L1 inhibits melanoma and lung carcinoma growth and metastasis by preventing angiogenesis." Cancer Res **67**(12): 5940-8.

Struyf, S., M. D. Burdick, et al. (2004). "Platelets release CXCL4L1, a nonallelic variant of the chemokine platelet factor-4/CXCL4 and potent inhibitor of angiogenesis." Circ Res **95**(9): 855-7.

Stuttfield, E. and K. Ballmer-Hofer (2009). "Structure and function of VEGF receptors." IUBMB Life **61**(9): 915-22.

Tanaka, T., Y. Manome, et al. (1997). "Viral vector-mediated transduction of a modified platelet factor 4 cDNA inhibits angiogenesis and tumor growth." Nat Med **3**(4): 437-42.

- Varga-Szabo, D., I. Pleines, et al. (2008). "Cell adhesion mechanisms in platelets." Arterioscler Thromb Vasc Biol **28**(3): 403-12.
- von Hundelshausen, P., R. R. Koenen, et al. (2005). "Heterophilic interactions of platelet factor 4 and RANTES promote monocyte arrest on endothelium." Blood **105**(3): 924-30.
- Von Hundelshausen, P., R. R. Koenen, et al. (2008). "Platelet-Mediated Enhancement of Leukocyte Adhesion." Microcirculation: 1-13.
- von Hundelshausen, P., F. Petersen, et al. (2007). "Platelet-derived chemokines in vascular biology." Thromb Haemost **97**(5): 704-13.
- von Hundelshausen, P. and C. Weber (2007). "Platelets as immune cells: bridging inflammation and cardiovascular disease." Circ Res **100**(1): 27-40.
- von Hundelshausen, P., K. S. Weber, et al. (2001). "RANTES deposition by platelets triggers monocyte arrest on inflamed and atherosclerotic endothelium." Circulation **103**(13): 1772-7.
- Walz, D. A., V. Y. Wu, et al. (1977). "Primary structure of human platelet factor 4." Thrombosis Research **11**(6): 893-898.
- Watson, J. B., S. B. Getzler, et al. (1994). "Platelet factor 4 modulates the mitogenic activity of basic fibroblast growth factor." J Clin Invest **94**(1): 261-8.
- Weber, C. and R. R. Koenen (2006). "Fine-tuning leukocyte responses: towards a chemokine 'interactome'." Trends Immunol **27**(6): 268-73.
- Weber, C., K. S. Weber, et al. (2001). "Specialized roles of the chemokine receptors CCR1 and CCR5 in the recruitment of monocytes and T(H)1-like/CD45RO(+) T cells." Blood **97**(4): 1144-6.
- Weber, C., A. Zernecke, et al. (2008). "The multifaceted contributions of leukocyte subsets to atherosclerosis: lessons from mouse models." Nat Rev Immunol **8**(10): 802-15.
- Woycechowsky, K. J., K. D. Wittrup, et al. (1999). "A small-molecule catalyst of protein folding in vitro and in vivo." Chem Biol **6**(12): 871-9.
- Zlotnik, A., O. Yoshie, et al. (2006). "The chemokine and chemokine receptor superfamilies and their molecular evolution." Genome Biol **7**(12): 243.

## IX Curriculum Vitae

### Personal data:

**Name:** Alisina Sarabi  
**Date of Birth:** 08.07.1978  
**Place of Birth:** Kabul, Afghanistan  
**Nationality:** Austria  
**Gender:** male

### EDUCATION

**1984-1987:** Volksschule (Elementary School) in Kabul, Afghanistan

**1988:** Volksschule (Elementary School), Märzstraße in Vienna, Austria

**1988-1992:** Hauptschule (High School), Märzstraße in Vienna, Austria

**1992-1997:** Gymnasium (High School) Diefenbachgasse in Vienna, Austria

**1997-2004:** Study of Biology / Genetics at the University of Vienna, Austria

**1998-1999:** Alternative civilian service at Caritas Wien and nursing home Liesing Vienna, Austria

**2003-2004:** Diploma thesis at the Medical University of Vienna  
(Title: Characterization of putative *Candida albicans* Zinc Cluster Transcription Factors)

**2005-2010:** PhD at the University Hospital RWTH Aachen,  
Institute for Molecular Cardiovascular Research (IMCAR)  
Aachen, Germany

**Publication:**

**Alisina Sarabi**, Birgit K Kramp, Maik Drechsler, Tilman M Hackeng, Oliver Soehnlein, Christian Weber, Rory R Koenen and Philipp von Hundelshausen (2010). CXCL4L1 inhibits angiogenesis and induces undirected endothelial cell migration without affecting endothelial cell proliferation and monocyte recruitment. *J Thromb Haemost* **9** (1): 209-19 [Epub ahead of print, DOI:10.1111/j.1538-7836.2010.04119.x.] PMID: 20961394

Nicole Schwarz, Jessica Pruessmeyer, Franz M Hess, Daniela Dreymueller, Elena Pantaler, Anne Koelsch, Reinhard Windoffer, Matthias Voss, **Alisina Sarabi**, Christian Weber, Antonio S Sechi, Stefan Uhlig, Andreas Ludwig (2010). Requirements for leukocyte transmigration via the transmembrane chemokine CX3CL1. *Cell Mol Life Sci* **67** (24): 4233-48

Rory R Koenen, Jessica Pruessmeyer, Oliver Soehnlein, Line Fraemohs, Alma Zerneck, Nicole Schwarz, Karina Reiss, **Alisina Sarabi**, Lennart Lindbom, Tilman M Hackeng, Christian Weber and Andreas Ludwig (2009). Regulated release and functional modulation of junctional adhesion molecule A by disintegrin metalloproteinases. *Blood* **113** (19): 4799-4809

Rory R Koenen, Philipp von Hundelshausen, Irina V Nesmelova, Alma Zerneck, Elisa A Liehn, **Alisina Sarabi**, Birgit K Kramp, Anna M Piccinini, Søren R Paludan, M Anna Kowalska, Andreas J Kunzl, Tilman M Hackeng, Kevin H Mayo & Christian Weber (2009). Disrupting functional interactions between platelet chemokines inhibits atherosclerosis in hyperlipidemic mice. *Nat Med* **15** (1): 97-103

Birgit K Kramp, **Alisina Sarabi**, Rory R Koenen, Christian Weber (2010). Heterophilic chemokine receptor interactions in chemokine signaling and biology. *Exp Cell Res in press* [Epub ahead of print] PMID: 21146524

**Poster:**

Functional Characterization of CXCL4L1/Platelet Factor 4alt

**Alisina Sarabi**, Rory R Koenen, Philipp von Hundelshausen, Tilman M Hackeng, Christian Weber

4th European Meeting on Vascular Biology and Medicine (EMVBM), 2007, September 14–17, University of Bristol, United Kingdom

Annual Meeting of the Society for Microcirculation and Vascular Biology (GfMVB), 2008, 25- 27 September, Aachen, Germany

Functional comparison of CXCL4 and CXCL4L1

**Alisina Sarabi**, Birgit K Kramp, Tilman M Hackeng, Christian Weber, Rory R Koenen and Philipp von Hundelshausen

5th European Meeting on Vascular Biology and Medicine (EMVBM), 2009, September 14–17, Palais des Congrès / Parc Chanot, Marseille, France